SISSA
Scuola
Internazionale
Superiore di
Studi Avanzati

Physics Area - PhD course in
Statistical Physics

Exact results for two-dimensional criticality. From local symmetries to correlated percolation

Candidate:
Youness Diouane

Advisor:
Gesualdo Delfino

Academic Year 2021-2022

Contents

To my parents Fatima and Ali Diouane

Foreword

Determining whether an additional local symmetry affects the universality class of a statistical model is an important issue in the theory of critical phenomena. A basic example is provided by the RP^{N-1} model, in which N-component spin variables at each lattice site interact through an Hamiltonian invariant under global $O(N)$ rotations and local spin reversals. The local symmetry makes the difference with the usual $O(N)$ model and amounts to the head-tail symmetry characteristic of liquid crystals. In three dimensions, the weak first order transition observed in numerical simulations of the ferromagnetic model is consistent with the mean field scenario. On the other hand, in the two-dimensional case – the one we focus on in this thesis – fluctuations are stronger and minimize the reliability of mean field predictions, as illustrated by the phase transition of the three-state Potts model, which becomes continuous on planar lattices. For the RP^{N-1} model, the absence of spontaneous breaking of continuous symmetry in two dimensions generically suggests that criticality is limited to zero temperature, and Monte Carlo studies for $T \to 0$ showed a fast growth of the correlation length which made particularly hard to reach the asymptotic limit and draw conclusions. On the other hand, the possibility of finite temperature topological transitions similar to the Berezinskii-Kosterlitz-Thouless (BKT) one – which should definitely occur for $RP^1 \sim O(2)$ – and mediated by "disclination" defects has also been debated in numerical studies. While two-dimensional criticality has allowed for an impressive amount of exact solutions thanks to lattice integrability and conformal field theory, models with local symmetries traditionally remained outside the range of application of these methods. In this thesis, however, we show how the renormalization group fixed points of the RP^{N-1} model and of its complex generalization, the CP^{N-1} model, can be accessed in an exact way. This is achieved in the scale invariant scattering framework which, as we review in the introductory part of the thesis, implements in the basis of particle excitations the infinite-dimensional conformal symmetry characteristic of

critical points in two dimensions and has provided in the last few years new results for pure and disordered systems.

In the last part of the thesis, we will exploit the generality of the scale invariant scattering method to progress with another long standing problem of two-dimensional criticality, namely that of spin clusters in Potts correlated percolation. It has been known for long time that the problem can be addressed considering two coupled Potts models, but the need to consider the number of states of one of these models as a continuous variable has severely limited the analytical or numerical study of the critical points. Also here, the ability of the scattering method to enforce conformal invariance for the internal symmetry characteristic of the universality class will allow us to obtain exact equations for the critical points and to determine their solutions in the relevant limits.

The thesis is based on the results of the following papers:

• Gesualdo Delfino, Youness Diouane and Noel Lamsen,
Absence of nematic quasi-long-range order in two-dimensional liquid crystals with three director components,
J. Phys. A: Math. Theor. 54 (2021) 03LT01

• Youness Diouane, Noel Lamsen and Gesualdo Delfino,
Critical points in the RP^{N-1} model,
J. Stat. Mech. (2021) 033214

• Youness Diouane, Noel Lamsen and Gesualdo Delfino,
Critical points in the CP^{N-1} model,
J. Stat. Mech. (2022) 023201

• Noel Lamsen, Youness Diouane and Gesualdo Delfino,
Critical points in coupled Potts models and correlated percolation,
arXiv:2208.14844

Chapter 1

Background

In this introductory chapter we recall basic notions of critical phenomena and the role of conformal symmetry in two dimensions. We then review scale invariant scattering theory and its application to the $O(N)$ and q-state Potts models.

1.1 Generalities of critical phenomena

Let us consider systems of equilibrium statistical mechanics [1] characterized by an Hamiltonian $\mathcal{H}$. The expectation value of an observable $\mathcal{O}$ is the average over configurations

$$\langle \mathcal{O} \rangle = \frac{1}{Z} \sum_{\text{configurations}} \mathcal{O}\, e^{-\mathcal{H}/T}, \tag{1.1}$$

with T the temperature and

$$Z = \sum_{\text{configurations}} e^{-\mathcal{H}/T} \tag{1.2}$$

the partition function. It is initially convenient to consider the degrees of freedom of a system as "spin" variables s_i located at sites i of a regular lattice corresponding to a discretization of the d-dimensional Euclidean space $\mathbb{R}^d$; the sums in (1.1) and (1.2) then correspond to sums over all spin configurations. Thoughtout this thesis we refer to systems with short range interactions among the site variables. In addition, the interactions are also homogeneous across the lattice, meaning that, for example, $\langle s_i \rangle$ is site-independent.

In the general case the site variable s_i has more than one component and carries a representation of the symmetry group G that leaves invariant the Hamiltonian[1]. A well

[1]We will focus on critical systems and directly consider Hamiltonians invariant under the symmetry

known example is provided by the vector model with Hamiltonian

$$\mathcal{H}_{O(N)} = -J \sum_{\langle i,j \rangle} \mathbf{s}_i \cdot \mathbf{s}_j \,, \tag{1.3}$$

where $\mathbf{s}_i$ is a N-component unit vector, the symmetry group G is the group $O(N)$, and the requirement of short distance interactions is implemented taking the sum over the nearest neighbor pairs of sites $\langle i, j \rangle$. For $N = 1$, and then $G = \mathbb{Z}_2$, one obtains the Ising model. The interaction is ferromagnetic for $J > 0$ and antiferromagnetic for $J < 0$. In this initial presentation we will refer to ferromagnets and will comment on antiferromagnets when relevant at a later stage.

Another very interesting generalization of the Ising model is offered by the q-state Potts model [2, 3], which is defined by the Hamiltonian

$$\mathcal{H}_{\text{Potts}} = -J \sum_{\langle i,j \rangle} \delta_{s_i, s_j} \,, \tag{1.4}$$

where $s_i = 1, 2, \ldots, q$. The Hamiltonian is left invariant by global permutations of the q values of the site variables (which we will often call "colors" in the following). As a consequence the symmetry of the model corresponds to the group S_q of permutations of q objects, and the $\mathbb{Z}_2$ symmetry which characterizes the Ising model is recovered when $q = 2$.

Returning to the general discussion, the "order parameter" $\langle s_i \rangle$ vanishes [2] when the temperature T is large enough, and becomes nonzero when T is brought below a critical value T_c. The latter is a phase transition point associated to the spontaneous breaking of the symmetry G. Indeed, below T_c the order parameter can take different values related by the symmetry. The phase transition is of the first order if the order parameter has a discontinuity at T_c, and of the second order (or, more generally, continuous) otherwise.

The spin-spin correlation function decays as

$$\langle s_i s_j \rangle - \langle s_i \rangle^2 \sim e^{-|i-j|/\xi} \tag{1.5}$$

when the distance $|i - j|$ between the two sites becomes large. The characteristic scale ξ introduced in this way is called correlation length. While it remains finite at a first order transition, it diverges as

$$\xi \sim |T - T_c|^{-\nu} \,, \qquad T \to T_c \tag{1.6}$$

group of the critical point.

[2] In the Potts model one takes $\langle \sigma_{\alpha,i} \rangle = \langle \delta_{s_i,\alpha} - \frac{1}{q} \rangle$, $\alpha = 1, 2, \ldots, q$.

when approaching a second order transition. This relation defines the correlation length critical exponent ν. A key point of the theory of critical phenomena is that the divergence of ξ at second order transition points leaves no characteristic scale at distances much larger than lattice spacing, and leads to scale invariance at T_c.

More generally, thermodynamical observables show a scaling behavior close to criticality; for the order parameter this reads

$$\langle s_i \rangle \sim (T_c - T)^\beta \,, \qquad T \to T_c^- \,, \tag{1.7}$$

a relation that defines the critical exponent β.

Importantly, the divergence of the correlation length as $T \to T_c$ allows a continuum description of the region close to criticality, provided that one is interested in the properties of the system over scales much larger than the lattice spacing (see e.g. [4]). This continuum description corresponds to a field theory, and the lattice variable s_i is replaced by a spin field $s(x)$, where $x = (x_1, \ldots, x_d)$ is a point in the Euclidean d-dimensional space $\mathbb{R}^d$. In a similar way the local spin-spin interaction $\sum_j s_i s_j$, where the sum is taken over neighbors of the site i, corresponds to an energy density field $\varepsilon(x)$. The sums in (1.1) and (1.2) are now taken over field configurations. In this continuum formulation, the Hamiltonian $\mathcal{H}$ continues to be invariant under the group G of internal symmetry, but also acquires invariance under continuous spatial translations (corresponding to homogeneity of the system) and under continuous rotations (corresponding to isotropy).

Scale invariance at critical points leads to a power law decay of correlation functions, which for a field $\Phi(x)$ takes the form

$$\langle \Phi(x_1) \Phi(x_2) \rangle = \frac{\text{constant}}{|x_1 - x_2|^{2X_\Phi}} \,. \tag{1.8}$$

This defines the scaling dimension X_Φ of Φ and implies that from the dimensional point of view the field behaves as length$^{-X_\Phi}$.

Let us denote by $\mathcal{A} = \mathcal{H}/T$ the reduced Hamiltonian, or Euclidean action, which characterizes a given theory. It is convenient to separate the near-critical action $\mathcal{A}$ into a scale invariant part $\mathcal{A}^*$ corresponding to T_c, plus a term taking into account the deviation from T_c, so that we write

$$\mathcal{A} = \mathcal{A}^* + \tau \int d^d x \, \varepsilon(x) \,, \tag{1.9}$$

where $\tau \sim T - T_c$. The expression (1.1) shows that $\mathcal{A}$ is dimensionless, and then that τ has the dimension of an inverse length to the power $d - X_\varepsilon$; it then provides the dimensionful

coupling that breaks scale invariance away from criticality. The fact that ξ is a length gives $\xi \propto |\tau|^{-1/(d-X_\varepsilon)}$ and, comparing with (1.6), the expression

$$\nu = 1/(d - X_\varepsilon) \tag{1.10}$$

for the correlation length critical exponent.

We are now in the position to recall some main ideas and terminology of the renormalization group (RG) that expresses the response of the system to a change of scale [4, 5]. Let $\Phi(x)$ be a field with given transformation properties under the action of the symmetry group G. Then the field theory contains infinitely many fields with growing scaling dimension and transforming in the same way (it is sufficient to think to the derivatives of $\Phi(x)$). In writing (1.9) we omitted the contribution of infinitely many G-invariant fields with scaling dimensions larger than d. The couplings conjugated to such fields have the dimension of a length to positive powers and become negligible for the description of the large distance properties of our interest. In this sense such fields are called "irrelevant" in the language of the RG. A scale invariant theory is called a RG fixed point. The action in which irrelevant fields are omitted and which describes the large distance properties is called the scaling action. It may contain more than one G-invariant field with scaling dimension smaller than d (these fields are called "relevant"). This occurs when more than one parameter needs to be tuned to reach the scale invariant point; such theories describe "multicritical" behavior. In light of these considerations, the field that we denote $\varepsilon(x)$ can be more precisely defined as the most relevant (smallest scaling dimension) G-invariant field; similarly, the spin field $s(x)$ is the most relevant field with the symmetry properties of the order parameter. Some theories also possess fields with scaling dimension equal to d ("marginal" fields). Marginality may be spoiled by logarithmic corrections induced by interaction. Depending on the theory, these corrections will effectively produce a "marginally relevant" or a "marginally irrelevant" field. If no logarithmic correction occurs, the addition to a fixed point action of such a "truly marginal" field does not break scale invariance and generates a line of fixed points.

In conclusion of this section we also notice that the order parameter scales as $\langle s(x) \rangle \sim \xi^{-X_s} \sim |\tau|^{\nu X_s}$, and that comparison with (1.7) gives

$$\beta = \nu X_s = X_s/(d - X_\varepsilon)\,. \tag{1.11}$$

Together with (1.10), this relation shows that the critical exponents are determined by the scaling dimensions, which should then be regarded as the fundamental critical indices.

1.2 The two-dimensional case

1.2.1 Conformal symmetry and minimal models

In this thesis we will be interested in critical systems in $d = 2$, and this is the case to which we now turn. When writing the correlation function (1.8) we considered the basic case in which the field Φ is a scalar, in the sense that it is invariant under spatial rotations. More generally, in our discussion of the two-dimensional case it will be relevant for us to consider fields $\Phi(x)$ with scaling dimension X_Φ that transform as

$$\Phi(0) \to e^{-is_\Phi \alpha}\Phi(0) \tag{1.12}$$

under a rotation by an angle α centered in the origin; s_Φ is called the "Euclidean spin" of the field. An important property of field theory, going under the name of operator product expansion (OPE), is that products of fields can be expanded onto an infinite-dimensional basis of fields [5]. In a scale invariant theory, the requirement that the result preserves the dimensional and rotational properties implies for the OPE the form

$$\begin{aligned}\Phi_i(x)\Phi_j(0) &= \sum_k C_{ij}^k \,(z\bar{z})^{(X_k - X_i - X_j)/2}(z\bar{z}^{-1})^{(s_k - s_i - s_j)/2}\,\Phi_k(0) \\ &= \sum_k C_{ij}^k \, z^{\Delta_k - \Delta_i - \Delta_j}\bar{z}^{\bar{\Delta}_k - \bar{\Delta}_i - \bar{\Delta}_j}\,\Phi_k(0)\,. \end{aligned} \tag{1.13}$$

Here we introduced the complex coordinates on the plane

$$z = x_1 + ix_2\,, \qquad \bar{z} = x_1 - ix_2\,, \tag{1.14}$$

which transform under rotations as $z \to e^{i\alpha}z$, $\bar{z} \to e^{-i\alpha}\bar{z}$, and the dimensions Δ_Φ, $\bar{\Delta}_\Phi$ such that

$$X_\Phi = \Delta_\Phi + \bar{\Delta}_\Phi\,, \tag{1.15}$$

$$s_\Phi = \Delta_\Phi - \bar{\Delta}_\Phi\,. \tag{1.16}$$

The C_{ij}^k's in (1.13) are called OPE coefficients, and we used the shortened notations $X_{\Phi_i} = X_i$, ... A relevant implication is that the final expression of (1.13) allows to treat a field $\Phi(x)$ as the product of a z-dependent part with dimension Δ_Φ, and a $\bar{z}$-dependent part with dimension $\bar{\Delta}_\Phi$. The OPE also allows to introduce the useful notion of mutual locality. In ordinary physical cases one expects the correlation functions $\langle \cdots \Phi_i(x)\Phi_j(0)\cdots\rangle$ to be

invariant if x is taken around the origin and brought to the original position, namely under the continuation $z \to e^{2i\pi} z$, $\bar{z} \to e^{-2i\pi} \bar{z}$. If this is the case, the fields Φ_i and Φ_j are said to be mutually local. The OPE (1.13) shows that the condition is satisfied if

$$s_i + s_j - s_k \in \mathbb{Z} \tag{1.17}$$

for all k's in the sum.

One of the important benefits of the field theoretical framework is that it allows to show (see e.g. [6]) that scale invariant theories are actually invariant under the larger group of conformal transformations, i.e. tranformations in which the change of scale, instead of being global, varies smoothly with the coordinate. Due to this property, the scale invariant field theories describing statistical systems at criticality actually correspond to conformal field theories (CFTs). This circumstance has its most powerful implications in the two-dimensional case of interest in this thesis, because in this case conformal transformations correspond to variations $\delta z = f(z)$, $\delta \bar{z} = \bar{f}(\bar{z})$, where f (resp. $\bar{f}$) is any analytic function of z (resp. $\bar{z}$). It follows that in $d = 2$ the conformal group has the crucial peculiarity of possessing infinitely many generators. These generators can be shown to correspond [6, 7] to operators L_n which satisfy the Virasoro algebra

$$[L_n, L_m] = (n - m) L_{n+m} + \frac{c}{12} (n^3 - n) \delta_{n,-m} \,, \tag{1.18}$$

where c is a fundamental parameter of the critical system which goes under the name of "central charge".

We now briefly recall some implications of the algebra (1.18) referring the reader to [6, 7] for the derivations. In the first place the space of fields in critical theories splits into families corresponding to lowest weight representations of the algebra. Considering the z-dependent part (a similar structure holds for the $\bar{z}$-dependent part), a family $[\phi]$ contains a "primary" field $\phi(z)$ with dimension (often referred to as conformal dimension) Δ_ϕ, together with "descendants" with dimension $\Delta_\phi + l$; $l = 1, 2, \ldots$ is the "level" of the descendant. The derivatives of ϕ are examples of descendants. An important role is played by the reducible representations of the algebra, namely representations $[\phi]$ containing another representation $[\phi_0]$ whose primary ϕ_0 is a descendant of ϕ at a level l_0. The irreducible representation that one obtains factoring out $[\phi_0]$ is said to be "degenerate" at level l_0, and ϕ is said to be a degenerate primary. The construction can be shown to lead to differential equations for multi-point correlation functions containing a degenerate primary.

It will be particularly relevant for our purposes to recall the characterization of the space of CFTs with central charge $c \leq 1$. For $c < 1$ it is convenient to introduce the parameter $p > 0$ and write

$$c = 1 - \frac{6}{p(p+1)} \,. \tag{1.19}$$

Then the degenerate primaries can be written as $\Phi_{m,n}(z)$, with m and n positive integers, and their dimension $\Delta_{m,n}$ is determined by[3]

$$\Delta_{\mu,\nu} = \frac{[(p+1)\mu - p\nu]^2 - 1}{4p(p+1)} \,. \tag{1.20}$$

The OPE of two degenerate primary fields takes the form

$$\Phi_{m_1,n_1} \cdot \Phi_{m_2,n_2} = \sum_{k=0}^{min(m_1,m_2)-1} \sum_{l=0}^{min(n_1,n_2)-1} \left[\Phi_{|m_1-m_2|+1+2k,|n_1-n_2|+1+2l}\right] \,, \tag{1.21}$$

where we have suppressed the coordinate dependence, which is generally determined by (1.13); the notation $[\Phi]$ in the r.h.s. indicates contribution from the whole family of fields. As we saw, a field is the product of a z-dependent part and a $\bar{z}$-dependent part, and (1.21) separately applies to each of them. One can also consider fields $\Phi_{\mu,\nu}(z)$ with dimension (1.20) and noninteger indices; they are nondegenerate and their OPE with degenerate fields reads

$$\Phi_{m,n} \cdot \Phi_{\mu,\nu} = \sum_{k=0}^{m-1} \sum_{l=0}^{n-1} \left[\Phi_{\mu-m+1+2k,\nu-n+1+2l}\right] \,. \tag{1.22}$$

The critical points arising in ordinary spin systems satisfy "reflection positivity", a property implying a spectrum of conformal dimension $\{\Delta_i\}$ without negative values, and then ensuring that correlations decay with distance. For central charge $c < 1$ reflection positivity turns out to be satisfied only by (1.19) with $p = 3, 4, \ldots$ [8]. For these values of c the OPE (1.21) closes on a finite number of operator families originating from degenerate primaries [7], giving rise to the so called reflection positive "minimal models". For these theories the conformal dimensions $\Delta_{m,n}$ of the primary fields are given by (1.20) with $m = 1, 2, \ldots, p-1$, $n = 1, 2, \ldots, p$. Notice that the number of primaries, and then the number of families, grows with c. The fact that the central charge gives a measure of the number of degrees of freedom is a general property of reflection positive CFTs [9].

Not surprisingly the minimal field content ($p = 3$, $c = 1/2$) corresponds to the Ising critical point, with $\Delta_{1,1} = \Delta_{2,3} = 0$, $\Delta_{1,2} = \Delta_{2,2} = 1/16$ and $\Delta_{1,3} = \Delta_{2,1} = 1/2$

[3] In (1.20) we use indices μ, ν that are not necessarily integer, since this will be useful later.

corresponding to the identity, the spin field and the energy density field, respectively. These scalar fields have $\Delta = \bar{\Delta}$, and the scaling dimensions $X_s = 1/8$ and $X_\varepsilon = 1$ determine through (1.10) and (1.11) the Ising critical exponents, in agreement with lattice results [10, 11]. The Ising spectrum of conformal dimensions also allows to build the fermions (i.e. fields with half-integer spin) ψ and $\bar{\psi}$ with dimensions $(\Delta, \bar{\Delta})$ equal to $(1/2, 0)$ and $(0, 1/2)$, respectively. Since dimension 0 corresponds to the identity, and does not carry a coordinate dependence, we have[4] $\bar{\partial}\psi = \partial\bar{\psi} = 0$, which are the equations of motion of free fermions. The fact that the two-dimensional Ising model (without external field) corresponds to a free fermionic theory is known since the lattice results of [12].

For $p > 3$ minimal models generally correspond to multicritical points associated to the spontaneous breaking of $\mathbb{Z}_2$ symmetry [13, 14]. In particular $p = 4$ gives the tricritical Ising model, with tricriticality realized, for example, allowing also for vacant sites. However, the values $p = 5, 6$ also allow a restriction to a smaller set of primaries [15, 16, 17] corresponding to the critical ($p = 5$) and tricritical ($p = 6$) three-state Potts model.

1.2.2 Gaussian model

In $d = 2$ the Gaussian model plays a special role that it does not possess in higher dimensions. At criticality it corresponds to the theory of a free scalar field with action

$$\mathcal{A}_0 = \frac{1}{4\pi} \int d^2x \, (\nabla\varphi)^2 \, . \tag{1.23}$$

The fact that $\varphi(x)$ is dimensionless leads to the logarithmic correlator

$$\langle \varphi(x)\varphi(0) \rangle = -\ln|x| = -\frac{1}{2}(\ln z + \ln \bar{z}) \, , \tag{1.24}$$

which is consistent with the equation of motion $\partial\bar{\partial}\varphi = 0$ and the decomposition

$$\varphi(x) = \phi(z) + \bar{\phi}(\bar{z}) \, . \tag{1.25}$$

Instead of ϕ, which has $\langle \phi(z)\phi(0) \rangle \propto \ln z$, proper scaling primary fields of the theory are the exponentials

$$V_p(z) = e^{2ip\phi(z)} \, . \tag{1.26}$$

[4] Our notation is $\partial = \partial_z$ and $\bar{\partial} = \bar{\partial}_{\bar{z}}$.

Their dimension easily follows from free field methods (see [6]) and is given by

$$\Delta_{V_p} \equiv \Delta_p = p^2 \,. \tag{1.27}$$

One also has $\bar{V}_{\bar{p}}(\bar{z}) = e^{2i\bar{p}\bar{\phi}(\bar{z})}$, in such a way that the generic primary $V_p\bar{V}_{\bar{p}}$ has dimensions $(\Delta_p, \Delta_{\bar{p}})$. The Gaussian OPE has the form

$$V_{p_1} \cdot V_{p_2} = [V_{p_1+p_2}] \,, \tag{1.28}$$

and, together with (1.17) and (1.27), implies that two fields $V_{p_1}\bar{V}_{\bar{p}_1}$ and $V_{p_2}\bar{V}_{\bar{p}_2}$ are mutually local if

$$2(p_1p_2 - \bar{p}_1\bar{p}_2) \in \mathbb{Z} \,. \tag{1.29}$$

The energy density field in this theory is generically written as $\varepsilon = V_b\bar{V}_b + V_{-b}\bar{V}_{-b} \propto \cos 2b\varphi$, with $\Delta_\varepsilon = \bar{\Delta}_\varepsilon = b^2$, and physically interesting fields are local with respect to ε. A field $V_p\bar{V}_{\bar{p}}$ satisfies this condition if $\pm 2b(p - \bar{p})$ is an integer, i.e. if

$$p - \bar{p} = \frac{m}{2b} \,, \qquad m \in \mathbb{Z} \,. \tag{1.30}$$

When $m = 1$ we can build the complex fermion

$$\Psi = (\psi, \bar{\psi}) = \left(V_{\frac{1}{4b}+\frac{b}{2}}\bar{V}_{-\frac{1}{4b}+\frac{b}{2}}, V_{\frac{1}{4b}-\frac{b}{2}}\bar{V}_{-\frac{1}{4b}-\frac{b}{2}} \right) \,, \tag{1.31}$$

with spin $p^2 - \bar{p}^2$ equal to $1/2$ for ψ and to $-1/2$ for $\bar{\psi}$. The decomposition $\Psi = \Psi_1 + i\Psi_2$ defines two real fermions $\Psi_i = (\psi_i, \bar{\psi}_i)$. When $b^2 = 1/2$ we have $\bar{\partial}\psi = \partial\bar{\psi} = 0$, which are free fermionic equations of motion; it follows that for $b^2 = 1/2$ the theory (1.23) can be represented in terms of free fermions. On the other hand, for $b^2 \neq 1/2$ the fermions are coupled by the four-fermion term, which can be shown to be truly marginal; it follows that the action (1.23) with energy density field $\cos 2b\varphi$ can be expressed as [18, 19]

$$\mathcal{A}_0 = \int d^2x \left[\sum_{i=1,2} (\psi_i\bar{\partial}\psi_i + \bar{\psi}_i\partial\bar{\psi}_i) + g(b^2)\psi_1\bar{\psi}_1\psi_2\bar{\psi}_2 \right] \,, \tag{1.32}$$

with $g(1/2) = 0$; the field $\cos 2b\varphi$ corresponds to the fermionic mass term $\psi_1\bar{\psi}_1 + \psi_2\bar{\psi}_2$.

The form (1.32) of the action shows that the two-dimensional Gaussian model actually corresponds to a line a fixed points parametrized by b^2. Since at $b^2 = 1/2$ we have two free neutral fermions, namely two decoupled Ising models, the central charge is twice the Ising one, namely $c = 1$. On the other hand, this value holds generically for the Gaussian

model, since the interaction ($g \neq 0$) does not change the field content. The form (1.32) of the theory gives a direct description of the critical properties of the Ashkin-Teller model [20, 21], which corresponds to two Ising models coupled by energy-energy interaction. The Ashkin-Teller model indeed possesses a critical line with continuously varying critical exponents.

The fact that a same theory possesses a scalar (bosonic) description (1.23) and a fermionic description (1.32) is a remarkable property of the two-dimensional case. It also allows to unveil a symmetry that is not obvious in the representation (1.23). Indeed, the fermionic property $\psi_i^2 = \bar{\psi}_i^2 = 0$ allows to write $\psi_1\bar{\psi}_1\psi_2\bar{\psi}_2 \propto (\sum_i \psi_i\bar{\psi}_i)^2$. It follows that the action (1.32) is left invariant by $O(2)$ rotations of the vector (ψ_1, ψ_2); these are in turn $U(1)$ transformations for the complex fermion, and the integer m in (1.30) corresponds to the $U(1)$ charge. While for central charge $c < 1$ we only found discrete internal symmetries, we see that the case $c = 1$ allows for the simplest continuous symmetry, $G = O(2) \sim U(1)$. The Gaussian model then describes the critical properties of the $N = 2$ vector model (1.3), also known as XY model. The components of the spin field $\mathbf{s}(x) = (s_1(x), s_2(x))$ are obtained picking up the scalar fields with $m = \pm 1$, namely

$$s_\pm = s_1 \pm i s_2 = V_{\pm 1/4b}\bar{V}_{\mp 1/4b}\,, \tag{1.33}$$

with $\Delta_{s_\pm} = 1/16b^2$. While continuous symmetries do not break spontaneously in two dimensions [22, 23, 24], the XY model exhibits a different type of transition known as Berezinskii-Kosterlitz-Thouless (BKT) transition [25, 26]. The order parameter $\langle \mathbf{s}(x) \rangle$ vanishes at all temperatures, but a value T_{BKT} separates a high temperature phase with exponential decay of correlations from a low temperature phase (BKT phase) with power law decay. The Gaussian model naturally accounts for this phenomenon once b^2 is identified as a decreasing function of the temperature (see e.g. [4]). The transition is driven by the $O(2)$-invariant ($m = 0$) field ε, which has $X_\varepsilon = 2b^2$. Then for $b^2 > b^2(T_{BKT}) = 1$ the field is irrelevant and scale invariance is preserved at large distances, thus explaining the BKT phase. Since we know from (1.33) that $\Delta_s = 1/16$ at $b^2 = 1$, we have

$$\langle \mathbf{s}(x) \cdot \mathbf{s}(0) \rangle_{T=T_{BKT}} \sim |x|^{-1/4}\,. \tag{1.34}$$

We will also be interested in the chiral (i.e. with $\Delta = 0$ or $\bar{\Delta} = 0$) fields satisfying (1.30) and having lowest charge $m = \pm 1$. They correspond to $\eta_\pm = V_{\pm 1/2b}$ and $\bar{\eta}_\pm = \bar{V}_{\pm 1/2b}$, where the nonzero conformal dimensions are given by

$$\Delta_{\eta_\pm} = \bar{\Delta}_{\bar{\eta}_\pm} = \frac{1}{4b^2}\,. \tag{1.35}$$

1.3 Scattering framework

1.3.1 Basic notions

In this thesis we will largely exploit the fact that a field theory describing the near-critical properties of a statistical system also possesses a formulation in momentum space. In this formulation the fundamendal degrees of freedom are the particle modes describing the excitations with respect to the ground state. These particle modes describe collective excitations of the degrees of freedom in real space and should not be confused with individual particles (atoms, molecules) of a fluid system. For our applications to critical phenomena we are interested in field theories possessing translation and rotation invariance (Euclidean field theories), and in $d = 2$ we denote by $x = (x_1, x_2)$ a point in real space. Performing the identification

$$x_2 = it\,, \tag{1.36}$$

an Euclidean field theory defines a quantum field theory with spatial coordinate x_1 and time coordinate t. The quantum theory has the same field content as the Euclidean theory, and correlation functions in the two cases are related by the analytic continuation (1.36). The particle modes correspond to excitations above a minimum energy (vacuum) state $|0\rangle$. The spontaneous symmetry breaking of an internal symmetry G leads to several degenerate vacua below T_c (see e.g. [27]). Through the continuation (1.36) rotation invariance (isotropy) in Euclidean space is mapped onto relativistic invariance in space-time. As a consequence the particle modes have the relativistic dispersion relation

$$E = \sqrt{p^2 + m^2}\,, \tag{1.37}$$

where E is the energy, p the momentum and m the mass. In our natural units the mass has the dimension of an inverse length, and is related to the correlation length as

$$\xi \propto 1/m\,. \tag{1.38}$$

The S-matrix [27, 28] encodes the particle description of field theory. The elements of this matrix are the probability amplitudes that a set of particles at $t = -\infty$ evolves into a set of particles at $t = +\infty$ as a result of scattering. In general relativistic scattering conserves total energy and momentum, but not the number of particles. For a given an initial state, the sum of the transition probabilities over all possible final states has to be

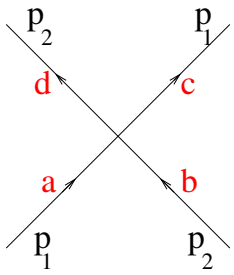

Figure 1.1: Scattering process associated to the amplitude that we denote $S_{ab}^{cd}(s)$. Time runs upwards.

one, implying the unitarity of the S-matrix. A scattering process in which the number of particles is preserved is said to be "elastic", and a two-particle elastic process is depicted in figure 1.1. We consider particles with the same mass, and in $d = 2$ conservation of energy and momentum implies that the momenta p_1 and p_2 are individually conserved. In general the particles form multiplets carrying a representation of the group G of internal symmetry, and the indices a, b, c, d in the figure label components of the multiplets.

Relativistic invariance requires that the scattering amplitude of figure 1.1 depends on the only relativistic invariant that can be built out of the two energy-momenta, i.e. the square of the center of mass energy

$$s = (E_1 + E_2)^2 - (p_1 + p_2)^2 \,. \tag{1.39}$$

Denoting the amplitude by $S_{ab}^{cd}(s)$, it satisfies the relations

$$S_{ab}^{cd}(s) = S_{ba}^{dc}(s) \,, \tag{1.40}$$

$$S_{ab}^{cd}(s) = S_{cd}^{ab}(s) \,, \tag{1.41}$$

$$S_{ab}^{cd}(s) = S_{\bar{c}\bar{d}}^{\bar{a}\bar{b}}(s) \,, \tag{1.42}$$

expressing invariance under spatial inversion, time reversal and charge conjugation, respectively. Let us also recall that the amplitude also satisfies the following analytic properties as a function of s, formally considered as a complex variable [28]. In the first place the amplitude is an analytic function up to singularities possessing a physical meaning. As a consequence of unitarity the minimal energy values (thresholds) $s = (km)^2$ needed to produce a final state with $k \geq 2$ particles correspond to branch points of the amplitude. Instead, a pole at $s = \tilde{m}^2 \in (0, 4m^2)$ corresponds to a particle of mass $\tilde{m}$ appearing as a

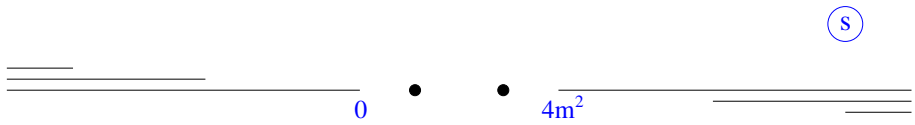

Figure 1.2: The figure illustrates the analytic structure of the scattering amplitude in the complex s-plane. The unitarity branch cuts are those on the right and the crossing cuts those on the left. Two poles are also shown.

bound state of the two scattering particles. The unitarity branch cuts are taken along the positive real axis in the complex s-plane (figure 1.2), and the physical values of the amplitude are given by the limit towards the real axis from above ($S^{cd}_{ab}(s+i\epsilon)$ with $s \geq 4m^2$, $\epsilon \to 0^+$). These values lie on the first (called "physical") sheet of the cut s-plane. Other sheets are accessed through the branch cuts. When s does not exceed the first inelastic threshold s_1 the unitarity condition reads

$$\sum_{e,f} S^{ef}_{ab}(s+i\epsilon) \left[S^{cd}_{ef}(s+i\epsilon)\right]^* = \delta_{ac}\delta_{bd}\,, \qquad (2m)^2 < s < s_1\,. \tag{1.43}$$

Crossing symmetry is a further important property of relativistic scattering. It states that the amplitude for the direct scattering channel (figure 1.1 with time running upwards) is related by analytic continuation to the amplitude for the crossed scattering channel (figure 1.1 with time running from left to right). When passing to the crossed channel, the particles b and d, whose arrows point in the 'wrong' direction, are replaced with antiparticles $\bar{b}$ and $\bar{d}$, and their energy and momentum is reversed ($E_2, p_2 \to -E_2, -p_2$, corresponding to $s \to 4m^2 - s$). It follows that the crossing relation takes the form

$$S^{cd}_{ab}(s+i\epsilon) = S^{\bar{b}c}_{\bar{d}a}(4m^2 - s - i\epsilon)\,, \tag{1.44}$$

with s real. This relation implies that an amplitude acquires crossed channel branch cuts running along the negative real axis, as well as crossing images of bound state poles. These features are illustrated in figure 1.2. In addition, the property of "real analyticity" states that the values of the amplitude on opposite edges of a cut are related by complex conjugation,

$$S^{cd}_{ab}(s+i\epsilon) = \left[S^{cd}_{ab}(s-i\epsilon)\right]^*\,. \tag{1.45}$$

We finally observe that the state created by the action of a field ϕ on the vacuum state $|0\rangle$ can be expanded on the basis of multi-particle states. If this expansion includes the

one-particle state $|p\rangle$, namely if

$$F_\phi(p) \equiv \langle p|\phi(0)|0\rangle \neq 0\,, \tag{1.46}$$

we say that ϕ creates the particle. Throughout this thesis we will adopt the usual normalization condition $\langle p_1|p_2\rangle = 2\pi E_1 \delta(p_1 - p_2)$ for the states. Since rotations in Euclidean space correspond to relativistic transformations in space-time under which (E, p) transforms as a vector, $E \pm p$ has Euclidean spin ± 1. It then follows from (1.12), (1.15) and (1.16) that

$$F_\phi(p) = a_\phi (E+p)^{\Delta_\phi} (E-p)^{\bar{\Delta}_\phi}\,, \tag{1.47}$$

with a_ϕ a dimensionless number.

1.3.2 Specialization to criticality

Remarkable simplifications occurs in the scattering problem at a scale invariant point in two dimensions [29]. Indeed, we have to take into account that infinite-dimensional conformal symmetry implies that infinitely many quantities (instead than just energy and momentum) have to be conserved in the time evolution. The consequence is that the final state will be kinematically identical (same number of particles, same energies, same momenta) to the initial one, a property that we call "complete elasticity". In addition, since the correlation length $\xi = \infty$, the particles are massless and the dispersion relation (1.37) shows that their energy and momentum are related as $p = E > 0$ (right movers) or $p = -E < 0$ (left movers). It then follows from (1.46) and (1.47) that at criticality the particles are created by chiral fields $\eta(z)$ (for right movers) and $\bar{\eta}(\bar{z})$ (for left movers), namely fields with $\bar{\Delta}_\eta = 0$ and $\Delta_{\bar{\eta}} = 0$. For the spin of these fields we have

$$s_\eta = -s_{\bar{\eta}} = \Delta_\eta = \bar{\Delta}_{\bar{\eta}}\,. \tag{1.48}$$

On the other hand, scale invariance implies that the theory does not possess dimensionful parameters, with the consequence that the scattering amplitude S of a right-mover with a left-mover cannot depend on the variable (1.39), which is the only relativistic invariant in the process and is dimensionful. The interpretation of the energy-independence of the amplitude is that the particles have no dynamical interaction, but this does not imply $S = 1$. Indeed, we must recall that scattering in one spatial dimension involves position exchange on the line, which in general produces a statistical factor. This can

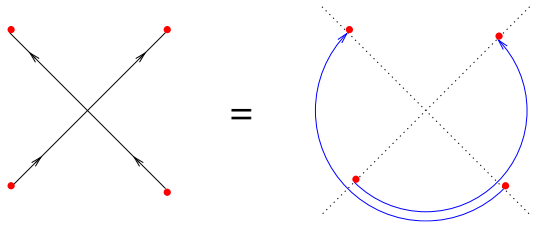

Figure 1.3: Pictorial illustration of equation (1.49).

be determined observing that, in absence of dynamical interaction, the scattering, i.e. the passage from the initial to the final state, can also be realized by π-rotations (see figure 1.3), and is then ruled by the Euclidean spin (1.48) of the fields that create the particles. The scattering (statistical) amplitude [29]

$$S = e^{-i\pi(s_\eta - s_{\bar{\eta}})} = e^{-2i\pi\Delta_\eta} \,. \tag{1.49}$$

is then obtained recalling (1.12). We see that S is 1 for bosons (Δ_η integer) and -1 for fermions (Δ_η half-integer), while generalized statistics will account for other values.

In this argument we considered the simplest case of a single particle species. More generally, the particles carry indices and we have the amplitudes S_{ab}^{cd} of the previous subsection, with the difference that they no longer depend on the center of mass energy. With respect to the general analyticity structure of figure 1.2, complete elasticity eliminates all branch points, apart from the elastic one at $s = 4m^2$ and its crossing image at $s = 0$. Hence, the limit $m \to 0$ relevant for the present case does not involve any collapse of infinitely many branch points on top of each other, and remains well defined. Since there are no inelastic thresholds ($s_1 = \infty$) and $m = 0$, the unitarity equation (1.43) holds for any s, consistently with the s-independence of the amplitudes; it now becomes [29]

$$\sum_{e,f} S_{ab}^{ef} \left[S_{ef}^{cd}\right]^* = \delta_{ac}\delta_{bd} \,. \tag{1.50}$$

On the other hand, (1.44) and (1.45) can be combined to obtain

$$S_{ab}^{cd} = \left[S_{\bar{d}a}^{\bar{b}c}\right]^* \,. \tag{1.51}$$

If there is a single particle species, (1.50) yields an amplitude S which is a phase, consistently with (1.49). In presence of more species a phase satisfying (1.49) is obtained by diagonalization of the scattering. We now illustrate this procedure through the examples of the $O(N)$ and q-state Potts models.

1.4 $O(N)$ model

1.4.1 Fixed point equations

For a first illustration of the use of the scale invariant scattering theory of section 1.3.2 we consider the vector model defined on the lattice by the Hamiltonian (1.3). The $O(N)$ symmetry is represented by a vector multiplet of massless particles which we denote by an index $a = 1, 2, \ldots, N$. We further denote by $|ab\rangle$ a state containing two particles a and b, and we omit the specification of momenta since we have seen that scattering at criticality does not depend on them. As the product of two vector representations, the initial state $|ab\rangle$ possesses a tensorial structure which needs to be preserved by the scattering. We then write the effect of the latter as

$$|ab\rangle \to \delta_{ab}\, S_1 \sum_{c=1}^{N} |cc\rangle + S_2\, |ab\rangle + S_3\, |ba\rangle\,, \tag{1.52}$$

where S_1, S_2 and S_3 are annihilation, transmission and reflection amplitudes, respectively. They are depicted in figure 1.4. In the present case the particles are self-conjugated ($a = \bar{a}$) and the crossing symmetry relations (1.51) take the form

$$S_1 = S_3^* \equiv \rho_1 e^{i\phi}\,, \tag{1.53}$$

$$S_2 = S_2^* \equiv \rho_2\,, \tag{1.54}$$

where we have introduced parametrizations in terms of $\rho_1 \geq 0$, and ρ_2 and ϕ real. The unitarity equations (1.50) then take the form [29]

$$\rho_1^2 + \rho_2^2 = 1\,, \tag{1.55}$$

$$\rho_1 \rho_2 \cos\phi = 0\,, \tag{1.56}$$

$$N\rho_1^2 + 2\rho_1\rho_2 \cos\phi + 2\rho_1^2 \cos 2\phi = 0\,, \tag{1.57}$$

corresponding respectively to the choices $(c = a, d = b)$, $(c = b, d = a)$, and $(a = b, c = d)$. It can be observed that in these equations N enters as a parameter that does not need to be an integer. The possibility to continue the model to noninteger values of N is already known on the lattice, as we recall in the next subsection. The solutions of the equations (1.55)-(1.57) give the critical points (RG fixed points) of the $O(N)$ model. They are listed in table 1.1 and shown in figure 1.5. We now discuss their physical meaning.

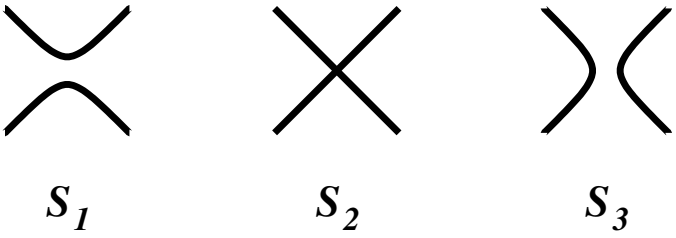

Figure 1.4: The scattering amplitudes S_1, S_2 and S_3 of the $O(N)$ model. Time runs upwards.

Solution	N	ρ_2	$\cos\phi$
$\mathrm{P1}_\pm$	$(-\infty,\infty)$	± 1	-
$\mathrm{P2}_\pm$	$[-2,2]$	0	$\pm\frac{1}{2}\sqrt{2-N}$
$\mathrm{P3}_\pm$	2	$\pm\sqrt{1-\rho_1^2}$	0

Table 1.1: The solutions of the equations (1.55)-(1.57) correspond to the RG fixed points with $O(N)$ symmetry.

1.4.2 Nonintersecting loops

Let us begin our discussion with the solutions $P2_\pm$, which are defined for $N \in [-2,2]$. At $N=2$ they coincide with the point $S_2=0$ of the solution $P3$ which, as will be seen in a moment, corresponds to a CFT with central charge $c=1$. The fact that the central charge increases with the number of degrees of freedom, and then with N, implies that the CFTs corresponding to the solutions $P2_\pm$ have $c \leq 1$. This means that we are in the CFT subspace of section 1.2.1, where we have seen that a main role is played by the degenerate primary fields with conformal dimensions (1.20). In particular, the energy density field $\varepsilon(x)$ is expected to be a degenerate field, and at $N=1$ for one of the two solutions $P2_\pm$ it should have the dimension $\Delta_\varepsilon = 1/2$ of the Ising model. This leads to the identification[5] $\Delta_\varepsilon = \bar{\Delta}_\varepsilon = \Delta_{1,3}$.

We can use this result and the OPE (1.21) to idenfity the chiral field η which creates the particles as the most relevant chiral field local with respect to ε. The result $\Delta_\eta = \Delta_{2,1}$ determine Δ_η as a function of the parameter p entering (1.19). On the other hand, it

[5]We will see below that the alternative choice $\Delta_{2,1}$ corresponds to the q-state Potts model.

follows from (1.52) that the state $\sum_{a=1}^{N} |aa\rangle$ scatters into itself with the amplitude

$$S = NS_1 + S_2 + S_3\,, \tag{1.58}$$

which for the solutions $P2_\pm$ is equal to $-e^{3i\phi}$. The requirement $S = -1$ for $N = 1$ (Ising free fermion) selects $P2_-$. As a consequence, for this solution we know Δ_η as a function of N, through (1.49), and as a function of p. Once we compare the two results we obtain

$$N = 2\cos\frac{\pi}{p}\,. \tag{1.59}$$

The result $\Delta_s = \bar{\Delta}_s = \Delta_{1/2,0}$ for the dimensions of the spin field can be obtained through a slightly more general analysis [29] exploiting the OPE (1.22) with nondegenerate fields yields.

The solution $P2_+$ can be quickly identified [30] once we recall that adding the field $\Phi_{1,3}$ to the CFT with central charge (1.19) induces a RG flow to the fixed point with central charge corresponding to $p-1$ [9]. Since $\Phi_{1,3} = \varepsilon$ preserves $O(N)$ symmetry, the infrared line of fixed points obtained in this way corresponds to $P2_+$ and has $N = 2\cos\frac{\pi}{p+1}$. Together with $S = -e^{3i\phi}$ this relation leads to $\Delta_\eta = \Delta_{1,2}$, a result that differs from $\Delta_{2,1}$ for $P2_-$ for the interchange of the indices. This interchange is preserved by the mutual locality analysis based on the OPEs (1.21) and (1.22), and gives $\Delta_\varepsilon = \Delta_{3,1}$ and $\Delta_s = \Delta_{0,1/2}$ for the solution $P2_+$. We summarize in table 1.2 the results obtained in this way for the critical lines $P2_\pm$.

We also notice that the critical lines $P2_\pm$ have $S_2 = 0$, and then correspond to particle trajectories that do not intersect (recall figure 1.4). On the other hand, it is known (see e.g. [4]) that the partition function of the $O(N)$ model can be mapped onto that of a loop gas,

$$Z_{\text{loops}} = \sum_{\mathcal{G}} K^{n_b} N^{n_l}\,, \tag{1.60}$$

where $\mathcal{G}$ are configurations of loops on the lattice, K is the coupling in the spin formulation, n_l is the number of loops, and n_b is the number of edges occupied by the loops. This loop formulation implements on the lattice the continuation to noninteger values of N, and for $N \to 0$ is known to describe the statistics of self-avoiding walks [31]. The loop model is exactly solvable on the honeycomb lattice [32], on which the loops do not intersect. The solution produces two critical lines defined in the interval $N \in [-2, 2]$ and coinciding at $N = 2$. Their critical exponents were shown in [33] to correspond to the

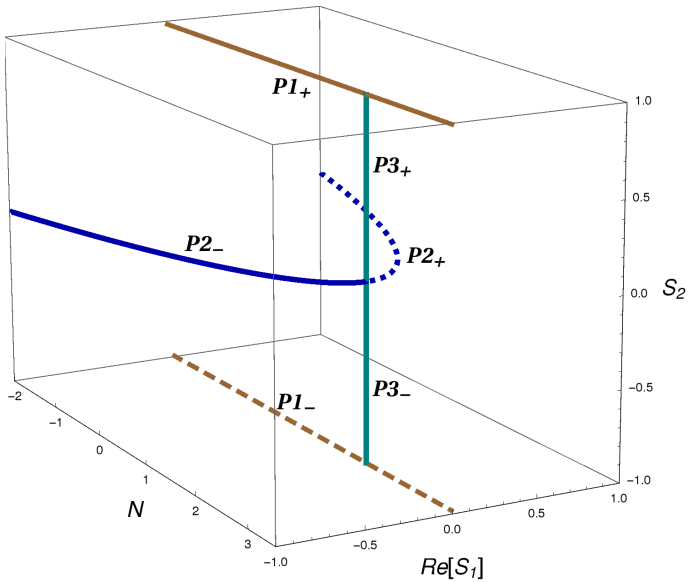

Figure 1.5: Solutions of the fixed point equations (1.55)-(1.57) of the $O(N)$ model. $P2_-$ and $P2_+$ are the critical lines for the dilute and dense regimes of nonintersecting loops, $P3_+$ corresponds to the BKT phase of the XY model, and for $N > 2$ $P1_+$ gives the zero temperature critical point.

conformal dimensions Δ_s and Δ_ε that we deduced above for the solutions $P2_\pm$. The two critical lines of the loop model are referred to as "dilute" and "dense" with reference to the loop properties that they control. They correspond to the solutions $P2_-$ and $P2_+$, respectively. For the off-critical case the analogy between particle trajectories and loop paths was observed in [34].

1.4.3 BKT phase at $N = 2$

We now notice that the solutions $P3_\pm$, defined only for $N = 2$, can also be written in the form

$$\rho_1 = \sin\alpha\,, \qquad \rho_2 = \cos\alpha\,, \qquad \phi = -\frac{\pi}{2}\,. \tag{1.61}$$

The characteristic presence of the free parameter α perfectly matches the observation of section 1.2.2 that $O(2)$ symmetry actually allows for a line of RG fixed points with central charge $c = 1$. We have seen that this fixed line corresponds to the Gaussian theory (1.23), in which the energy density field $\varepsilon(x) = \cos 2b\varphi(x)$, with conformal dimension $\Delta_\varepsilon = b^2$, introduces the parameter b^2 providing the coordinate along the line. We also determined

Solution	N	c	Δ_η	Δ_ε	Δ_s
$\mathrm{P1}_-$	$(-\infty,\infty)$	$\frac{N}{2}$	$\frac{1}{2}$	$\frac{1}{2}$	$\frac{1}{16}$
$\mathrm{P1}_+$	$(-\infty,\infty)$	$N-1$	0	1	0
$\mathrm{P2}_-$	$2\cos\frac{\pi}{p}$	$1-\frac{6}{p(p+1)}$	$\Delta_{2,1}$	$\Delta_{1,3}$	$\Delta_{\frac{1}{2},0}$
$\mathrm{P2}_+$	$2\cos\frac{\pi}{p+1}$	$1-\frac{6}{p(p+1)}$	$\Delta_{1,2}$	$\Delta_{3,1}$	$\Delta_{0,\frac{1}{2}}$
$\mathrm{P3}_\pm$	2	1	$\frac{1}{4b^2}$	b^2	$\frac{1}{16b^2}$

Table 1.2: Conformal data (central charge c and conformal dimensions Δ) for the solutions of table 1.1. $\Delta_{\mu,\nu}$ is given by (1.20).

in (1.35) as a function of b^2 the dimension of the chiral fields that create the particles. On the other hand, for the solution (1.61) the scattering phase (1.58) takes the form $S = e^{-i\alpha}$, in such a way that (1.49) yields the relation

$$\alpha = \frac{\pi}{2b^2} \tag{1.62}$$

between the free parameter of the scattering theory and that of the Gaussian model. We also notice that S takes the value -1 when $b^2 = 1/2$, in full agreement with the fact that at such a point the Gaussian model has the fermionic representation (1.32) with $g = 0$. When b^2 takes generic values, the particles $a = 1, 2$ of the scattering theory can be identified with the two neutral fermions in (1.32). An additional piece of information we possess is that the $O(2)$ spin vector field has the bosonic representation (1.33) with dimension $\Delta_s = 1/16b^2$.

The solutions $P3_+$ and $P3_-$ correspond to the two intervals $\alpha \in [0, \pi/2]$ and $\alpha \in [\pi/2, \pi]$, respectively. As seen in section 1.2.2, the BKT phase of the XY model corresponds to the portion of the line of fixed points where $\varepsilon(x)$ is irrelevant, and then to solution $P3_+$. $P3_+$ and $P3_-$ meet at the point $\alpha = \pi/2$, which is also the meeting point of the solutions $P2_\pm$, as can be seen in figure 1.5. This is the BKT transition point, where the field ε is marginal ($\Delta_\varepsilon = 1$).

1.4.4 Zero temperature criticality for $N > 2$

The solutions $P1_+$ and $P1_-$, which are the only ones to be defined for any N, are purely transmissive and correspond respectively to free bosons ($S_2 = 1$) and free fermions ($S_2 = -1$). $P1_-$ corresponds to N neutral fermions, for a total central charge $c = N/2$ (a single

neutral fermion (Ising) has $c = 1/2$), and is not relevant[6] for the critical behavior of the vector model (1.3) for generic N. For $N = 2$ this gives back the $c = 1$ theory (1.23) with $b^2 = 1/2$, or (1.32) with $g = 0$. As can be seen in figure (1.5), this is the contact point between $P1_-$ and $P3_-$. The conformal dimension $\Delta_s = 1/16$ that we give in table 1.2 for $P1_-$ is that of the spin fields $s_1, \ldots, s_N$ of the N decoupled Ising copies. Notice that, at the meeting point $b^2 = 1/2$, $P3_-$ has instead $\Delta_s = 1/8$. The reason is that the XY spin field (1.33) actually corresponds to $s_1 s_2$ [29].

The solution $P1_+$ describes two different cases. On one hand, it corresponds to N free bosons, i.e. the theory with action $\sum_{j=1}^{N} \int d^2x (\nabla\varphi_j)^2$, with $\Delta_\varepsilon = \Delta_{\varphi_j^2} = 0$, and $c = N$. On the other hand, and more interestingly, for $N = 2$ it also coincides with the limit $b^2 \to \infty$ of $P3_+$, which has $c = 1$. This is possible because, as we already observed, scattering on the line mixes statistics and interaction, so that the two fermions of the theory (1.32) can appear for $b^2 \to \infty$ as two free bosons ($S_2 = 1$). This subtle role of interaction continues for $N > 2$, where the $O(N)$ model is known to possess a zero temperature critical point and scaling properties described by the nonlinear sigma model (see e.g. [4])

$$\mathcal{A}_{\rm SM} = \frac{1}{T} \sum_{j=1}^{N} \int d^2x (\nabla\varphi_j)^2 \,, \qquad \sum_{j=1}^{N} \varphi_j^2 = 1 \,, \tag{1.63}$$

in which interaction is introduced by the constraint on the length of the vector $(\varphi_1, \ldots, \varphi_N)$. This theory is "asymptotically free", meaning that for $T \to 0$ the interaction amomg the bosons vanishes ($\Delta_s = \Delta_{\varphi_j} = 0$), while the energy density field is marginally relevant ($\Delta_\varepsilon = 1$, implying $\nu = \infty$ and exponentially diverging correlation length). The constraint in (1.63) reduces the central charge by one unit, to $c = N - 1$. These results for c and Δ_s agree with those for $N = 2$, $b^2 \to \infty$. In order to idenfity $\Delta_\varepsilon = 1$, we have to observe that for $b^2 > 1$ at $N = 2$ the field $\cos 2b\varphi$ is irrelevant, and that the most relevant $O(2)$-invariant field is the marginal one that generates the line of critical points. The sigma model interpretation of the solution $P1_+$ is the one that we report in table 1.2, together with the data discussed for the other solutions.

We conclude our discussion of the $O(N)$ scattering solutions observing that the case $N = 1$ allows some considerations that will be useful in the subsequent chapters. The symmetry $O(1) = \mathbb{Z}_2$ is that of the Ising model, which in two dimensions has a critical

[6]It must be noticed that, due to the quadratic nature of the unitarity equations (1.50), solutions differing for a change of sign of all amplitudes are always simultaneously present.

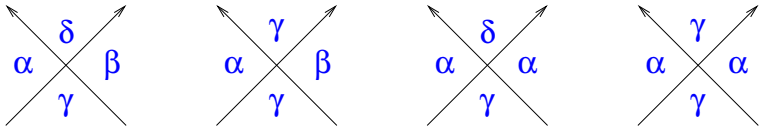

Figure 1.6: Scattering amplitudes S_0, S_1, S_2 and S_3 for the Potts model, with different letters denoting different colors. Time runs upwards.

point described by a free neutral fermion [6]. The corresponding amplitude $S_{11}^{11} = -1$ is of course realized by P1$_-$ in the purely transmissive form $S_{11}^{11} = S_2$. On the other hand, it is also realized by P2$_-$ in the form $S_{11}^{11} = S_1 + S_3$, as required by the fact that also the Ising partition function has a "geometrical" representation in terms of self-avoiding loops. This illustrates that a specific critical point may allow different diagrammatic realizations at the scattering level. Clearly, this is due to the fact that at $N = 1$ there is a single particle species, and transmission, reflection and annihilation are not physically distinguishable[7]. At the same time, some geometrical observables in the Ising model need to be computed in the limit $N \to 1$ [35, 36], and in this case solution P2$_-$ provides the right analytic continuation.

1.5 q-state Potts model

1.5.1 Fixed point equations

The q-state Potts model is defined on the lattice by the Hamiltonian (1.4) and is characterized by invariance under global permutations of the q values (colors) of the site variable, corresponding to the symmetry group $\mathbb{S}_q$. As always, the first step for the implementation of the scattering theory at criticality is the introduction of a particle basis that carries a representation of the symmetry. For the symmety $\mathbb{S}_q$ this is obtained considering particles that we denote $A_{\alpha\beta}$, with $\alpha, \beta = 1, 2, \ldots, q$, and $\alpha \neq \beta$. In the case of the Potts ferromagnet below critical temperature, such a particle basis corresponds to the kinks interpolating between pairs of the q degenerate vacua [37]; on the lattice a related representation of the symmetry was used in [38]. We will now see that this same basis allows to represent the symmetry also at criticality [29, 39] (where there are no kinks due to the coalescence of

[7] In a relativistic scattering process only the initial and final states are observable [28].

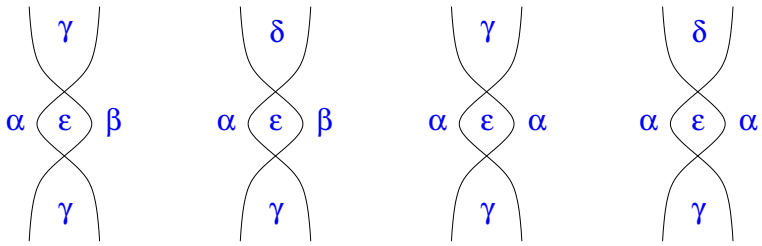

Figure 1.7: Configurations of the colors entering the unitarity equations (1.67)-(1.70), in that order. The interpretation is that the amplitude for the lower scattering multiplies the complex conjugate of the amplitude for the upper scattering; the sum over the internal color ε is also implied.

the vacua) and beyond the ferromagnetic case [40].

Let us consider the trajectory of a particle $A_{\alpha\beta}$ as a line separating a region of the two-dimensional space-time characterized by the color α from a region characterized by the color β. The permutational symmetry then allows for the four inequivalent amplitudes S_0, S_1, S_2 and S_3 depicted in figure 1.6. With this way of labeling the particles the crossing relations (1.51) become

$$S_0 = S_0^* \equiv \rho_0 \,, \tag{1.64}$$

$$S_1 = S_2^* \equiv \rho e^{i\phi} \,, \tag{1.65}$$

$$S_3 = S_3^* \equiv \rho_3 \,, \tag{1.66}$$

where the parametrizations in terms of $\rho \geq 0$, and ρ_0, ρ_3 and ϕ real have been introduced. With this parametrizations the unitarity equations (1.50) take the form [29] (see also figure 1.7)

$$(q-3)\rho_0^2 + \rho^2 = 1 \,, \tag{1.67}$$

$$(q-4)\rho_0^2 + 2\rho_0\rho\cos\phi = 0 \,, \tag{1.68}$$

$$(q-2)\rho^2 + \rho_3^2 = 1 \,, \tag{1.69}$$

$$(q-3)\rho^2 + 2\rho\rho_3\cos\phi = 0 \,. \tag{1.70}$$

The solutions of these equations, which give the Potts RG fixed points [29, 40], are listed in table 1.3 and will be discussed in the next subsections.

It must be observed that the equations (1.67)-(1.70) realize the analytic continuation of the model to noninteger values of q. The fact that this continuation is possible is well

known on the lattice, where the Potts partition function allows for the Fortuin-Kasteleyn expansion [41]

$$Z \propto \sum_{\mathcal{G}} p^{N_b}(1-p)^{\bar{N}_b} q^{N_c}\,, \tag{1.71}$$

where $\mathcal{G}$ is a graph made of bonds placed on the edges of the lattice, N_b is the number of bonds in $\mathcal{G}$, $\bar{N}_b$ is the number of edges without a bond, and N_c is the number of clusters in $\mathcal{G}$. A cluster corresponds to a set of connected bonds, but also to an isolated site. The quantity

$$p = 1 - e^{-J/T} \tag{1.72}$$

gives the relation with the coupling J of the spin representation. The Fortuin-Kasteleyn expansion is important, in particular, because implies that the percolation problem [42] can be studied as the limit $q \to 1$ of the Potts model. Indeed, in such a limit the weight $p^{N_b}(1-p)^{\bar{N}_b}$ of a bond configuration corresponds to random bond occupation with probability p. For q generic the reprentation (1.71) of the partition function defines a problem of "correlated percolation" in which each cluster can take q colors. In the following we will discuss the Potts model implying the continuation to q noninteger. While for q integer only the scattering amplitudes of figure 1.6 involving a number of colors not larger than q play a role, all of them participate to the analytic continuation to q noninteger[8].

1.5.2 Ferromagnetic criticality and tricriticality

The phase transition of the two-dimensional q-state Potts ferromagnet is of the second order up to $q = 4$, and of the first order above this value [43]. This implies that the ferromagnetic critical line corresponds to a solution of the fixed point equations (1.67)-(1.70) having $q = 4$ as upper endpoint, namely to one of the solutions $\mathrm{III}_{\pm}$ in table 1.3. The fact that for the Ising model ($q = 2$) the only physical amplitude $S_3 = \rho_3$ must take the free fermion value -1 uniquely identifies the solution III_{-}.

On the other hand, the $q = 4$ Potts model is a particular case of the Ashkin-Teller model[9], which we already saw has central charge $c = 1$. It follows that the Potts ferromagnetic critical line falls into the subspace of CFTs with $c \leq 1$ which we discussed in

[8] A detailed discussion of this point is given in [36].

[9] See [44, 45] for the scattering description of the Ashkin-Teller model, and [46] for that of the Potts model along the first order transition as $q \to 4^+$.

Solution	q	ρ_0	ρ	$2\cos\phi$	ρ_3
I	3	$0,\ 2\cos\phi$	1	$\in[-2,2]$	0
$\mathrm{II}_\pm$	$[-1,3]$	0	1	$\pm\sqrt{3-q}$	$\pm\sqrt{3-q}$
$\mathrm{III}_\pm$	$[0,4]$	±1	$\sqrt{4-q}$	$\pm\sqrt{4-q}$	$\pm(3-q)$
$\mathrm{IV}_\pm$	$[\frac{1}{2}(7-\sqrt{17}),3]$	$\pm\sqrt{\frac{q-3}{q^2-5q+5}}$	$\sqrt{\frac{q-4}{q^2-5q+5}}$	$\pm\sqrt{(3-q)(4-q)}$	$\pm\sqrt{\frac{q-3}{q^2-5q+5}}$
$\mathrm{V}_\pm$	$[4,\frac{1}{2}(7+\sqrt{17})]$	$\pm\sqrt{\frac{q-3}{q^2-5q+5}}$	$\sqrt{\frac{q-4}{q^2-5q+5}}$	$\mp\sqrt{(3-q)(4-q)}$	$\pm\sqrt{\frac{q-3}{q^2-5q+5}}$

Table 1.3: Solutions of Eqs. (1.67)-(1.70). They give the RG fixed points with $\mathbb{S}_q$ permutational symmetry.

section 1.2.1. The correspondence between CFT and scattering theory [29] then proceeds through steps anologous to those discussed in section 1.4.2 for the $O(N)$ case. One first identifies $\Delta_\varepsilon = \Delta_{2,1}$ and then searches for the field η that creates the particles as the most relevant chiral field local with respect to ε; this gives $\Delta_\eta = \Delta_{1,3}$, a function of the parameter p entering (1.19). At this point we observe that it follows in general from the amplitudes of figure 1.6 that the state $\sum_{\gamma\neq\alpha} A_{\alpha\gamma}A_{\gamma\alpha}$ scatters into itself with the amplitude

$$S = S_3 + (q-2)S_2\,, \tag{1.73}$$

which takes the value $S = e^{-4i\phi}$ for the solution III_-. This gives Δ_η as a function of q through (1.49), and the comparison with the previous result in function of p provides us with the relation

$$\sqrt{q} = 2\cos\frac{\pi}{p+1}\,. \tag{1.74}$$

The identification $\Delta_s = \Delta_{1/2,0}$ for the conformal dimension of the spin field for real values of q can be done exploiting the OPE (1.22) involving nondegenerate fields [29]. We report in table 1.4 these identifications of the central charge and conformal dimensions for the critical Potts ferromagnet. They match those obtained in [33] from the lattice determination of scaling dimensions [32].

We now recall the observation of section 1.2.1 that the critical points of the Potts ferromagnet for $q = 2, 3$ correspond to the CFT minimal models with $p = 3, 5$, respectively,

and that for the same values of q there are tricritical points that can be realized allowing for vacant sites; they correspond to $p = 4, 6$, respectively. This pairing, for a given q, of a critical point at p and and a tricritical point at $p + 1$ is actually known to extend to p generic (also noninteger) [9]. It follows that, together with the critical line (1.74), there is a tricritical line with

$$\sqrt{q} = 2 \cos \frac{\pi}{p} \,. \tag{1.75}$$

Since the introduction of vacancies does not affect color permutational symmetry, also the tricritical line must correspond to one of the scattering solutions in table 1.3. Critical and tricritical lines meet [47] at the endpoint $q = 4$ ($p = \infty$), and have conformal dimensions related by index exchange (see [40]), namely $\Delta_\varepsilon = \Delta_{1,2}$, $\Delta_s = \Delta_{0,1/2}$ and $\Delta_\eta = \Delta_{3,1}$ on the tricritical line. Inserting this value of Δ_η in (1.73) and using (1.75) one obtains again the result $S = e^{-4i\phi}$ corresponding to III$_-$; on the tricritical line, however, the sign of $\sin \phi$ is opposite to that for the critical line.

1.5.3 Antiferromagnets

The Potts model naturally offers us the occasion to enlarge our discussion to the case of antiferromagnetic interactions. Since the antiferromagnetic interaction tends to anti-align neighboring spins, it assigns an important role to the number of neighbors and to the structure of the lattice. This means that, while for ferromagnets quantities like critical exponents do not depend on the lattice structure (universality), antiferromagnenets have to be analyzed case by case. The fixed point equations (1.67)-(1.70) were obtained relying only on $\mathbb{S}_q$ symmetry, and this is common to ferromagnetic and antiferromagnetic Potts models. As a consequence the solutions of table 1.3 must also account for criticality in antiferromagnetic Potts models. What is presently known about the relations between the solutions of table 1.3 and Potts antiferromagnets can be summarized as follows.

The solution I, which is defined only for $q = 3$, contains ϕ as free parameter. This means that it describes a line of fixed points, and the simplest possibility is that it corresponds to the Gaussian line with central charge $c = 1$ of section 1.2.2. A confirmation comes from the fact that the $q = 3$ Potts antiferromagnet on the square lattice is known to possess a $T = 0$ Gaussian critical point [43, 48, 49] with $\Delta_\varepsilon = b^2 = 3/4$ [50]. Since we know that $\Delta_\eta = 1/4b^2$ on the Gaussian line, and (1.73) gives $S = S_2 = e^{-i\phi}$ for solution

I, (1.49) gives the relation

$$\phi = \frac{\pi}{2b^2} \tag{1.76}$$

between the scattering and the Gaussian parameters. The expectation [40] is that solution I corresponds to critical points of $q = 3$ antiferromagnets on lattices whose structure changes with b^2. Quite remarkably a family of lattices (self-dual quadrangulations with $T = 0$ criticality) realizing this phenomenon was recently found [51].

Hence, solution I corresponds to a family of different lattices for a fixed value of q. On the other hand, an early result for Potts antiferromagnets was obtained for the simplest lattice as a function of q. Indeed, Baxter showed that on the square lattice there is a second order transition for $q \in [0, 4]$ [52]. The critical temperature decreases as q increases, and we saw a moment ago that it is zero at $q = 3$, implying that for $q > 3$ the transition no longer corresponds to physical temperatures. Given its definition in the range $q \in [0, 4]$, the critical line has to corresponds to one of the scattering solutions of type III, and III$_-$ is selected by the fact that for $q = 2$ the square lattice ferromagnet and antiferromagnet can be mapped into. The square lattice critical line was found [53] (see also [54, 55, 40]) to have central charge[10]

$$c = \frac{2(N-1)}{N+2}\,, \tag{1.77}$$

with N related to q as

$$\sqrt{q} = 2\cos\frac{\pi}{(N+2)}\,. \tag{1.78}$$

The relations $\Delta_\varepsilon = (N-1)/N$ and $\Delta_\sigma = N/8(N+2)$ are also obtained. On the other hand, using (1.49) with $S = e^{-4i\phi}$ for solution III$_-$, one finds $\Delta_\eta = 2/(N+2)$.

The latter identification shows that solution III$_-$ with $\sin\phi > 0$ describes both the tricritical ferromagnetic line and the square lattice antiferromagnetic line, something made possible by the fact that the relation (1.49) allows for different values of Δ_η in correspondence of the same amplitude S. This illustrates how the solutions of table 1.3, although rather limited in number, are able to account for the diversity of antiferromagnetic critical behaviors.

Solution V of table 1.3 has to be noted for the fact that it sets to $(7+\sqrt{17})/2 = 5.56..$ the maximal value of q for which criticality with $\mathbb{S}_q$ symmetry can be realized in two dimensions[11], leaving room for a second order transition in a $q = 5$ antiferromagnet [40].

[10] It must be noted that this value of central charge is that of $\mathbb{Z}_N$ ferromagnets [56].

[11] Quenched disorder brings this maximal value to infinity [57, 58], see [39] for the analytical derivation.

$\sqrt{q}$	line	c	Δ_ε	Δ_η	Δ_s
$2\cos\frac{\pi}{p+1}$	F critical	$1-\frac{6}{p(p+1)}$	$\Delta_{2,1}$	$\Delta_{1,3}$	$\Delta_{\frac{1}{2},0}$
$2\cos\frac{\pi}{p}$	F tricritical	$1-\frac{6}{p(p+1)}$	$\Delta_{1,2}$	$\Delta_{3,1}$	$\Delta_{0,\frac{1}{2}}$
$2\cos\frac{\pi}{N+2}$	AF square lattice	$\frac{2(N-1)}{N+2}$	$\frac{N-1}{N}$	$\frac{2}{N+2}$	$\frac{N}{8(N+2)}$

Table 1.4: As discussed in the text, the scattering solution III$_-$ describes both Potts ferromagnetic (F) and antiferromagnetic (AF) critical lines. Here c is the central charge, while the conformal dimensions $\Delta_{\mu,\nu}$ are given by (1.20).

Numerical evidence in favor of such a transition in the five-state Potts antiferromagnet on the bisected hexagonal lattice was given in [59]. However, a more recent study concluded in favor of an extremely weak first order transition [60], so that the search for a lattice on which this transition can occur has to start over. Here we notice that the relation $S_0 + S_3 = S_1 + S_2$ among the Potts amplitudes was obtained in [36] for fixed points possessing an order-disorder duality[12]. Table 1.3 shows that only the solutions IV and V do not satisfy this relation, thus indicating that they do not allow for order-disorder duality. To conclude the survey of the solutions of table 1.3, we observe that solution IV appears as a counterpart of V in a lower range of q, while II allows a conformal identification [63] similar to that of the critical lines of section 1.4.2.

[12]Under this condition the relation extends away from criticality, without the need of integrability [36]. In particular, it is displayed by the solution for the off-critical ferromagnet, which is integrable [37]. Obviously, the relation relies on $\mathbb{S}_q$ symmetry, even if spontaneously broken. See [61, 62] for the effects on the spectrum of particle excitations of an explicit breaking of the symmetry induced by a magnetic field.

Chapter 2

Criticality in two-dimensional liquid crystals and the RP^{N-1} model

The isotropic-nematic transition in liquid crystals is described by the Lebwohl-Lasher model. In two dimensions, where its continuous symmetry cannot break spontaneously, this model has been numerically investigated since decades to verify, in particular, the conjecture of a topological transition leading to a nematic phase with quasi-long-range order. We use scale invariant scattering theory to exactly determine the renormalization group fixed points in the general case of N director components (RP^{N-1} model), which yields the Lebwohl-Lasher model for $N = 3$. For $N > 2$ we show that quasi-long-range order is absent and that criticality is restricted to zero temperature. For $N = 2$ the fixed point equations yield the Berezinskii-Kosterlitz-Thouless transition required by the correspondence $RP^1 \sim O(2)$.

2.1 Physical context

A liquid crystal cooled starting from its isotropic phase is generically expected to undergo a transition to a nematic phase with orientational order [64]. The head-tail symmetry of the elongated molecules distinguishes the isotropic-nematic (I-N) transition from the $O(3)$ ferromagnetic transition, and indeed in three dimensions the latter is second order while the former is observed to be first order, although weakly so [64]. In two dimensions (2D), on the other hand, the effect of fluctuations is stronger and the existence and nature of an I-N transition have been the object of debate. The absence of spontaneous

breaking of continuous symmetries [65] prevents a nematic phase with long range order, but leaves room for a defect-mediated (topological) transition similar to the Berezinskii-Kosterlitz-Thouless (BKT) one [66, 4]. In absence of analytical approaches, the matter has been considered within experimental studies (see [67] for a recent review) and, more specifically, through numerical simulations within the Lebwohl-Lasher (LL) lattice model [1], which encodes head-tail symmetry and successfully accounts for the weak first order transition in 3D [68]. The possibility in the 2D model of a topological transition driven by "disclination" defects [69, 70] and leading to a nematic phase with quasi-long-range order (QLRO) received support by some numerical studies [71, 72, 73, 74], with others concluding for the absence of a true transition [75, 76, 77, 78, 79]. The alternative scenario of criticality limited to zero temperature has also been the subject of several numerical studies [80, 81, 82, 83, 84, 85, 86], which tried to establish in the first place whether the head-tail symmetry is able to affect the universality class. Conclusions, however, have been made difficult by the very fast growth of the correlation length as the temperature is lowered.

Here we study the problem of critical behavior in the 2D LL model within the scale invariant scattering theory of section 1.3.2. Actually, we consider the more general case of N director components (RP^{N-1} model), which yields the LL model for $N = 3$. We show, in particular, that for $N > 2$ there is no QLRO, that criticality is limited to zero temperature, and that the local symmetry affects critical behavior. The analysis is performed for continuous values of N and allows to distinguish the range $N < N^* = 2.24421..$ characterized by a rich pattern of fixed points from the range $N > N^*$ in which the equations possess a single solution.

2.2 Preliminary remarks

As we saw in section 1.3.2, the special features of two-dimensional criticality are responsible for a substantial simplification of the unitarity and crossing equations that generally apply to relativistic scattering [28, 87]. Indeed, if we denote by $\mu = 1, 2, \ldots, k$ the particle species[1], by $\mathbb{S}$ the scattering operator, and by $S^{\rho\sigma}_{\mu\nu} = \langle\rho\sigma|\mathbb{S}|\mu\nu\rangle$ the amplitude for a scattering process with particles μ and ν in the initial state and particles ρ and σ in the

[1]In this chapter we can limit our discussion to self-conjugated particles.

Figure 2.1: *Left:* Pictorial representation of the scattering amplitude $S^{\rho\sigma}_{\mu\nu}$. *Right:* The product of amplitudes entering the unitarity equations (1.50).

final state (figure 2.1), we have [29]

$$S^{\rho\sigma}_{\mu\nu} = \left[S^{\rho\nu}_{\mu\sigma}\right]^* \tag{2.1}$$

for crossing and

$$\sum_{\lambda,\tau} S^{\lambda\tau}_{\mu\nu} \left[S^{\rho\sigma}_{\lambda\tau}\right]^* = \delta_{\mu\rho}\delta_{\nu\sigma} \tag{2.2}$$

for unitarity. The relations

$$S^{\rho\sigma}_{\mu\nu} = S^{\mu\nu}_{\rho\sigma} = S^{\sigma\rho}_{\nu\mu} \tag{2.3}$$

also hold and express invariance of the amplitudes under time reversal and spatial inversion.

In our study of the RP^{N-1} model it will be relevant to have in mind the results we discussed in section 1.4 for the vector model. It will also be convenient, in order to avoid confusion about the role of the parameter N, to refer to an $O(M)$ vector model defined on the lattice by the Hamiltonian

$$\mathcal{H}_1 = -J \sum_{\langle i,j \rangle} \mathbf{s}_i \cdot \mathbf{s}_j \,, \tag{2.4}$$

where $\mathbf{s}_i$ is a M-component unit vector. Then we know that the scattering amplitudes are those of figure 1.4, parametrized as in (1.53), (1.54), and satisfying the equations

$$\rho_1^2 + \rho_2^2 = 1 \,, \tag{2.5}$$

$$\rho_1\rho_2 \cos\phi = 0 \,, \tag{2.6}$$

$$M\rho_1^2 + 2\rho_1\rho_2\cos\phi + 2\rho_1^2\cos 2\phi = 0 \,. \tag{2.7}$$

The solutions of these $O(M)$ fixed point equations are those listed in table 2.1 and shown in figure 2.2; their physical interpretation was discussed in detail in section 1.4.

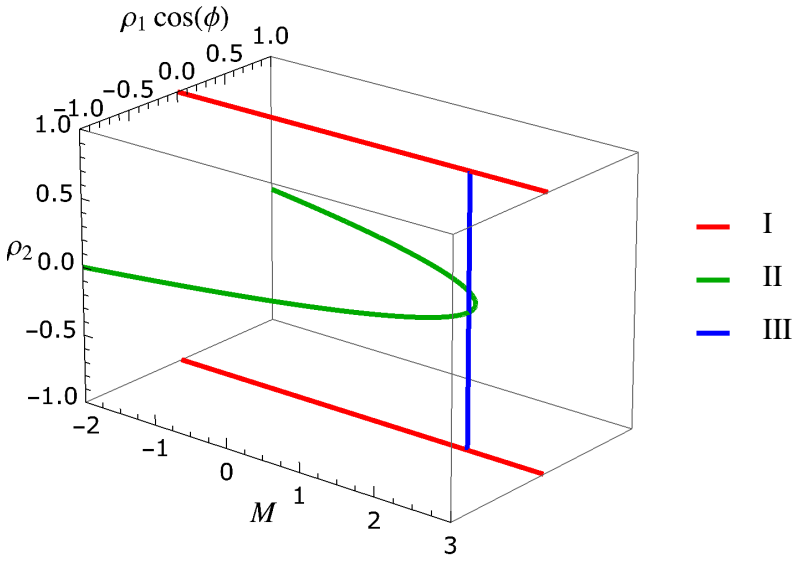

Figure 2.2: Solutions of the $O(M)$ fixed point equations (2.5)-(2.7). The two branches of II correspond to the critical lines for the dilute and dense phases of nonintersecting loops, III accounts for the BKT transition of the XY model, and the upper branch of I corresponds to the zero temperature critical point of the model for $M > 2$.

Solution	M	ρ_1	ρ_2	$\cos\phi$
$\mathrm{I}_\pm$	$(-\infty, \infty)$	0	± 1	-
$\mathrm{II}_\pm$	$[-2, 2]$	1	0	$\pm\frac{1}{2}\sqrt{2-M}$
$\mathrm{III}_\pm$	2	$[0, 1]$	$\pm\sqrt{1-\rho_1^2}$	0

Table 2.1: Solutions of equations (2.5)-(2.7), yielding the renormalization group fixed points with $O(M)$ symmetry.

2.3 Fixed point equations of the RP^{N-1} model

The RP^{N-1} lattice model is defined by the Hamiltonian

$$\mathcal{H}_2 = -J \sum_{\langle i,j \rangle} (\mathbf{s}_i \cdot \mathbf{s}_j)^2 \,, \tag{2.8}$$

where $\mathbf{s}_i$ is a N-component unit vector located at site i. The difference with respect to the Hamiltonian (1.3) is the square in the r.h.s., which makes (2.8) invariant under any local reversal $\mathbf{s}_i \to -\mathbf{s}_i$, thus ensuring head-tail symmetry. This means that $\mathbf{s}_i$ effectively takes values on the unit hypersphere with opposite points identified, namely in the real projective space the model is named after. The Lebwohl-Lasher case corresponds to $N = 3$. The global and local symmetries of the model are represented through an order parameter variable quadratic in the vector components s_i^a, namely by the symmetric tensor [64]

$$Q_i^{ab} = s_i^a s_i^b - \frac{1}{N} \delta_{ab} \,. \tag{2.9}$$

While $\sum_a s_i^a s_i^a = 1$ excludes the presence of an invariant linear in the order parameter components, $\mathrm{Tr}\, Q_i^{ab} = 0$ ensures that, upon diagonalization in generic dimension, the order parameter $\langle Q_i^{ab} \rangle$ vanishes in the isotropic phase. We denote by $\langle \cdots \rangle$ the average over configurations weighted by $e^{-\mathcal{H}_2/T}$.

The steps through which we implement scale invariant scattering for the two-dimensional RP^{N-1} model at criticality parallel those seen in section 1.4 for the vector model. The key difference is that, in the continuum limit, the order parameter field is now the symmetric tensor $Q_{ab}(x)$, which creates particles that we label by $\mu = ab$, with a and b going from 1 to N. The scattering processes corresponding to these particles are those shown in figure 2.3. Taking into account also the relations (1.40) and (1.41) in the massless limit, the scattering matrix is expressed in terms of the amplitudes $S_1, \ldots, S_{11}$ as

$$\begin{aligned}
S_{ab,cd}^{ef,gh} &= S_1\, \delta^{(2)}_{(ab),(cd)} \delta^{(2)}_{(ef),(gh)} + S_2\, \delta^{(2)}_{(ab),(ef)} \delta^{(2)}_{(cd),(gh)} + S_3\, \delta^{(2)}_{(ab),(gh)} \delta^{(2)}_{(cd),(ef)} \\
&+ S_4\, \delta^{(4)}_{(ab)(gh),(cd)(ef)} + S_5\, \delta^{(4)}_{(ab)(ef),(cd)(gh)} + S_6\, \delta^{(4)}_{(ab)(cd),(ef)(gh)} \\
&+ S_7 \left[\delta_{ab}\delta_{ef} \delta^{(2)}_{(cd),(gh)} + \delta_{cd}\delta_{gh} \delta^{(2)}_{(ab),(ef)} \right] + S_8 \left[\delta_{ab}\delta_{gh} \delta^{(2)}_{(cd),(ef)} + \delta_{cd}\delta_{ef} \delta^{(2)}_{(ab),(gh)} \right] \\
&+ S_9 \left[\delta_{ab} \delta^{(3)}_{(cd),(ef),(gh)} + \delta_{cd} \delta^{(3)}_{(ab),(ef),(gh)} + \delta_{ef} \delta^{(3)}_{(cd),(ab),(gh)} + \delta_{gh} \delta^{(3)}_{(cd),(ef),(ab)} \right] \\
&+ S_{10}\, \delta_{ab}\delta_{cd}\delta_{ef}\delta_{gh} + S_{11} \left[\delta_{ab}\delta_{cd} \delta^2_{(ef),(gh)} + \delta_{ef}\delta_{gh} \delta^{(2)}_{(ab),(cd)} \right] ,
\end{aligned} \tag{2.10}$$

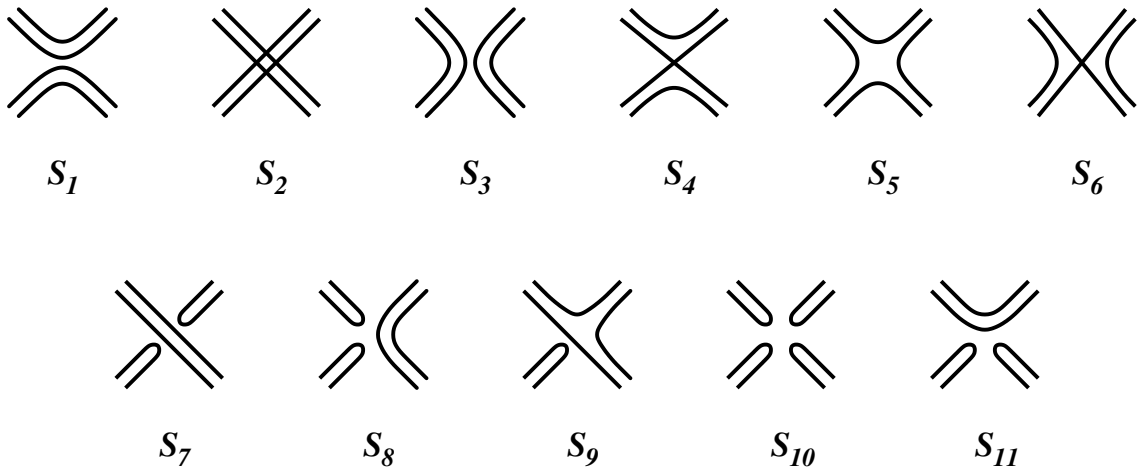

Figure 2.3: Scattering amplitudes appearing in (2.10). Time runs upwards.

where we introduced the notations

$$\delta^{(2)}_{(ab),(cd)} \equiv (\delta_{ac}\delta_{bd} + \delta_{ad}\delta_{bc})/2\,, \tag{2.11}$$

$$\begin{aligned}\delta^{(3)}_{(ab),(cd),(ef)} \equiv (&\delta_{af}\delta_{bd}\delta_{ce} + \delta_{ad}\delta_{bf}\delta_{ce} + \delta_{ae}\delta_{bd}\delta_{cf} + \delta_{ad}\delta_{be}\delta_{cf} \\ &+ \delta_{af}\delta_{bc}\delta_{de} + \delta_{ac}\delta_{bf}\delta_{de} + \delta_{ae}\delta_{bc}\delta_{df} + \delta_{ac}\delta_{be}\delta_{df})/8\,,\end{aligned} \tag{2.12}$$

$$\begin{aligned}\delta^{(4)}_{(ab)(cd),(ef)(gh)} \equiv (&\delta_{ah}\delta_{bf}\delta_{cg}\delta_{de} + \delta_{af}\delta_{bh}\delta_{cg}\delta_{de} + \delta_{ag}\delta_{bf}\delta_{ch}\delta_{de} + \delta_{af}\delta_{bg}\delta_{ch}\delta_{de} \\ &+ \delta_{ah}\delta_{be}\delta_{c,g}\delta_{df} + \delta_{a,e}\delta_{bh}\delta_{cg}\delta_{df} + \delta_{ag}\delta_{be}\delta_{ch}\delta_{df} + \delta_{ae}\delta_{bg}\delta_{ch}\delta_{df} \\ &+ \delta_{ah}\delta_{bf}\delta_{ce}\delta_{dg} + \delta_{af}\delta_{bh}\delta_{ce}\delta_{dg} + \delta_{ah}\delta_{be}\delta_{cf}\delta_{dg} + \delta_{ae}\delta_{bh}\delta_{cf}\delta_{dg} \\ &+ \delta_{ag}\delta_{bf}\delta_{ce}\delta_{dh} + \delta_{af}\delta_{bg}\delta_{ce}\delta_{dh} + \delta_{ag}\delta_{be}\delta_{cf}\delta_{dh} + \delta_{ae}\delta_{bg}\delta_{cf}\delta_{dh})/4\end{aligned} \tag{2.13}$$

to take into account the different ways of contracting the particle indices for a given process in figure 2.3. The fact that the indices of a particle aa can annihilate each other gives rise to the amplitudes $S_{i\geq 7}$.

Since the amplitudes $S_{i\leq 3}$ satisfy the crossing equations (1.53) and (1.54), we keep for them the same parametrization in terms of ρ_1, ρ_2 and ϕ. On the other hand, the crossing

relations for the remaining amplitudes lead to the parametrizations

$$S_4 = S_6^* \equiv \rho_4 e^{i\theta}\,, \tag{2.14}$$

$$S_5 = S_5^* \equiv \rho_5\,, \tag{2.15}$$

$$S_7 = S_7^* \equiv \rho_7\,, \tag{2.16}$$

$$S_8 = S_{11}^* \equiv \rho_8 e^{i\psi}\,, \tag{2.17}$$

$$S_9 = S_9^* \equiv \rho_9\,, \tag{2.18}$$

$$S_{10} = S_{10}^* \equiv \rho_{10}\,. \tag{2.19}$$

The unitarity equations (1.50) now take the explicit form

$$\sum_{e,f,g,h=1}^{N} S_{ab,cd}^{ef,gh} \left[S_{ef,gh}^{a'b',c'd'}\right]^* = \delta^{(2)}_{(ab),(a'b')}\delta^{(2)}_{(cd),(c'd')}\,, \tag{2.20}$$

which takes into account the present way of indexing the particles. The different possible choices of external indices (see table 2.2) then yield the equations

$$1 = \rho_1^2 + \rho_2^2 + 4\rho_4^2, \tag{2.21}$$

$$0 = 2\rho_1\rho_2\cos\phi + 4\rho_4^2, \tag{2.22}$$

$$\begin{aligned} 0 = {} & (M_N+1)\rho_1^2 + 2\rho_1^2\cos 2\phi + 2\rho_1\rho_2\cos\phi + 4\rho_1\rho_4\cos(\phi+\theta) + 4(\rho_4^2+\rho_5^2+2\rho_4\rho_5\cos\theta) \\ & + 4(N+1)(\rho_1\rho_4\cos(\phi-\theta) + \rho_1\rho_5\cos\phi) + 2N\rho_1\rho_8\cos(\phi+\psi) + 8\rho_4\rho_8\cos(\theta-\psi) \\ & + 8\rho_4\rho_8\cos(\theta+\psi) + 8\rho_5\rho_8\cos\psi + N^2\rho_8^2 + 4\rho_1\rho_9\cos\phi + 4N\rho_8\rho_9\cos\psi + 2\rho_9^2, \end{aligned} \tag{2.23}$$

$$\begin{aligned} 0 = {} & 2\rho_2\rho_5 + 2\rho_1\rho_4\cos(\phi+\theta) + 2\rho_4^2\cos 2\theta + 2(N+3)\rho_4\rho_5\cos\theta + 4\rho_4\rho_9\cos\theta \\ & + 2\rho_5\rho_9 + \tfrac{1}{4}N\rho_9^2, \end{aligned} \tag{2.24}$$

$$\begin{aligned} 0 = {} & 2\rho_1\rho_5\cos\phi + 2\rho_2\rho_4\cos\theta + 2\rho_4^2\cos 2\theta + 2\rho_4\rho_5\cos\theta + (N+2)(\rho_4^2+\rho_5^2) \\ & + 4\rho_4\rho_9\cos\theta + 2\rho_5\rho_9 + \tfrac{1}{4}N\rho_9^2, \end{aligned} \tag{2.25}$$

$$0 = 2\rho_1\rho_4\cos(\phi-\theta) + 2\rho_2\rho_4\cos\theta + 2\rho_4^2, \tag{2.26}$$

$$\begin{aligned} 0 = {} & 2\rho_1\rho_7\cos\phi + 2\rho_2\rho_8\cos\psi + 2N\rho_7\rho_8\cos\psi + 2\rho_4\rho_9\cos\theta + 2\rho_7\rho_9 + 2\rho_8\rho_9\cos\psi \\ & + \tfrac{1}{4}(N+2)\rho_9^2, \end{aligned} \tag{2.27}$$

$$\begin{aligned} 0 = {} & 2\rho_1\rho_8\cos(\phi+\psi) + 2\rho_2\rho_7 + N(\rho_7^2+\rho_8^2) + 2\rho_4\rho_9\cos\theta + 2\rho_7\rho_9 + 2\rho_8\rho_9\cos\psi \\ & + \tfrac{1}{4}(N+2)\rho_9^2, \end{aligned} \tag{2.28}$$

$$
\begin{aligned}
0 = {} & 4\rho_8\rho_4 e^{i\psi}\cos\theta + 2e^{-2i\theta}\rho_4^2 + 2e^{-i\theta}\rho_5\rho_4 + 4\rho_7\rho_4\cos\theta + 2\rho_9\rho_4\cos\theta + \frac{1}{2}e^{-i\theta}N\rho_9\rho_4 \\
& + \frac{1}{2}N\rho_8\rho_9 e^{i\psi} + \left(\frac{N}{2}+1\right)\rho_5\rho_9 + \frac{1}{2}N\rho_7\rho_9 + 2\rho_5\rho_8 e^{i\psi} + \rho_1\rho_9\cos\phi + \rho_9^2 + 2\rho_5\rho_7 \\
& + \rho_2\rho_9, \qquad (2.29)
\end{aligned}
$$

$$
\begin{aligned}
0 = {} & 4\rho_4\rho_8\cos(\theta-\psi) + (M_N+3)\,\rho_8^2 + N^2\rho_{10}^2 + 2(N+1)\rho_8\rho_9\cos\psi + 6N\rho_8\rho_{10}\cos\psi \\
& + 4N\rho_7\rho_{10} + 8\rho_7\rho_8\cos\psi + 4\rho_8^2\cos 2\psi + 2\rho_1\rho_{10}\cos\phi + 2\rho_7^2 + \rho_9^2 + 2\rho_2\rho_{10} + 4\rho_9\rho_{10}, \qquad (2.30)
\end{aligned}
$$

$$
\begin{aligned}
0 = {} & 4\rho_1\rho_4 e^{-i(\theta+\phi)} + 4\rho_4\rho_9 e^{-i\theta} + 16\rho_4\rho_{10}\cos\theta + 2(M_N+1)\rho_1\rho_8 e^{-i(\psi+\phi)} + 4\rho_1\rho_8 e^{-i(\phi-\psi)} \\
& + 4\rho_1\rho_8\cos(\phi-\psi) + 2N^2\rho_8\rho_{10}e^{i\psi} + 4\left(2\cos\theta + e^{-i\theta}N\right)\rho_4\rho_8 e^{-i\psi} + N\left(2+4e^{2i\psi}\right)\rho_8^2 \\
& + 4N\rho_7\rho_8 e^{i\psi} + 4(N+1)\rho_5\rho_8 e^{-i\psi} + 2N\rho_1\rho_{10}e^{-i\phi} + 2(N+1)\rho_1\rho_9 e^{-i\phi} + 4N\rho_9\rho_{10} \\
& + 4\left(2\cos\psi + e^{i\psi}\right)\rho_8\rho_9 + 4\rho_2\rho_8\cos\psi + 4\rho_1\rho_7 e^{-i\phi} + 4\rho_5\rho_9 + 4\rho_7\rho_9 + 8\rho_5\rho_{10} \qquad (2.31)
\end{aligned}
$$

where M_N is given by

$$
M_N \equiv \frac{1}{2}N(N+1) - 1 \qquad (2.32)
$$

and coincides with the number of independent components of the order parameter variable (2.9). In table 2.2 different latin letters correspond to different values from 1 to N; we checked that no new constraints arise from different choices.

At this stage we did not yet take into account the fact that the field $Q_{ab}(x)$ that creates the particles is traceless. We do this now defining $\mathcal{T} = \sum_a aa$ and requiring the trace decoupling condition

$$
\mathbb{S}|(ab)\mathcal{T}\rangle = S_0|(ab)\mathcal{T}\rangle\,, \qquad S_0 = \pm 1 \qquad (2.33)
$$

for any particle state $|(ab)\rangle = |ab\rangle + |ba\rangle$. In other words, we require that the trace mode $\mathcal{T}$ is a noninteracting[2] (and then decoupled) particle that can be discarded, thus yielding the desired sector with $\mathrm{Tr}\, Q_{ab} = 0$. The condition (2.33) gives the relations

$$
\begin{aligned}
& S_2 + S_9 + NS_7 - S_0 = S_1 + S_9 + NS_{11} = S_3 + S_9 + NS_8 = \\
& \qquad 4(S_4 + S_5 + S_6) + NS_9 = S_7 + S_8 + S_{11} + NS_{10} = 0\,, \qquad (2.34)
\end{aligned}
$$

[2]The sign factor S_0 takes into account that the trace mode can decouple as a free boson or a free fermion.

Equation	μ	ν	ρ	σ
(2.21)	ab	cd	ab	cd
(2.22)	ab	cd	cd	ab
(2.23)	ab	ba	cd	dc
(2.24)	ab	bc	cd	da
(2.25)	ab	bc	ad	dc
(2.26)	ab	cd	ac	bd
(2.27)	aa	bc	bc	dd
(2.28)	aa	bc	dd	bc
(2.29)	aa	bc	bd	dc
(2.30)	aa	bb	cc	dd
(2.31)	aa	bb	cd	dc

Table 2.2: External indices used in (1.50) to obtain the equations (2.21)-(2.31).

which we use to express the amplitudes $S_{i\geq 7}$ in terms of $S_{i\leq 6}$, namely

$$\rho_7 = -\frac{1}{N}(\rho_2 - S_0) + \frac{4}{N^2}(2\rho_4 \cos\theta + \rho_5), \tag{2.35}$$

$$\rho_8 \cos\psi = -\frac{1}{N}\rho_1 \cos\phi + \frac{4}{N^2}(2\rho_4 \cos\theta + \rho_5), \tag{2.36}$$

$$\rho_8 \sin\psi = \frac{1}{N}\rho_1 \sin\phi, \tag{2.37}$$

$$\rho_9 = -\frac{4}{N}(2\rho_4 \cos\theta + \rho_5), \tag{2.38}$$

$$\rho_{10} = \frac{1}{N^2}\Big(2\rho_1 \cos\phi + \rho_2 - S_0 - \frac{12}{N}(2\rho_4 \cos\theta + \rho_5)\Big). \tag{2.39}$$

Upon substitution of these expressions in (2.21)-(2.31), the imaginary parts of (2.29) and (2.31) vanish, while the real parts as well as the equations (2.27), (2.28) and (2.30) become linear combinations of (2.21)-(2.26). The latter are the only remaining equations and can

Solution	N	ρ_1	ρ_2	$\cos\phi$	ρ_4	ρ_5	$\cos\theta$
$A1_\pm$	$(-\infty,\infty)$	0	±1	$-$	0	0	$-$
$A2_\pm$	$[-3,2]$	1	0	$\pm\frac{1}{2}\sqrt{2-M_N}$	0	0	$-$
A3	$-3,2$	$\sqrt{1-\rho_2^2}$	$[-1,1]$	0	0	0	$-$
B1	2	$\frac{1-\rho_2^2}{\sqrt{1+3\rho_2^2}}$	$[-1,1]$	$-\frac{2\rho_2}{\sqrt{1+3\rho_2^2}}$	$\lvert\rho_2\rvert\sqrt{\frac{1-\rho_2^2}{1+3\rho_2^2}}$	$\frac{\rho_2(1-\rho_2^2)}{1+3\rho_2^2}$	$-\mathrm{sgn}(\rho_2)\sqrt{\frac{1-\rho_2^2}{1+3\rho_2^2}}$
$B2_\pm$	2	$\sqrt{1+2x\rho_2-\rho_2^2}$	$\alpha_\pm(x)$	$\frac{x}{\sqrt{1+2x\rho_2-\rho_2^2}}$	$\sqrt{\frac{-x\rho_2}{2}}$	$\frac{-x}{2}$	$\frac{x+2\rho_2}{2\sqrt{-2x\rho_2}}$
$B3_\pm$	3	$\frac{2}{3}$	$\pm\frac{1}{3}$	∓1	$\frac{1}{3}$	$\pm\frac{1}{3}$	±1

Table 2.3: Analytic solutions of the equations (2.40)-(2.45). In the expression of $B2_\pm$, $x\in\left[-\frac{1}{\sqrt{2}}\frac{1}{\sqrt{2}}\right]$ is a free parameter, and $\alpha_\pm(x)\equiv x\,\frac{2x^2-3\pm\sqrt{2(x^2-4)(2x^2-1)}}{2(6x^2+1)}$.

be written in the form

$$1=\rho_1^2+\rho_2^2+4\rho_4^2\,, \tag{2.40}$$

$$0=2\rho_1\rho_2\cos\phi+4\rho_4^2\,, \tag{2.41}$$

$$\begin{aligned}0=\;&M_N\rho_1^2+2\rho_1^2\cos2\phi+2\rho_1\rho_2\cos\phi+4\left(1-\frac{2}{N}+N\right)\rho_1\rho_4\cos(\phi-\theta)\\&+4\left(1-\frac{2}{N}\right)\rho_1\rho_4\cos(\phi+\theta)+\frac{32}{N^2}\rho_4^2\cos2\theta+4\left(1-\frac{2}{N}+N\right)\rho_1\rho_5\cos\phi\\&+8\left(1+\frac{8}{N^2}\right)\rho_4\rho_5\cos\theta+4\left(1+\frac{8}{N^2}\right)\rho_4^2+4\left(1+\frac{4}{N^2}\right)\rho_5^2\,,\end{aligned} \tag{2.42}$$

$$\begin{aligned}0=\;&2\rho_2\rho_5+2\rho_1\rho_4\cos(\phi+\theta)-\frac{8}{N}\rho_4^2+2\left(1-\frac{4}{N}\right)\rho_4^2\cos2\theta\\&+2\left(3-\frac{8}{N}+N\right)\rho_4\rho_5\cos\theta-\frac{4}{N}\rho_5^2\,,\end{aligned} \tag{2.43}$$

$$\begin{aligned}0=\;&2\rho_2\rho_4\cos\theta+\left(2-\frac{8}{N}+N\right)\rho_4^2+2\left(1-\frac{4}{N}\right)\rho_4^2\cos2\theta+2\rho_1\rho_5\cos\phi\\&+2\left(1-\frac{8}{N}\right)\rho_4\rho_5\cos\theta+\left(2-\frac{4}{N}+N\right)\rho_5^2\,,\end{aligned} \tag{2.44}$$

$$0=2\rho_1\rho_4\cos(\phi-\theta)+2\rho_2\rho_4\cos\theta+2\rho_4^2\,. \tag{2.45}$$

The solutions of these equations yield the renormalization group fixed points of the RP^{N-1} model in two dimensions. Since the equations were obtained relying only on the symmetries of the Hamiltonian (2.8), their space of solutions contains the fixed points that arise in the ferromagnetic case ($J>0$) as well as in antiferromagnets ($J<0$).

2.4 Solutions

The solutions of the equations (2.40)-(2.45) that we could determine analytically are listed in appendix 2.A and summarized in table 2.3. The remaining solutions, which we determined numerically, are discussed in section 2.4.2 below.

Since for $\rho_4 = \rho_5 = 0$ the equations (2.40)-(2.45) reduce to (2.5)-(2.7) with $M = M_N$, the RP^{N-1} model possesses, in particular, the FPs of the $O(M_N)$ model. Notice that, for $\rho_4 = \rho_5 = 0$, equation (2.38) also implies $\rho_9 = 0$. Hence, for this class of solutions we have the vanishing of the amplidutes S_4, S_5, S_6 and S_9, namely of the amplitudes responsible for mixing indices coming from different particles (see figure 2.3). This is why in the following we refer to these solutions as nonmixing; they are all determined analytically.

On the other hand, not all solutions of equations (2.40)-(2.45) are nonmixing. We now discuss the different solutions, starting from the case $N = 2$.

2.4.1 $N = 2$

The equations (2.40)-(2.45) with $N = 2$ admit the solutions A3, B1 and B2 of appendix 2.A and table 2.3. The common feature of these solutions is that they possess a free parameter, so that each of them describes a line of fixed points at $N = 2$. The presence of a continuum of fixed points at $N = 2$ is expected due to the topological correspondence $RP^1 \sim O(2)$. The solution A3 directly corresponds to the $O(2)$ solution P3 of table 1.1, which we saw accounts for the BKT transition. We now see that the RP^1 fixed point equations also allow for the realization of such a transition via the mixing solutions B1 and B2. This results into several lines of fixed points meeting at the BKT transition point (figure 2.4). A similar concurrence of lines of fixed points at the BKT transition occurs in the Ashkin-Teller model, for which it was originally argued on perturbative grounds [88] and has recently been shown exactly [89].

2.4.2 Other solutions for $N < 3$

Besides the $N = 2$ solutions of the previous subsection, the other solutions with $N < 3$ of the fixed point equations (2.40)-(2.45) that we determined analytically are the solutions A1 and A2 of table 2.3. These are nonmixing solutions corresponding to P1 and P2, respectively, of the $O(M_N)$ case (see also appendix 2.B). The fact that M_N is quadratic

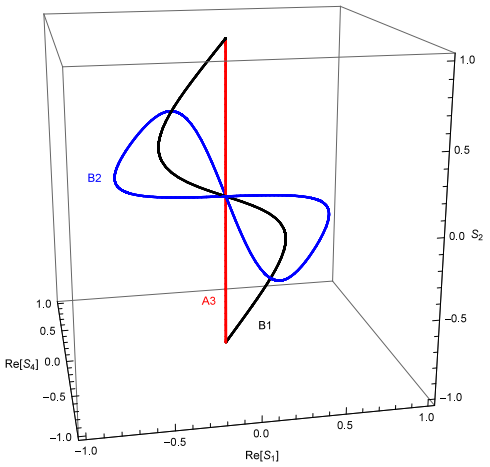

Figure 2.4: The $N = 2$ solutions A3, B1 and B2. They all meet at the BKT transition point.

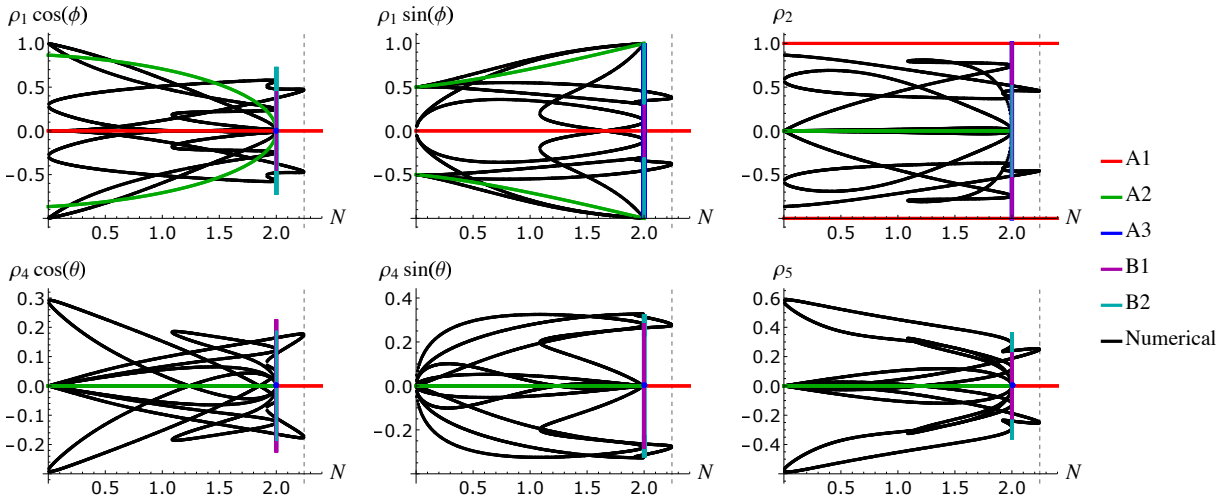

Figure 2.5: The solutions of the fixed point equations (2.40)-(2.45) in the interval $N \in (0, N^*)$, with $N^* = 2.24421..$ indicated by the dashed vertical line. The dotted lines correspond to numerical solutions, and the continuous ones to the analytic solutions of table 2.3.

in N is responsible for the fact that solution A3 exists also at $N = -3$ ($M_{-3} = M_2 = 2$), and that A2 extends down to $N = -3$.

Besides these analytic solutions, equations (2.40)-(2.45) admit for $N < 3$ solutions that we determined numerically. All these numerical solutions are of the mixing type (ρ_4 and/or ρ_5 nonzero) and turn out to extend up to a maximal value $N^* = 2.24421..$. These solutions do not possess free parameters for fixed N, and for $N = 2$ reduce to particular cases of the solutions discussed in the previous subsection. The numerical solutions form a rich pattern and are shown, together with the analytical ones, in figure 2.5 in the range $N \in (0, N^*)$.

Apart from the case $N = 2$, the fixed points for $N < 3$ only make sense from the point of view of the analytical continuation in N. This is true also for $N = 1$, since the RP^0 model possesses no degrees of freedom. On the other hand, the fixed points obtained for $N \to 1$ can have a physical meaning, in the same way that those obtained for $N \to 0$ in the $O(N)$ model are relevant for the critical behavior of self-avoiding walks.

2.4.3 $N \geq 3$

The rich pattern of fixed points with $N < 3$ visible in figure 2.5 has to be contrasted with the fact that solutions A1 and B3 of table 2.3 are the only ones existing for $N \geq 3$. The circumstance appears as a manifestation of the fact that continuous symmetries – integer values of $N > 1$ in the present case – cannot break spontaneously in two dimensions [65], thus confining criticality to zero temperature or to topological transitions. In the latter respect, the fact that the RP^{N-1} fixed point solutions do not allow for free parameters at fixed $N > 2$ excludes the presence in this range of BKT-like transitions yielding quasi-long-range order. The possibility of such a transition driven by disclination defects had been debated in numerical studies [75, 71, 72, 73, 76, 77, 78, 74, 79].

Solution A1 is the only one for $N > 3$. Its fermionic version $\mathrm{A1}_-$ is not expected to play a role for the RP^{N-1} Hamiltonian (2.8), so that we restrict our attention to $\mathrm{A1}_+$. This solution corresponds to solution $\mathrm{P1}_+$ of table 1.1, which describes a zero temperature fixed point in the $O(M_N)$ universality class. Hence, we see that the RP^{N-1} model allows for criticality displaying enhanced symmetry $O(M_N)$. On the other hand, we have to remember that the space of solutions in the scale invariant scattering framework contains the fixed points for both ferromagnetic and antiferromagnetic interactions, and that a single scattering solution can correspond to different fixed points (recall the discussion of section 1.5 for the Potts model). Hence, solution $\mathrm{A1}_+$ describes a zero temperature

fixed point, with the symmetry enhancement applying to the antiferromagnetic case[3], similarly to the Potts case of [40]. In any case, for $N \neq 2$ both the ferromagnetic and antiferromagnetic universality classes differ from the $O(N)$ universality class, since the RP^{N-1} and $O(N)$ order parameters have a different number of components.

These considerations are expected to apply for all N larger than 2. From this point of view, the existence for $N = 3$ – and only for this value – of the additional solution B3 is at first sight not easy to interpret. As a matter of fact, it can be checked that solution B3 is equivalent to solution A1, since it leads to the same scattering matrix (2.10). We will discuss in more detail other examples of this identification mechanism in the next chapter.

We finally mention that if, for $N \geq 2$, the square in (2.8) is replaced by a power p, a first order transition is known to arise when p becomes large enough [91, 92, 93, 94]. For the RP^{N-1} Hamiltonian (2.8) a first order transition was deduced for $N = \infty$ [95, 96] and debated for the case of N large [97, 98, 99], while it was shown to be absent in numerical simulations performed up to $N = 40$ [71]. Our results concern the fixed points of the renormalization group, at which the correlation length diverges, and do not add to the debate about the possibility of a first order transition at large N.

2.A Appendix. Analytic solutions

We give here the analytic solutions of the fixed point equations (2.40)-(2.45), using also (2.35)-(2.39) to express the amplitudes $S_{i>6}$.

- Solution A1a$_\pm$ is defined for $N \in \mathbb{R}$ and reads

$$\begin{aligned} &\rho_2 = S_0\,, \quad \rho_1 = \rho_4 = \rho_5 = 0, \\ &\rho_7 = \rho_8 = \rho_9 = \rho_{10} = 0. \end{aligned} \tag{2.46}$$

- Solution A1b$_\pm$ is defined for $N \in \mathbb{R}$ and reads

$$\begin{aligned} &\rho_2 = -S_0\,, \quad \rho_1 = \rho_4 = \rho_5 = 0, \\ &\rho_7 = \frac{2S_0}{N}\,, \quad \rho_8 = \rho_9 = 0\,, \quad \rho_{10} = -\frac{\rho_7}{N}. \end{aligned} \tag{2.47}$$

[3]In three dimensions the continuous symmetry can break spontaneously, and finite temperature criticality in the $O(5)$ universality class has been identified numerically for the RP^2 antiferromagnet on the cubic lattice [90].

- Solution A2$_\pm$ is defined for $N \in [-3, 2]$ and reads

$$\rho_1 = 1\,, \quad \cos\phi = (\pm)\frac{1}{2}\sqrt{2 - M_N}\,, \quad \sin\phi = (\pm)\frac{1}{2}\sqrt{2 + M_N}\,, \quad \rho_2 = \rho_4 = \rho_5 = 0,$$
$$\rho_7 = \frac{S_0}{N}\,, \quad \rho_8 = \frac{1}{|N|}\,, \quad \psi = \pi u(N) - \phi\,, \quad \rho_9 = 0\,, \quad \rho_{10} = \frac{2}{N^2}\rho_1\cos\phi - \frac{1}{N}\rho_7, \tag{2.48}$$

with $u(N) = \begin{cases} 1\,, & N \geq 0 \\ 0\,, & \text{otherwise.} \end{cases}$

Here and below, signs in parenthesis are both allowed.

- Solution A3$_\pm$ is defined for $N = -3, 2$ and reads

$$\begin{aligned} &\rho_1 = \sqrt{1 - \rho_2^2}\,, \quad \phi = (\pm)\frac{\pi}{2}\,, \quad \rho_2 \in [-1, 1]\,, \quad \rho_4 = \rho_5 = 0, \\ &\rho_7 = \frac{S_0}{N} - \frac{\rho_2}{N}\,, \quad \rho_8 = \frac{1}{|N|}\rho_1\,, \quad \psi = \mathrm{sgn(N)}\phi\,, \quad \rho_9 = 0\,, \quad \rho_{10} = -\frac{\rho_7}{N}. \end{aligned} \tag{2.49}$$

- Solution B1$_\pm$ is defined for $N = 2$ and reads

$$\rho_1 = \frac{1 - \rho_2^2}{\sqrt{1 + 3\rho_2^2}}\,, \quad \cos\phi = -\frac{2\rho_2}{\sqrt{1 + 3\rho_2^2}}\,, \quad \sin\phi = \pm\frac{\sqrt{1 - \rho_2^2}}{\sqrt{1 + 3\rho_2^2}}\,, \quad \rho_2 \in [-1, 1]\,,$$
$$\rho_4\cos\theta = -\frac{\rho_2(1 - \rho_2^2)}{1 + 3\rho_2^2}\,, \quad \rho_4\sin\theta = -\frac{2\rho_2^2}{1 - \rho_2^2}\rho_1\sin\phi\,, \quad \rho_5 = -\frac{1}{2}\rho_1\cos\phi\,,$$
$$\rho_7 = \frac{S_0}{2} - \frac{\rho_2}{2} - \rho_5\,, \quad \rho_8 = \frac{1}{2}\rho_1|\sin\phi|\,, \quad \psi = \pm\frac{\pi}{2}\,, \quad \rho_9 = 2\rho_5\,, \quad \rho_{10} = -\frac{\rho_7}{2}\,. \tag{2.50}$$

- Solution B2$_\pm$ is defined for $N = 2$ and reads

$$x \in \left[-\tfrac{1}{\sqrt{2}}, \tfrac{1}{\sqrt{2}}\right]\,, \quad y = (\pm)\sqrt{1 - (x - \rho_2)^2}\,, \quad \rho_2 = x\frac{2x^2 - 3 \pm \sqrt{2(x^2 - 4)(2x^2 - 1)}}{2(1 + 6x^2)}$$
$$u = \frac{x + 2\rho_2}{4}\,, \quad v = -\mathrm{sgn(y)}\sqrt{-\frac{x\rho_2}{2} - \left(\frac{x + 2\rho_2}{4}\right)^2}\,, \quad \rho_5 = -\frac{x}{2}\,, \tag{2.51}$$
$$\rho_7 = \frac{S_0}{2} + \frac{\rho_2}{2}\,, \quad p = \rho_2 + \rho_5\,, \quad q = \frac{y}{2}\,, \quad \rho_9 = -2\rho_2\,, \quad \rho_{10} = -\frac{\rho_7}{2} - p\,,$$

where $x = \rho_1\cos\phi$, $y = \rho_1\sin\phi$, $u = \rho_4\cos\theta$, $v = \rho_4\sin\theta$, $p = \rho_8\cos\psi$, $q = \rho_8\sin\psi$.

S'_1 S'_2 S'_3 S'_4 S'_5 S'_6 S'_7

Figure 2.6: Scattering processes of a vector particle multiplet (continuous lines) and a scalar particle (dashed lines). Time runs upwards.

- Solution B3$_\pm$ is defined for $N = 3$ and reads

$$\begin{aligned} &\rho_1 = \frac{2}{3}\,, \quad \phi = \pi - \theta = \pi - \psi = \frac{\pi}{2} \pm \frac{\pi}{2}\,, \quad \rho_2 = \pm\frac{1}{3}\,, \quad \rho_4 = \frac{1}{3}\,, \quad \rho_5 = \rho_2, \\ &\rho_7 = \frac{S_0}{3} + \rho_2\,, \quad \rho_8 = \rho_1\,, \quad \rho_9 = \mp\frac{4}{3}\,, \quad \rho_{10} = \frac{\rho_9 - \rho_7}{3}. \end{aligned} \tag{2.52}$$

The results for the scattering parameters entering equation (2.40)-(2.45) are summarized in table 2.3. We show in the next appendix that solutions (2.46) and (2.47) only differ for the trace mode decoupling as a free boson or a free fermion; for this reason they both appear as solution A1 in table 2.3.

2.B Appendix. Rewriting nonmixing solutions

In this appendix we show how the nonmixing ($\rho_4 = \rho_5 = \rho_9 = 0$) solutions of the RP^{N-1} fixed point equations can be written as those of a system consisting of a $O(M_N)$ vector and a scalar that are decoupled. The scattering amplitudes for such a system, in which the vector and the scalar in general interact [89], are shown in figure 2.6 and take the form

$$S'_1 = S'^*_3 \equiv \rho'_1 e^{i\phi'}, \tag{2.53}$$

$$S'_2 = S'^*_2 \equiv \rho'_2, \tag{2.54}$$

$$S'_4 = S'^*_6 \equiv \rho'_4 e^{i\theta'}, \tag{2.55}$$

$$S'_5 = S'^*_5 \equiv \rho'_5, \tag{2.56}$$

$$S'_7 = S'^*_7 \equiv \rho'_7, \tag{2.57}$$

where ρ'_1 and ρ'_4 are non negative, while ρ'_2, ρ'_5, ρ'_7, ϕ' and θ' are real.

For the purpose of the mapping, we reorganize the particles $\mu = ab$ of the RP^{N-1} model into the new basis

$$|\Phi_\mu\rangle = \begin{cases} |\Phi_0\rangle = \frac{1}{N}\sum_{a=1}^{N}|aa\rangle \\ \frac{1}{\sqrt{2}}\left(|ab\rangle + |ba\rangle\right), \quad \mu = (ab), \;\; a \neq b \\ \frac{1}{\sqrt{k(k+1)}}\left(\sum_{j=1}^{k}|jj\rangle - k|(k+1)(k+1)\rangle\right), \quad \mu = kk, \;\; k = 1, \ldots N-1 \end{cases} \tag{2.58}$$

with $\langle\Phi_\mu|\Phi_\nu\rangle = \delta_{\mu\nu}$ and the trace mode Φ_0 playing the role of the scalar of the vector-scalar system. Then, in the nonmixing case, the RP^{N-1} scattering matrix can be expressed as

$$\begin{aligned} S^{\rho,\sigma}_{\mu,\nu} = &\left(S'_1\delta_{\mu,\nu}\delta^{\rho,\sigma} + S'_2\delta^\rho_\mu\delta^\sigma_\nu + S'_3\delta^\sigma_\mu\delta^\rho_\nu\right)\bar{\delta}^0_\mu\bar{\delta}^0_\nu\bar{\delta}^\rho_0\bar{\delta}^\sigma_0 + S'_4(\delta_{\mu,\nu}\delta^\rho_0\delta^\sigma_0 + \delta^0_\mu\delta^0_\nu\delta^{\rho,\sigma}) \\ &+ S'_5\delta^0_\mu\delta^0_\nu\delta^\rho_0\delta^\sigma_0 + S'_6(\delta^\sigma_\mu\delta^0_\nu\delta^\rho_0 + \delta^0_\mu\delta^\sigma_0\delta^\rho_\nu) + S'_7(\delta^\rho_\mu\delta^0_\nu\delta^\sigma_0 + \delta^0_\mu\delta^\rho_0\delta^\sigma_\nu), \end{aligned} \tag{2.59}$$

where $\bar{\delta}^\nu_\mu = 1 - \delta^\nu_\mu$ and

$$S'_1 = \langle\Phi_\nu\Phi_\nu|\mathbb{S}|\Phi_\mu\Phi_\mu\rangle = S_1, \tag{2.60}$$

$$S'_2 = \langle\Phi_\mu\Phi_\nu|\mathbb{S}|\Phi_\mu\Phi_\nu\rangle = S_2, \tag{2.61}$$

$$S'_3 = \langle\Phi_\nu\Phi_\mu|\mathbb{S}|\Phi_\mu\Phi_\nu\rangle = S_3, \tag{2.62}$$

$$S'_4 = \langle\Phi_0\Phi_0|\mathbb{S}|\Phi_\mu\Phi_\mu\rangle = \langle\Phi_\nu\Phi_\nu|\mathbb{S}|\Phi_0\Phi_0\rangle = S_1 + NS_{11}, \tag{2.63}$$

$$S'_5 = \langle\Phi_0\Phi_0|\mathbb{S}|\Phi_0\Phi_0\rangle = S_1 + S_2 + S_3 + 2N(S_7 + S_8 + S_{11}) + N^2S_{10}, \tag{2.64}$$

$$S'_6 = \langle\Phi_\mu\Phi_0|\mathbb{S}|\Phi_0\Phi_\mu\rangle = \langle\Phi_0\Phi_\nu|\mathbb{S}|\Phi_\nu\Phi_0\rangle = S_3 + NS_8, \tag{2.65}$$

$$S'_7 = \langle\Phi_0\Phi_\mu|\mathbb{S}|\Phi_0\Phi_\mu\rangle = \langle\Phi_\nu\Phi_0|\mathbb{S}|\Phi_\nu\Phi_0\rangle = S_2 + NS_7. \tag{2.66}$$

The condition (2.34) translate into the relations

$$S'_4 = S'_6 = 0 \;, \;\; S'_5 = S'_7 = S_0, \tag{2.67}$$

which express the decoupling between the vector and the scalar (see figure 2.6, recalling that $S_0 = \pm 1$). The explicit form of the RP^{N-1} nonmixing solutions in terms of the vector-scalar amplitudes is given in table 2.4. Notice, in particular, that solutions $\mathrm{A1a}_\pm$ and $\mathrm{A1b}_\mp$ only differ for the fermionic or bosonic nature of the decoupled scalar.

Solution	N	ρ_1'	ρ_2'	$\cos\phi'$	ρ_4'	$\cos\theta'$	ρ_5'	ρ_7'
$\mathrm{A1a}_\pm$	$\mathbb{R}$	0	S_0	$-$	0	$-$	S_0	S_0
$\mathrm{A1b}_\pm$	$\mathbb{R}$	0	$-S_0$	$-$	0	$-$	S_0	S_0
$\mathrm{A2}_\pm$	$[-2,2]$	1	0	$(\pm)\frac{1}{2}\sqrt{2-M_N}$	0	$-$	S_0	S_0
$\mathrm{A3}_\pm$	2	$\sqrt{1-\rho_2^2}$	$[-1,1]$	0	0	$-$	S_0	S_0

Table 2.4: Mapping between nonmixing RP^{N-1} solutions and decoupled vector-scalar solutions. Signs in parenthesis are both allowed.

Chapter 3

Critical points in the CP^{N-1} model

In this chapter we use scale invariant scattering theory to obtain the exact equations determining the renormalization group fixed points of the two-dimensional CP^{N-1} model, for N real. Also due to special degeneracies at $N = 2$ and 3, the space of solutions for $N \geq 2$ allows only for zero temperature criticality. For $N < 2$ the space of solutions becomes larger, with the appearance of new branches of fixed points relevant for criticality in gases of intersecting loops

3.1 Fixed point equations

We consider the basic lattice model with a continuous – $U(1)$ – local symmetry, namely the CP^{N-1} model realized in terms of complex N-component spin vectors at lattice sites. In two dimensions, this model has been studied in the high energy context (since [100, 101, 102]) for the similarities – in particular asymptotic freedom – which it shares with quantum chromodynamics, in statistical mechanics in relation with loop gases [103], and in condensed matter in relation with quantum antiferromagnets (see e.g. [98]). The remarks that we made in the previous chapter for RP^{N-1} concerning the continuous nature of the symmetry, zero temperature criticality, the possibility of topological transitions, and the absence of previous exact results, apply to CP^{N-1} as well. We then turn to the search of critical points within the scattering framework of section 1.3.2. For this purpose, we denote by $\mu = 1, 2, \ldots k$ the particle species, by $\mathbb{S}$ the scattering operator, and by $S^{\rho\sigma}_{\mu\nu} = \langle \rho\sigma|\mathbb{S}|\mu\nu\rangle$ the scattering amplitude for a process with particles μ and ν in the initial state and particles ρ and σ in the final state (figure 2.1). Taking into account that

in this chapter we will deal with particles that are not self-conjugated, the unitarity and crossing equations take the form (2.2) and

$$S_{\mu\nu}^{\rho\sigma} = \left[S_{\mu\bar{\sigma}}^{\rho\bar{\nu}}\right]^* , \tag{3.1}$$

respectively, where we denote by $\bar{\mu}$ the antiparticle of μ. Invariance under charge conjugation, time reversal and spatial inversion provides the relations

$$S_{\mu\nu}^{\rho\sigma} = S_{\bar{\mu}\bar{\nu}}^{\bar{\rho}\bar{\sigma}} = S_{\nu\mu}^{\sigma\rho} = S_{\rho\sigma}^{\mu\nu} . \tag{3.2}$$

The CP^{N-1} lattice model is defined by the Hamiltonian

$$\mathcal{H}_{CP^{N-1}} = -J \sum_{\langle i,j \rangle} |\mathbf{s}_i \cdot \mathbf{s}_j^*|^2, \tag{3.3}$$

where $\mathbf{s}_j$ is a N-component complex vector at site j satisfying $\mathbf{s}_j \cdot \mathbf{s}_j^* = 1$. The Hamiltonian (3.3) is invariant under global $U(N)$ transformations ($\mathbf{s}_j \to U\mathbf{s}_j$, $U \in U(N)$) and site-dependent $U(1)$ transformations ($\mathbf{s}_j \to e^{i\alpha_j}\mathbf{s}_j$, $\alpha_j \in \mathbb{R}$). These symmetries are represented through the tensorial order parameter variable

$$Q_i^{ab} = s_i^a (s_i^b)^* - \frac{1}{N}\delta_{ab} . \tag{3.4}$$

The presence of an invariant linear in the order parameter components is excluded by the constraint $\mathbf{s}_j \cdot \mathbf{s}_j^* = 1$, which in turn makes Q_i^{ab} traceless.

In order to implement scale invariant scattering for the two-dimensional CP^{N-1} model we first of all observe that in the continuum limit the order parameter field is the Hermitian tensor $Q_{ab}(x)$, which creates particles that we label by $\mu = ab$, with a and b taking values from 1 to N. A state containing a particle ab transforms under the $U(N)$ symmetry as

$$|ab\rangle \longrightarrow |a'b'\rangle = \sum_{a,b} U_{a',a} U_{b',b}^* |ab\rangle , \tag{3.5}$$

so that a scattering amplitude $S_{ab,cd}^{ef,gh} = \langle ef, gh|\mathbb{S}|ab, cd\rangle$ with particles ab and cd in the initial state and particles ef and gh in the final state transforms into

$$S_{a'b',c'd'}^{e'f',g'h'} = \sum_{a,b,c,d} \sum_{e,f,g,h} U_{a',a} U_{b',b}^* U_{c',c} U_{d',d}^* U_{e',e}^* U_{f',f} U_{g',g}^* U_{h',h} S_{ab,cd}^{ef,gh} . \tag{3.6}$$

Taking also into account the massless limit of the relations (1.40), (1.41) and (1.42), which can now be written as

$$S_{ab,cd}^{ef,gh} = S_{ba,dc}^{fe,hg} = S_{cd,ab}^{gh,ef} = S_{ef,gh}^{ab,cd} , \tag{3.7}$$

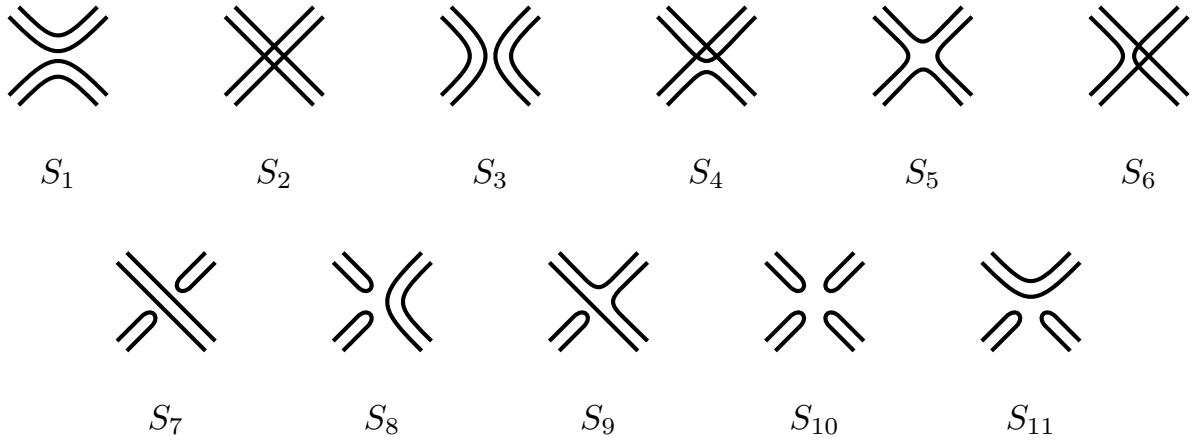

Figure 3.1: Amplitudes entering (3.8). Time runs upwards

$U(N)$-invariance corresponds to

$$\begin{aligned}
S^{ef,gh}_{ab,cd} = {} & S_1\,\delta_{a,d}\delta_{b,c}\delta_{e,h}\delta_{f,g} + S_2\,\delta_{a,e}\delta_{b,f}\delta_{c,g}\delta_{d,h} + S_3\,\delta_{a,g}\delta_{b,h}\delta_{c,e}\delta_{d,f} \\
& + S_4\,(\delta_{a,d}\delta_{b,f}\delta_{c,g}\delta_{e,h} + \delta_{b,c}\delta_{a,e}\delta_{d,h}\delta_{f,g}) + S_5\,(\delta_{b,c}\delta_{a,g}\delta_{d,f}\delta_{e,h} + \delta_{a,d}\delta_{b,h}\delta_{c,e}\delta_{f,g}) \\
& + S_6\,(\delta_{a,e}\delta_{b,h}\delta_{d,f}\delta_{c,g} + \delta_{b,f}\delta_{a,g}\delta_{c,e}\delta_{d,h}) + S_7\,(\delta_{a,b}\delta_{e,f}\delta_{c,g}\delta_{d,h} + \delta_{c,d}\delta_{g,h}\delta_{a,e}\delta_{b,f}) \\
& + S_8\,(\delta_{c,d}\delta_{e,f}\delta_{a,g}\delta_{b,h} + \delta_{a,b}\delta_{g,h}\delta_{c,e}\delta_{d,f}) + S_9\big[\delta_{e,f}\,(\delta_{a,d}\delta_{b,h}\delta_{c,g} + \delta_{b,c}\delta_{a,g}\delta_{d,h}) \\
& \qquad + \delta_{c,d}\,(\delta_{b,f}\delta_{a,g}\delta_{e,h} + \delta_{a,e}\delta_{b,h}\delta_{f,g})\,\delta_{a,b}\,(\delta_{d,f}\delta_{c,g}\delta_{e,h} + \delta_{c,e}\delta_{d,h}\delta_{f,g}) \\
& \qquad + \delta_{g,h}\,(\delta_{a,d}\delta_{b,f}\delta_{c,e} + \delta_{b,c}\delta_{a,e}\delta_{d,f})\big] + S_{10}\,\delta_{a,b}\delta_{c,d}\delta_{e,f}\delta_{g,h} \\
& + S_{11}\,(\delta_{a,b}\delta_{c,d}\delta_{e,h}\delta_{f,g} + \delta_{e,f}\delta_{g,h}\delta_{a,d}\delta_{b,c})\ ,
\end{aligned} \tag{3.8}$$

with amplitudes $S_1, \ldots, S_{11}$ depicted in figure 3.1. In this figure each incoming or outgoing particle has two terminals corresponding to its two indices, and a line connecting two indices corresponds to a Kronecker delta identifying them.

Crossing symmetry (1.51) translates into

$$S^{ef,gh}_{ab,cd} = \left[S^{ef,dc}_{ab,hg}\right]^* . \tag{3.9}$$

The crossing equations for the amplitudes $S_{i\leq 3}$ preserve the form (1.53) and (1.54), and we keep for these amplitudes the same parametrization in terms of ρ_1, ρ_2 and ϕ. The crossing relations and the corresponding parametrizations for the remaining amplitudes

are the ones given in equations

$$S_4 = S_6^* \equiv \rho_4 e^{i\theta}, \tag{3.10}$$

$$S_5 = S_5^* \equiv \rho_5, \tag{3.11}$$

$$S_7 = S_7^* \equiv \rho_7, \tag{3.12}$$

$$S_8 = S_{11}^* \equiv \rho_8 e^{i\psi}, \tag{3.13}$$

$$S_9 = S_9^* \equiv \rho_9, \tag{3.14}$$

$$S_{10} = S_{10}^* \equiv \rho_{10}\,, \tag{3.15}$$

The unitarity condition (1.50) can be written as

$$\sum_{i,j=1}^{N} \sum_{k,l=1}^{N} S_{ab,cd}^{ij,kl} \left[S_{ij,kl}^{ef,gh} \right]^* = \delta_{a,e}\delta_{b,f}\delta_{c,g}\delta_{d,h}\,, \tag{3.16}$$

and gives rise to the 11 independent equations

$$1 = \rho_1^2 + \rho_2^2 + 2\rho_4^2, \tag{3.17}$$

$$0 = 2\rho_1\rho_2\cos\phi + 2\rho_4^2, \tag{3.18}$$

$$\begin{aligned} 0 = {} & N^2\rho_1^2 + 2\rho_1^2\cos 2\phi + 2\rho_1\rho_2\cos\phi + 4N\rho_1\rho_4\cos(\theta-\phi) + 4N\rho_1\rho_5\cos\phi \\ & + 2\rho_4^2 + 4\rho_4\rho_5\cos\theta + 2\rho_5^2 + 2N\rho_1\rho_8\cos(\psi+\phi) + 8\rho_1\rho_9\cos\phi + 4\rho_5\rho_8\cos\psi \\ & + 8\rho_4\rho_8\cos\theta\cos\psi + 8N\rho_8\rho_9\cos\psi + N^2\rho_8^2 + 8\rho_9^2 \end{aligned} \tag{3.19}$$

$$0 = 2\rho_1\rho_5\cos\phi + 2\rho_2\rho_4\cos\theta + N\rho_4^2 + N\rho_5^2 + 8\rho_4\rho_9\cos\theta + 4\rho_5\rho_9 + 2N\rho_9^2, \tag{3.20}$$

$$0 = 2\rho_1\rho_4\cos(\theta+\phi) + 2\rho_2\rho_5 + 2N\rho_4\rho_5\cos\theta + 8\rho_4\rho_9\cos\theta + 4\rho_5\rho_9 + 2N\rho_9^2, \tag{3.21}$$

$$0 = 2\rho_1\rho_4\cos(\theta-\phi) + 2\rho_2\rho_4\cos\theta, \tag{3.22}$$

$$0 = 2\rho_1\rho_8\cos(\psi+\phi) + 2\rho_2\rho_7 + 4\rho_9(\rho_4\cos\theta + \rho_7 + \rho_8\cos\psi) + N(\rho_7^2 + \rho_8^2 + 2\rho_9^2), \tag{3.23}$$

Equation	μ	ν	ρ	σ
(3.17)	ab	cd	ab	cd
(3.18)	ab	cd	cd	ab
(3.19)	ab	ba	cd	dc
(3.20)	ab	bc	ad	dc
(3.21)	ab	bc	dc	ad
(3.22)	ab	cd	ad	cb
(3.23)	aa	cd	bb	cd
(3.24)	aa	cd	cd	bb
(3.25)	aa	cd	bd	cb
(3.26)	aa	bb	dd	cc
(3.27)	aa	bb	cd	dc

Table 3.1: External indices used in (1.50), (3.16) to obtain the unitarity equations (3.17)-(3.27).

$$0 = 2\rho_1\rho_7\cos\phi + 2\rho_2\rho_8\cos\psi + 4\rho_9(\rho_4\cos\theta + \rho_7 + \rho_8\cos\psi) + 2N(\rho_7\rho_8\cos\psi + \rho_9^2), \tag{3.24}$$

$$\begin{aligned} 0 = {} & 2\rho_1\rho_9\cos\phi + 2\rho_2\rho_9 + \rho_4^2 e^{-2i\theta} + \rho_4\rho_5 e^{-i\theta} + 2\rho_4\rho_7\cos\theta + 2\rho_4\rho_8 e^{i\psi}\cos\theta \\ & + N\rho_4\rho_9 e^{-i\theta} + \rho_5\rho_7 + \rho_5\rho_8 e^{i\psi} + N\rho_5\rho_9 + N\rho_7\rho_9 + N\rho_8\rho_9 e^{i\psi} + 4\rho_9^2, \end{aligned} \tag{3.25}$$

$$\begin{aligned} 0 = {} & 2\rho_1\rho_{10}\cos\phi + 2\rho_2\rho_{10} + 4\rho_4\rho_8\cos(\theta-\psi) + 8\rho_7\rho_8\cos\psi + 4N\rho_7\rho_{10} + 6N\rho_8\rho_{10}\cos\psi \\ & + 2\rho_7^2 + 4\rho_8^2\cos 2\psi + \left(N^2+2\right)\rho_8^2 + 8N\rho_8\rho_9\cos\psi + 8\rho_9^2 + 8\rho_9\rho_{10} + N^2\rho_{10}^2, \end{aligned} \tag{3.26}$$

$$\begin{aligned} 0 = {} & 2\rho_1\rho_4 e^{-i(\theta+\phi)} + 4e^{-i\theta}\rho_4\rho_9 + 2e^{-i\theta}\rho_4\rho_{10} + 2e^{i\theta}\rho_4\rho_{10} + N^2\rho_8\rho_{10}e^{i\psi} + N^2\rho_1\rho_8 e^{-i(\psi+\phi)} \\ & + 2N\rho_4\rho_8 e^{-i(\theta+\psi)} + 2N\rho_8^2 e^{2i\psi} + 2N\rho_5\rho_8 e^{-i\psi} + 2N\rho_7\rho_8 e^{i\psi} + 4N\rho_1\rho_9 e^{-i\phi} \\ & + N\rho_1\rho_{10}e^{-i\phi} + N\rho_8^2 + 4N\rho_9\rho_{10} + \rho_2\rho_8 e^{-i\psi} + \rho_2\rho_8 e^{i\psi} + 4\rho_8\rho_9 e^{-i\psi} + 8\rho_8\rho_9 e^{i\psi} \\ & + \rho_1\rho_8 e^{i(\phi-\psi)} + 3\rho_1\rho_8 e^{i(\psi-\phi)} + 2\rho_1\rho_7 e^{-i\phi} + 4\rho_5\rho_9 + 4\rho_7\rho_9 + 2\rho_5\rho_{10}\,. \end{aligned} \tag{3.27}$$

The choices of the indices yielding these equations are given in table 3.1, where the notation ab implies $a \neq b$; we checked that no new constraints arise from different choices.

We still need to take into account that the field $Q_{ab}(x)$ that creates the particles is

traceless. We do this requiring that the trace mode

$$\mathcal{T} = \sum_{a=1}^{N} aa \tag{3.28}$$

does not interact with the generic particle cd and can be discarded. This corresponds to

$$\mathbb{S}|\mathcal{T}cd\rangle = S_0|\mathcal{T}cd\rangle\,, \qquad S_0 = \pm 1, \tag{3.29}$$

where the sign factor S_0 takes into account that the trace mode can decouple as a boson or a fermion. The last equation translates into $\sum_a S^{ef,gh}_{aa,cd} = S_0\delta_{ef}\delta_{cg}\delta_{dh}$ and yields the relations

$$S_0 = \rho_2 + N\rho_7 + 2\rho_9, \tag{3.30}$$

$$0 = \rho_1 e^{i\phi} + N\rho_8 e^{-i\psi} + 2\rho_9, \tag{3.31}$$

$$0 = 2\rho_4\cos\theta + \rho_5 + N\rho_9, \tag{3.32}$$

$$0 = \rho_7 + 2\rho_8\cos\psi + N\rho_{10}\,. \tag{3.33}$$

These can be used to express $S_{i\geq 7}$ in terms of $S_{i\leq 6}$ through

$$\rho_7 = \tfrac{1}{N}\left(S_0 - \rho_2 + \tfrac{2}{N}\big(2\rho_4\cos\theta + \rho_5\big)\right), \tag{3.34}$$

$$\rho_8\cos\psi = \tfrac{1}{N}\left(-\rho_1\cos\phi + \tfrac{2}{N}\big(2\rho_4\cos\theta + \rho_5\big)\right), \tag{3.35}$$

$$\rho_8\sin\psi = \tfrac{1}{N}\rho_1\sin\phi, \tag{3.36}$$

$$\rho_9 = -\tfrac{1}{N}\big(2\rho_4\cos\theta + \rho_5\big), \tag{3.37}$$

$$\rho_{10} = \tfrac{1}{N^2}\left(2\rho_1\cos\phi + \rho_2 - S_0 - \tfrac{6}{N}\big(2\rho_4\cos\theta + \rho_5\big)\right). \tag{3.38}$$

When substituting (3.34)-(3.38) in (3.17)-(3.27), the imaginary parts of (3.25) and (3.27) vanish, while their real parts as well as (3.23), (3.24), (3.26) become linear combinations of the first six equations. This reduces the unitarity equations (3.17)-(3.27) to six

Solutions	N	ρ_1	ρ_2	$\cos\phi$	ρ_4	ρ_5	$\cos\theta$
$A1_\pm$	$\mathbb{R}$	0	±1	$-$	0	0	$-$
$A2_\pm$	$[-\sqrt{3},\sqrt{3}]$	1	0	$\pm\frac{1}{2}\sqrt{3-N^2}$	0	0	$-$
$A3_\pm$	$\pm\sqrt{3}$	$\sqrt{1-\rho_2^2}$	$[-1,1]$	0	0	0	$-$
$B_\pm$	3	$\frac{1}{2}$	$\pm\frac{1}{2}$	∓1	$\frac{1}{2}$	ρ_2	±1

Table 3.2: Analytic solutions of the CP^{N-1} fixed point equations (3.39)-(3.44).

independent equations given by

$$1 = \rho_1^2 + \rho_2^2 + 2\rho_4^2\,, \tag{3.39}$$

$$0 = 2\rho_1\rho_2\cos\phi + 2\rho_4^2\,, \tag{3.40}$$

$$\begin{aligned} 0 = {} & (N^2-1)\rho_1^2 + 2\rho_1^2\cos 2\phi + 2\rho_1\rho_2\cos\phi + 4\left(N-\tfrac{1}{N}\right)\rho_1\left(\rho_4\cos(\theta-\phi)+\rho_5\cos\phi\right) \\ & - \tfrac{4}{N}\rho_1\rho_4\cos(\theta+\phi) + \tfrac{8}{N^2}\rho_4^2\cos 2\theta + 2\left(1+\tfrac{4}{N^2}\right)\rho_4\left(\rho_4+2\rho_5\cos\theta\right) \\ & + 2\left(1+\tfrac{2}{N^2}\right)\rho_5^2\,, \end{aligned} \tag{3.41}$$

$$\begin{aligned} 0 = {} & 2\rho_1\rho_5\cos\phi + 2\rho_2\rho_4\cos\theta - \tfrac{4}{N}\rho_4^2\cos 2\theta + \left(N-\tfrac{4}{N}\right)\rho_4^2 - \tfrac{8}{N}\rho_4\rho_5\cos\theta \\ & + \left(N-\tfrac{2}{N}\right)\rho_5^2\,, \end{aligned} \tag{3.42}$$

$$0 = 2\rho_1\rho_4\cos(\theta+\phi) + 2\rho_2\rho_5 - \tfrac{4}{N}\rho_4^2\cos 2\theta - \tfrac{4}{N}\rho_4^2 + 2\left(N-\tfrac{4}{N}\right)\rho_4\rho_5\cos\theta - \tfrac{2}{N}\rho_5^2\,, \tag{3.43}$$

$$0 = 2\rho_1\rho_4\cos(\theta-\phi) + 2\rho_2\rho_4\cos\theta\,. \tag{3.44}$$

The solutions of these equations, which we discuss in the next section, correspond to the renormalization group fixed points with CP^{N-1} symmetry in two dimensions. As in the previous chapter, since we derived the equations relying only on the symmetries of the Hamiltonian (3.3), the space of solutions contains both the fixed points of the ferromagnetic case ($J > 0$) and those of the antiferromagnetic case ($J < 0$).

3.2 Solutions

The solutions of the equations (3.39)-(3.44) that we determined analytically are listed in appendix 3.A and summarized in table 3.2. The remaining solutions, which we dermined numerically for $N > 0$, are shown in figure 3.2 together with the analytical ones. The figure shows values of N up to 2, since it turns out that only the solutions A1 and B exists beyond this value. Another visualization of the solutions is given in figure 3.3.

We start the discussion of the solutions observing that when $\rho_4 = \rho_5 = 0$ equations (3.39)-(3.44) reduce to the equations (1.55)-(1.57) of the $O(M = N^2 - 1)$ model[1]. As a consequence, the CP^{N-1} model contains in particular the fixed points of the $O(N^2 - 1)$ model. The solutions A1, A2 and A3 of table 2.3 as corresponding to the $O(M = N^2 - 1)$ solutions P1, P2 and P3, respectively, of table 1.2. The fact that $N^2 - 1 = 2$ when $N = \pm\sqrt{3}$ explains the domain of definition of solutions A2 and A3.

Since continuous symmetries do not break spontaneously in two dimensions [65], the Hamiltonian (3.3) is expected to possess only a zero temperature fixed point for $N \geq 2$. For $N > 3$ we only have solution[2] A1, which corresponds in particular to an $O(N^2 - 1)$ zero temperature fixed point and to a symmetry enhancement. However, as we did in the previous chapter for the RP^{N-1} case, we have to recall that the space of solutions contains both ferromagnetic and antiferromagnetic fixed points, and that the a single solution can correspond to different fixed points. Hence, solution A1 describes both the ferromagnetic and the antiferromagnetic zero temperature fixed points, with symmetry enhancement applying to the antiferromagnetic case[3] (as for the Potts model [40]).

For $N = 3$ the situation is apparently complicated by the existence of solution B. However, while solutions A1 and B clearly differ at the level of the amplitudes $S_1, \ldots, S_{11}$, it can be checked that they yield the same scattering matrix (3.8). Hence, through the same mechanism we illustrated in the end of section 1.4 for the Ising model, the solutions A1 and B of the CP^2 model are equivalent at $N = 3$. This is possible because for $N < 4$ the particle indices do not take enough different values to make physically distinguishable all the terms entering the decomposition (3.8).

Having clarified what happens for $N > 2$, let us now consider $N = 2$. Figures 3.2 and 3.3 show that $N = 2$ is the value at which several pairs of solutions existing for $N < 2$ meet and terminate. The list of solutions at $N = 2$ is given in table 3.3 in appendix 3.A. Such a proliferation is at first sight problematic, since we already argued that for $N \geq 2$ the Hamiltonian (3.3) should possess only a zero temperature critical point. This is also fully consistent with the fact that CP^1 corresponds to the Riemann sphere, and

[1] $N^2 - 1$ is the number of independent real components of the order parameter variable (3.4).

[2] When discussing the Hamiltonian (3.3) we refer to the bosonic realization $A1_+$ of the symmetry. The fermionic realization $A1_-$ is not relevant for that Hamiltonian.

[3] In three dimensions, where the symmetry can break spontaneously, a finite temperature critical point in the $O(8)$ universality class has been observed in numerical simulations of the antiferromagnetic CP^2 model [104].

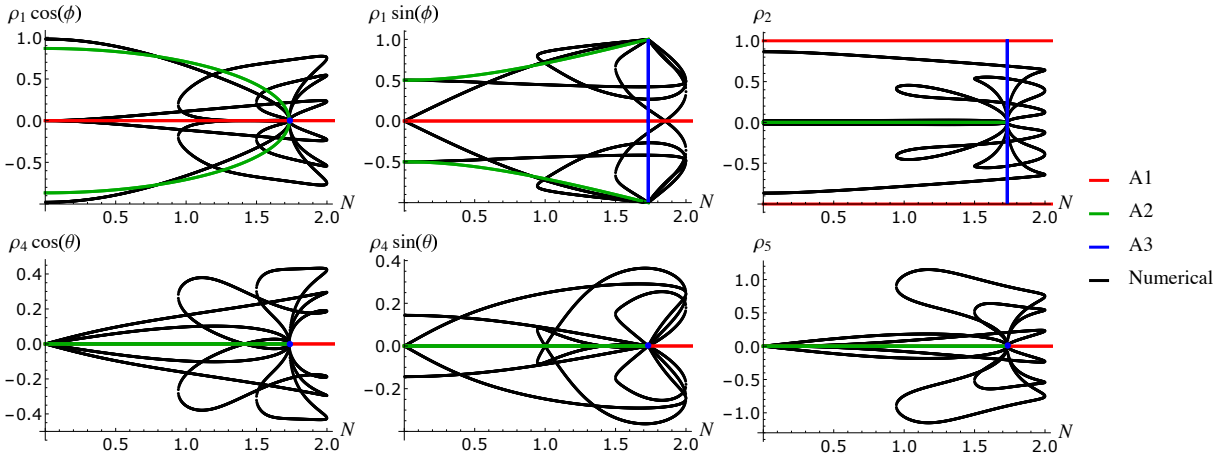

Figure 3.2: Solutions of the CP^{N-1} fixed point equations (2.40)-(2.45).

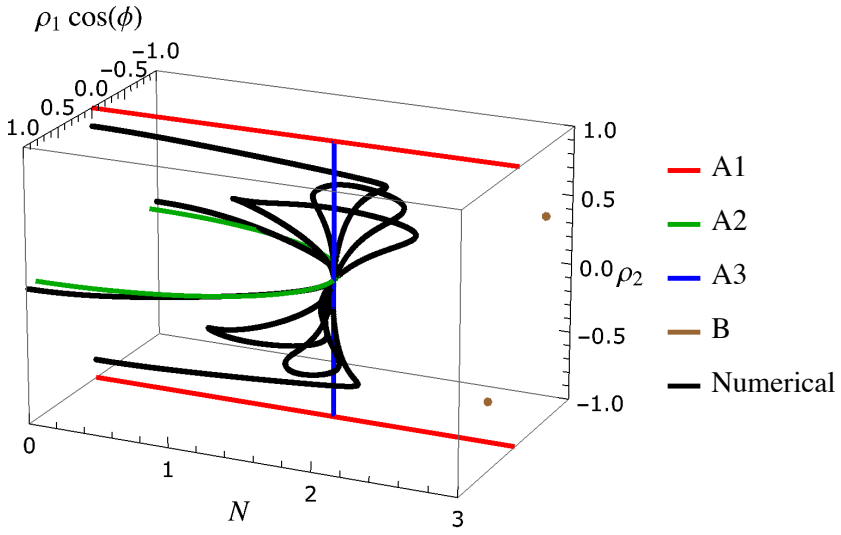

Figure 3.3: Solutions of the CP^{N-1} fixed point equations (2.40)-(2.45) in the parameter subspace $(\rho_1 \cos\phi,\ \rho_2)$.

then to $O(3)$. We can then suspect that, by the same mechanism observed for solution B at $N = 3$, the solutions of table 3.3 reconstruct the same scattering matrix (3.8) than solution A1, and we checked that this is indeed the case. More specifically, solutions C3, C4, C7, C8, D3 and D4 correspond to A1_+, while C1, C2, C5, C6, D1 and D2 correspond to A1_-.

Let us now consider the solutions that we determined numerically, which extend up

to $N = 2$, where they meet in pairs (see figures 3.2 and 3.3). Since the meeting points at $N = 2$ are $O(3)$ fixed points, and the $O(M)$ model does not possess branches of fixed points terminating at $M = 3$, we can anticipate that the CP^{N-1} branches terminating at $N = 2$ correspond to new universality classes. We illustrate this fact considering the $U(N)$-invariant two-particle state

$$|\psi\rangle = \sum_{a,b=1}^{N} \left(|ab, ba\rangle - \frac{1}{N}|aa, bb\rangle \right), \tag{3.45}$$

which scatters into itself, i.e. satisfies $\mathbb{S}|\psi\rangle = \lambda|\psi\rangle$, with an amplitude λ which is a phase by unitarity and is given by

$$\lambda = (N^2 - 1)S_1 + S_2 + S_3 + 2\left(N - \frac{1}{N}\right)(S_4 + S_5) - \frac{2}{N}S_6\,. \tag{3.46}$$

Such a phase is related to the conformal dimension Δ_η of the chiral field that creates the particles as [29, 105]

$$\lambda = e^{-2\pi i \Delta_\eta}. \tag{3.47}$$

The values of Δ_η obtained through (3.46) and (1.49) for the different solutions of the fixed point equations (2.40)-(2.45) are shown in figure 3.4. Equation (1.49) defines Δ_η modulo integers[4], and we plot the most relevant (in the renormalization group sense) interval $\Delta_\eta \in (0, 1)$. The values 0 and 1/2 correspond to the $O(N^2 - 1)$ sigma model (solution $\mathrm{A1}_+$) and to the fermionic realization (solution $\mathrm{A1}_-$), respectively[5]. The figure clearly exhibits the collapse on the solution A1 of the additional solutions existing at $N = 2, 3$. We also see that the numerical solutions at $N < 2$ correspond to values of Δ_η – and then to fixed points – different from those associated to A1, A2 and A3.

It appears from figure 3.2 that the numerical solutions have nonvanishing ρ_2 and ρ_4. Hence, they correspond to intersecting particle trajectories (see figure 3.1) and should describe criticality in gases of intersecting loops. Actually, the relevance of RP^{N-1} and CP^{N-1} models for gases of intersecting loops was discussed in [103]. Here we are finding the corresponding CP^{N-1} fixed points and showing that they exist up to $N = 2$.

We see that for $N \geq 2$ there are only solutions with $\rho_4 = \rho_5 = 0$ (or equivalent to them at $N = 2, 3$). When moving away from criticality, on the other hand, ρ_4 and ρ_5

[4]This corresponds to the fact that in conformal field theory, given a primary field with dimension Δ, there are descendants with dimension $\Delta + n$, $n = 1, 2, \ldots$. In addition, the duplication of solutions pointed out in footnote 6 causes Δ_η to go into itself under shifts by half-integers.

[5]See [106] for details about Δ_η in the $O(M)$ model.

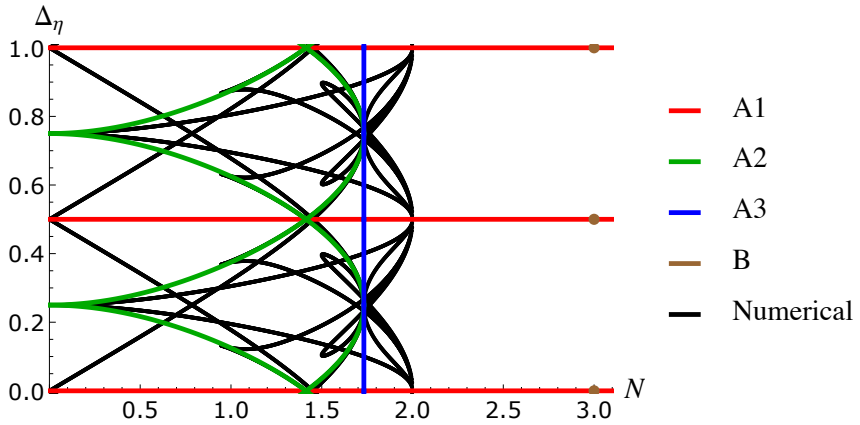

Figure 3.4: The conformal dimension Δ_η (modulo integers) for the different solutions of the CP^{N-1} fixed point equations (2.40)-(2.45).

may[6] in general develop nonvanishing values. This is expected for the ferromagnetic case, thus making explicit away from criticality the difference with the $O(N^2-1)$ universality class[7].

3.3 Parallels with the RP^{N-1} model

We briefly point out similarities and differences between the above results for the CP^{N-1} model and those of the previous chapter for the RP^{N-1} model. The RP^{N-1} model differs from CP^{N-1} for the fact that the spin variable $\mathbf{s}_i$ is real, leading to an order parameter that is a traceless symmetric tensor. This allows a larger number of contractions between pairs of particle indices, but there are still 11 amplitudes $S_1, \ldots, S_{11}$ parametrized as in (1.53), (1.54), (3.10)-(3.15). When $\rho_4 = \rho_5 = 0$, the fixed point equations reduce to those of the $O(M_N)$ model, with $M_N = N(N+1)/2 - 1$. As a consequence, there are solutions A1, A2 and A3 that correspond to the solutions P1, P2 and P3, respectively, of table 1.1 with $M = M_N$. A1 is the only solution for $N > 2.24421\ldots$ More precisely, at $N = 3$ there is an isolated solution B3, but is equivalent to A1 by the same mechanism discussed in the previous section for solution B in CP^2. At $N = 2$, solution A3 goes along with two additional solutions, B1 and B2, which also possess a free parameter and provide

[6]Not for $N = 2$, given that $CP^1 \sim O(3)$.

[7]In particular, contrary to the $O(N^2-1)$ model [107], the CP^{N-1} model is not expected to be exactly solvable away from criticality [108, 109].

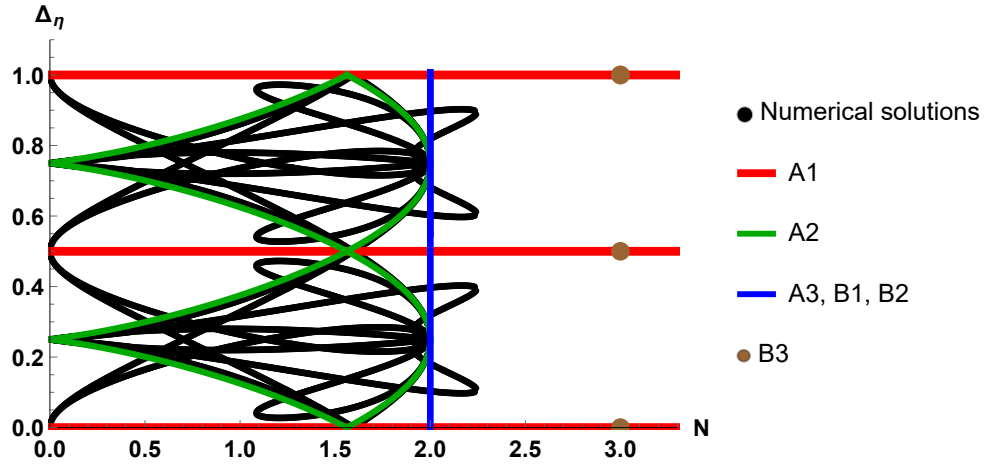

Figure 3.5: Δ_η (modulo integers) for the different RP^{N-1} solutions.

alternative realizations of the BKT phase in the $RP^1 \sim O(2)$ model. Finally, we showed in figure 2.5 how for $N < 2.24421..$ there is a rich pattern of solutions that we determined numerically.

We can again use (1.49) to determine the conformal dimension Δ_η, taking into account that (3.46) is now replaced by

$$\tfrac{(N-1)(N+2)}{2} S_1 + S_2 + S_3 + 2\tfrac{(N-1)(N+2)}{N}(S_4 + S_5) + 2\tfrac{N-2}{N} S_6 \,, \tag{3.48}$$

in terms of the RP^{N-1} amplitudes S_i. The result for the different solutions is shown in figure 3.5. $N = 2.24421..$ is the threshold value below which the space of solutions enlarges, a threshold that in CP^{N-1} occurs at $N = 2$. While in the previous section the correspondence $CP^1 \sim O(3)$ allowed us to anticipate that all the "threshold solutions" should be equivalent to A1, a similar argument is absent at the RP^{N-1} threshold, and indeed figure 3.5 illustrates that the solutions at $N = 2.24421..$ are not related to A1.

3.A Appendix. Analytic solutions

We list in this appendix the solutions of the fixed point equations (3.39)-(3.44) that we determined analytically. With respect to table 3.2, we also use the equations (3.34)-(3.38) to express the amplitudes $S_{i\geq 7}$.

• Solution A1a$_\pm$ is defined for $N \in \mathbb{R}$ and reads

$$\rho_2 = S_0 \ , \ \rho_1 = \rho_4 = \rho_5 = \rho_8 = \rho_7 = \rho_9 = \rho_{10} = 0 \,. \tag{3.49}$$

• Solution A1b$_\pm$ is defined for $N \in \mathbb{R}$ and reads

$$\begin{aligned} &\rho_2 = -S_0 \ , \ \rho_1 = \rho_4 = \rho_5 = \rho_8 = \rho_9 = 0 \, , \\ &\rho_7 = \frac{2S_0}{N} \ , \ \rho_{10} = -\frac{\rho_7}{N}, \end{aligned} \tag{3.50}$$

• Solution A2$_\pm$ is defined for $N \in [-\sqrt{3}, \sqrt{3}]$ and reads[8]

$$\begin{aligned} &\rho_1 = 1 \ , \ \rho_2 = \rho_4 = \rho_5 = \rho_9 = 0 \ , \ \cos\phi = (\pm)\frac{1}{2}\sqrt{3 - N^2} \, , \\ &\sin\phi = (\pm)\frac{1}{2}\sqrt{1 + N^2} \ , \ \rho_7 = \frac{S_0}{N} \ , \ \rho_8 = \frac{1}{|N|} \ , \ \cos\psi = -\mathrm{sgn}(N)\cos\phi, \\ &\sin\psi = \mathrm{sgn}(N)\sin\phi \ , \ \rho_{10} = \frac{2\cos\phi}{N^2} - \frac{S_0}{N^2} \, . \end{aligned} \tag{3.51}$$

• Solution A3$_\pm$ is defined for $N = \pm\sqrt{3}$ and reads

$$\begin{aligned} &\rho_1 = \sqrt{1 - \rho_2^2} \ , \ \rho_2 \in [-1, 1] \ , \ \rho_4 = \rho_5 = \rho_9 = 0 \ , \ \phi = (\pm)\frac{\pi}{2} \ , \ \psi = \pm\phi, \\ &\rho_8 = \frac{1}{|N|}\sqrt{1 - \rho_2^2} \ , \ \rho_7 = \frac{S_0 - \rho_2}{N} \ , \ \rho_{10} = -\frac{\rho_7}{N} \, . \end{aligned} \tag{3.52}$$

• Solution B$_\pm$ is defined for $N = 3$ and reads

$$\begin{aligned} &\rho_1 = \rho_4 = \rho_8 = \frac{1}{2} \ , \ \rho_2 = \rho_5 = \rho_9 = \pm\frac{1}{2} \ , \ \phi = \frac{\pi}{2} \pm \frac{\pi}{2} = \theta + \pi = \psi + \pi, \\ &\rho_7 = \frac{\rho_2 + S_0}{3} \ , \ \rho_{10} = -\frac{\rho_7}{3} \mp \frac{1}{3} \, . \end{aligned} \tag{3.53}$$

In the next appendix we show that solutions (3.49) and (3.50) differ only for the way the trace mode decouples (as a free fermion or a free boson); this is why they both appear in table 2.3 as solution A1. Table 3.3 gives the solutions at $N = 2$.

3.B Appendix. Mapping of nonmixing solutions

Equation (3.37) shows that the solutions with $\rho_4 = \rho_5 = 0$ also have $\rho_9 = 0$, and then $S_4 = S_5 = S_6 = S_9 = 0$. Figure 3.1 shows that the vanishing of these amplitudes eliminates the mixing of indices coming from different particles, and for this reason we refer to this type of solutions as "nonmixing". We now show how, through a change of basis, these nonmixing solutions can all be expressed as those of a system consisting of an

[8] Signs enclosed in parenthesis are both allowed.

Solution	$\rho_1 \cos\phi$	$\rho_1 \sin\phi$	$\rho_4 \cos\theta$	$\rho_4 \sin\theta$	ρ_2	ρ_5
C1	$\frac{1}{32}\left(-5-3\sqrt{17}\right)$	$-\frac{1}{16}\sqrt{\frac{1}{2}\left(95-7\sqrt{17}\right)}$	$\frac{1}{64}\left(-23-\sqrt{17}\right)$	$\frac{1}{32}\sqrt{\frac{1}{2}\left(95-7\sqrt{17}\right)}$	$\frac{1}{8}\left(\sqrt{17}-1\right)$	$\frac{1}{32}\left(5+3\sqrt{17}\right)$
C2	$\frac{1}{32}\left(-5-3\sqrt{17}\right)$	$\frac{1}{16}\sqrt{\frac{1}{2}\left(95-7\sqrt{17}\right)}$	$\frac{1}{64}\left(-23-\sqrt{17}\right)$	$-\frac{1}{32}\sqrt{\frac{1}{2}\left(95-7\sqrt{17}\right)}$	$\frac{1}{8}\left(\sqrt{17}-1\right)$	$\frac{1}{32}\left(5+3\sqrt{17}\right)$
C3	$\frac{1}{32}\left(5-3\sqrt{17}\right)$	$-\frac{1}{16}\sqrt{\frac{1}{2}\left(95+7\sqrt{17}\right)}$	$\frac{1}{64}\left(23-\sqrt{17}\right)$	$\frac{1}{32}\sqrt{\frac{1}{2}\left(95+7\sqrt{17}\right)}$	$\frac{1}{8}\left(1+\sqrt{17}\right)$	$\frac{1}{32}\left(3\sqrt{17}-5\right)$
C4	$\frac{1}{32}\left(5-3\sqrt{17}\right)$	$\frac{1}{16}\sqrt{\frac{1}{2}\left(95+7\sqrt{17}\right)}$	$\frac{1}{64}\left(23-\sqrt{17}\right)$	$-\frac{1}{32}\sqrt{\frac{1}{2}\left(95+7\sqrt{17}\right)}$	$\frac{1}{8}\left(1+\sqrt{17}\right)$	$\frac{1}{32}\left(3\sqrt{17}-5\right)$
C5	$\frac{1}{32}\left(3\sqrt{17}-5\right)$	$-\frac{1}{16}\sqrt{\frac{1}{2}\left(95+7\sqrt{17}\right)}$	$\frac{1}{64}\left(\sqrt{17}-23\right)$	$\frac{1}{32}\sqrt{\frac{1}{2}\left(95+7\sqrt{17}\right)}$	$\frac{1}{8}\left(-1-\sqrt{17}\right)$	$\frac{1}{32}\left(5-3\sqrt{17}\right)$
C6	$\frac{1}{32}\left(3\sqrt{17}-5\right)$	$\frac{1}{16}\sqrt{\frac{1}{2}\left(95+7\sqrt{17}\right)}$	$\frac{1}{64}\left(\sqrt{17}-23\right)$	$-\frac{1}{32}\sqrt{\frac{1}{2}\left(95+7\sqrt{17}\right)}$	$\frac{1}{8}\left(-1-\sqrt{17}\right)$	$\frac{1}{32}\left(5-3\sqrt{17}\right)$
C7	$\frac{1}{32}\left(5+3\sqrt{17}\right)$	$-\frac{1}{16}\sqrt{\frac{1}{2}\left(95-7\sqrt{17}\right)}$	$\frac{1}{64}\left(23+\sqrt{17}\right)$	$\frac{1}{32}\sqrt{\frac{1}{2}\left(95-7\sqrt{17}\right)}$	$\frac{1}{8}\left(1-\sqrt{17}\right)$	$\frac{1}{32}\left(-5-3\sqrt{17}\right)$
C8	$\frac{1}{32}\left(5+3\sqrt{17}\right)$	$\frac{1}{16}\sqrt{\frac{1}{2}\left(95-7\sqrt{17}\right)}$	$\frac{1}{64}\left(23+\sqrt{17}\right)$	$-\frac{1}{32}\sqrt{\frac{1}{2}\left(95-7\sqrt{17}\right)}$	$\frac{1}{8}\left(1-\sqrt{17}\right)$	$\frac{1}{32}\left(-5-3\sqrt{17}\right)$
D1	$-\frac{3}{4}$	$-\frac{\sqrt{15}}{8}$	$-\frac{3}{16}$	$\frac{\sqrt{15}}{16}$	$\frac{1}{8}$	$\frac{3}{4}$
D2	$-\frac{3}{4}$	$\frac{\sqrt{15}}{8}$	$-\frac{3}{16}$	$-\frac{\sqrt{15}}{16}$	$\frac{1}{8}$	$\frac{3}{4}$
D3	$\frac{3}{4}$	$-\frac{\sqrt{15}}{8}$	$\frac{3}{16}$	$\frac{\sqrt{15}}{16}$	$-\frac{1}{8}$	$-\frac{3}{4}$
D4	$\frac{3}{4}$	$\frac{\sqrt{15}}{8}$	$\frac{3}{16}$	$-\frac{\sqrt{15}}{16}$	$-\frac{1}{8}$	$-\frac{3}{4}$

Table 3.3: Solutions of equations (2.40)-(2.45) at $N = 2$; we omit A1.

$O(N^2-1)$ vector and a scalar that are decoupled. The amplitudes for such a system, in which the scalar and the vector in general interact [89], are shown in figure 3.6 and take the form

$$S'_1 = S'^*_3 \equiv \rho'_1 e^{i\phi'}, \tag{3.54}$$

$$S'_2 = S'^*_2 \equiv \rho'_2, \tag{3.55}$$

$$S'_4 = S'^*_6 \equiv \rho'_4 e^{i\theta'}, \tag{3.56}$$

$$S'_5 = S'^*_5 \equiv \rho'_5, \tag{3.57}$$

$$S'_7 = S'^*_7 \equiv \rho'_7\,. \tag{3.58}$$

The change of basis that we perform in the CP^{N-1} model is

$$|\Phi_\mu\rangle = \begin{cases} |\Phi_0\rangle = \frac{1}{\sqrt{N}} \sum_{a=1}^{N} |aa\rangle\,, \\ \frac{1+i}{2}|ab\rangle + \frac{1-i}{2}|ba\rangle\,, \quad \mu = ab\,, \qquad a \neq b\,, \\ \frac{1}{\sqrt{k(k+1)}} \left(\sum_{j=1}^{k} |jj\rangle - k|(k+1)(k+1)\rangle \right)\,, \quad \mu = kk\,, \quad k = 1, \ldots, N-1, \end{cases} \tag{3.59}$$

with $\langle \Phi_\mu | \Phi_\nu \rangle = \delta_{\mu\nu}$, and the trace mode Φ_0 being the scalar of the vector-scalar system. The scattering matrix for the non-mixing case of the CP^{N-1} model can now be expressed

S_1' S_2' S_3' S_4' S_5' S_6' S_7'

Figure 3.6: Scattering processes for a vector particle multiplet (continuous lines) and a scalar particle (dashed lines).

as

$$S_{\mu,\nu}^{\rho,\sigma} = \left(S_1'\delta_{\mu,\nu}\delta^{\rho,\sigma} + S_2'\delta_\mu^\rho\delta_\nu^\sigma + S_3'\delta_\mu^\sigma\delta_\nu^\rho\right)\bar\delta_\mu^0\bar\delta_\nu^0\bar\delta_0^\rho\bar\delta_0^\sigma + S_4'(\delta_{\mu,\nu}\delta_0^\rho\delta_0^\sigma\bar\delta_\mu^0\bar\delta_\nu^0 + \delta_\mu^0\delta_\nu^0\delta^{\rho,\sigma}\bar\delta_0^\rho\bar\delta_0^\sigma)$$
$$+ S_5'\delta_\mu^0\delta_\nu^0\delta_0^\rho\delta_0^\sigma + S_6'(\delta_\mu^\sigma\delta_\nu^0\delta_0^\rho\bar\delta_\mu^0\bar\delta_0^\sigma + \delta_\mu^0\delta_0^\sigma\delta_\nu^\rho\bar\delta_\nu^0\bar\delta_0^\rho) + S_7'(\delta_\mu^\rho\delta_\nu^0\delta_0^\sigma\bar\delta_\mu^0\bar\delta_0^\rho + \delta_\mu^0\delta_0^\rho\delta_\nu^\sigma\bar\delta_\nu^0\bar\delta_0^\sigma)\,, \tag{3.60}$$

where $\bar\delta_\mu^\nu \equiv 1 - \delta_\mu^\nu$, and

$$S_1' = \langle\Phi_\nu\Phi_\nu|\mathbb{S}|\Phi_\mu\Phi_\mu\rangle = S_1, \tag{3.61}$$
$$S_2' = \langle\Phi_\mu\Phi_\nu|\mathbb{S}|\Phi_\mu\Phi_\nu\rangle = S_2, \tag{3.62}$$
$$S_3' = \langle\Phi_\nu\Phi_\mu|\mathbb{S}|\Phi_\mu\Phi_\nu\rangle = S_3, \tag{3.63}$$
$$S_4' = \langle\Phi_0\Phi_0|\mathbb{S}|\Phi_\mu\Phi_\mu\rangle = \langle\Phi_\nu\Phi_\nu|\mathbb{S}|\Phi_0\Phi_0\rangle = S_1 + NS_{11} \tag{3.64}$$
$$S_5' = \langle\Phi_0\Phi_0|\mathbb{S}|\Phi_0\Phi_0\rangle = S_1 + S_2 + S_3 + 2N(S_7 + S_8) + N^2S_{10} + 2NS_{11}, \tag{3.65}$$
$$S_6' = \langle\Phi_\mu\Phi_0|\mathbb{S}|\Phi_0\Phi_\mu\rangle = \langle\Phi_0\Phi_\nu|\mathbb{S}|\Phi_\nu\Phi_0\rangle = S_3 + NS_8, \tag{3.66}$$
$$S_7' = \langle\Phi_0\Phi_\mu|\mathbb{S}|\Phi_0\Phi_\mu\rangle = \langle\Phi_\nu\Phi_0|\mathbb{S}|\Phi_\nu\Phi_0\rangle = S_2 + NS_7\,. \tag{3.67}$$

Using the trace decoupling equations (3.34)-(3.38) the relations (3.61)-(3.67) reduce to

$$S_1' = S_1\ ,\ S_2' = S_2\ ,\ S_3' = S_3\ ,\ S_4' = S_6' = 0\ ,\ S_5' = S_7' = S_0\,, \tag{3.68}$$

which exhibit the decoupling between the vector and the scalar (recall that $S_0 = \pm 1$). Table 3.4 gives the explicit form of the CP^{N-1} nonmixing solutions in terms of the vector-scalar amplitudes. One sees, in particular, that solutions A1a$_\pm$ and A1b$_\mp$ only differ for the nature of the decoupled scalar (fermionic or bosonic).

Solution	N^2-1	ρ_1'	ρ_2'	$\cos\phi'$	ρ_4'	ρ_5'	ρ_7'
$\mathrm{A1a}_\pm$	$\mathbb{R}$	0	S_0	$-$	0	S_0	S_0
$\mathrm{A1b}_\pm$	$\mathbb{R}$	0	$-S_0$	$-$	0	S_0	S_0
$\mathrm{A2}_\pm$	$[-2,2]$	1	0	$(\pm)\frac{1}{2}\sqrt{3-N^2}$	0	S_0	S_0
$\mathrm{A3}_\pm$	2	$\sqrt{1-\rho_2^2}$	$[-1,1]$	0	0	S_0	S_0

Table 3.4: Nonmixing solutions of the CP^{N-1} model in terms of the amplitudes of the vector-scalar system. Signs in parenthesis are both allowed, and $S_0 = \pm 1$.

Chapter 4

Critical points in coupled Potts models and correlated percolation

In this chapter, we use scale invariant scattering theory to exactly determine the renormalization group fixed points of a q-state Potts model coupled to an r-state Potts model in two dimensions. For integer values of q and r the fixed point equations are very constraining and show in particular that scale invariance in coupled Potts ferromagnets is limited to the Ashkin-Teller case ($q = r = 2$). Since our results extend to continuous values of the number of states, we can access the limit $r \to 1$ corresponding to correlated percolation, and show that the critical properties of Potts spin clusters cannot in general be obtained from those of Fortuin-Kasteleyn clusters by analytical continuation.

4.1 Spin vs Fortuin-Kasteleyn clusters

The idea that ferromagnetic transitions correspond to the percolation of clusters of like spins has been present since the early days of the theory of critical phenomena [110] (see [42] for a review). However, numerical studies for the three-dimensional Ising model [111] showed that the natural clusters obtained drawing a link between nearest neighboring spins with the same sign – we simply call them *spin clusters* – do not percolate at the critical temperature T_c of the magnetic transition. The picture of the ferromagnetic transition as a percolative transition was rescued in [112], where it was observed that, in any dimension, a different type of clusters – the Fortuin-Kasteleyn (FK) clusters [41] obtained drawing the link between nearest neighboring like spins with a probability determined

by the Ising coupling – do percolate at T_c. The FK clusters also satisfy the requirement that their fractal dimension is determined by the scaling dimension of the magnetic order parameter, and allow the coincidence of percolative and magnetic critical exponents.

A particularly interesting picture emerged in two dimensions, where it was shown that also the Ising spin clusters percolate at T_c [113], with a new fractal dimension [114]. Hence FK and spin clusters yield, at the same Ising temperature, two different universality classes of *correlated* percolation, which in turn differ from basic (*random*) percolation in which there is no interaction among lattice sites [42]. As random percolation is conveniently brought in the framework of magnetic transitions through its mapping onto the limit $r \to 1$ of the r-state Potts model [41], Ising-correlated percolation can be described in terms of coupled Ising and r-state Potts models, which amount to a dilute Potts model in which the former Ising variables determine if sites are occupied or empty. It is always understood that the auxiliary Potts variables are eventually eliminated by the limit $r \to 1$. The universality classes of FK and spin clusters in the Ising model were then identified in [112] as corresponding to two different renormalization group (RG) fixed points of this dilute $r \to 1$ Potts model. The fact that the dilute Potts model displays, as r varies, a critical and a tricritical branch [47, 115, 116] accomodates for the fixed point of FK clusters on the former and for that of spin clusters on the latter, and led to an exact identification of the fractal dimension of Ising spin clusters [117].

Much insight is usually gained extending to the q-state Potts model what has been learned for Ising ($q = 2$). The generalization of the above RG picture to q-state Potts correlated percolation was studied in [118]. Now the site variable takes q values, and spin and FK clusters are obtained drawing a link between nearest neighboring sites with the same value, with probability 1 for the former and interaction-dependent for the latter. In [118] the q-state Potts model coupled to the auxiliary r-state Potts model was studied by an approximated RG approach, in the relevant limit $r \to 1$. Two fixed points were found as a function of q and were associated to the universality classes of FK and spin clusters. It was conjectured that the two branches coalesce and terminate at the value of q above which the *ordinary* Potts transition becomes first order; in two dimensions this value is known to be $q = 4$ [119, 43]. This conjecture, however, could never be checked, since the approximate RG of [118] was unable to see a transition to a first order regime, and the model cannot be numerically simulated in the limit $r \to 1$. The conjecture was extended in [120], where it was proposed that the two branches of fixed points of the coupled q-state

and r-state Potts models can be related, for $r \to 1$, to the critical and tricritical branches of the q-state Potts model, which coalesce at $q = 4$ and are analytical continuation of each other [115, 116]. The idea that the critical properties of spin clusters are related in this way to those of FK clusters was used in [120] to propose an exact formula for the fractal dimension of Potts spin clusters as a function of q. Given the good agreement of this formula with numerical studies of spin clusters at[1] $q = 3$ [120, 122], the conjecture about analytic continuation was accepted.

The three-point connectivity (i.e. the probability that three points are in the same cluster) of q-state Potts FK clusters at criticality was exactly determined in [35], and was shown to agree with numerical simulations performed for random percolation ($q \to 1$) in [123] and for q generic in [124]. As the only exact analytical result for correlations in critical clusters on the infinite plane after the critical exponents [115], this connectivity formula also provided a new test for the conjectured analytic continuation for spin clusters. Numerical determination for Potts spin clusters performed in [125] showed the failure of the conjecture for this observable, a finding that reopened the question of the theoretical understanding of spin clusters[2].

Here we use scale invariant scattering to obtain the first exact determination of the RG fixed points for a q-state Potts model coupled to an r-state Potts model in two dimensions. Since our results are obtained for continuous values of q and r, we have in particular access to the limit $r \to 1$ relevant for Potts correlated percolation. The subtleties of this limit[3] require that, for a complete description of critical spin clusters, the degrees of freedom of the q-state sector and the auxiliary degrees of freedom of the $(r = 1 + \epsilon)$-state sector are simultaneously critical. We do not find any critical line in the coupled regime along which this requirement is fulfilled with continuity in the whole interval $q \in [2, 4]$. One implication is that the conjectured analytical continuation cannot hold in general, thus explaining the failures observed in [125, 126]. On the other hand, it may happen, that specific quantities can be evaluated directly *at* $r = 1$, where the number of r-state degrees

[1] Numerical studies of the Potts model at $q = 4$ are notoriously complicated by logarithmic corrections to scaling [121].

[2] A similar failure of the analytic continuation was then observed in [126] from simulations for the cluster number in geometries with corners, which for FK clusters can be related [127] to the Potts central charge [33]. Tests of conformal invariance for critical Potts spin clusters have recently been performed in [128].

[3] See [35] for an analytically exact illustration in the context or random percolation.

of freedom is strictly zero and the discontinuities coming from this sector can be ignored. This leaves open the possibility that the formula for the fractal dimension of spin clusters conjectured in [120] – which up to now has been found in agreement with numerical simulations (see also [125]) – is exact. We now turn to the derivation of the results.

4.2 Coupled q-state and r-state Potts models

4.2.1 Fixed point equations

We want to determine the RG fixed points associated to the symmetry $\mathbb{S}_q \times \mathbb{S}_r$, which can be realized coupling a q-state Potts model to an r-state Potts model, namely considering the Hamiltonian

$$\mathcal{H}_{q,r} = -J_1 \sum_{\langle i,j \rangle} \delta_{s_{i,1},s_{j,1}} - J_2 \sum_{\langle i,j \rangle} \delta_{s_{i,2},s_{j,2}} - J \sum_{\langle i,j \rangle} \delta_{s_{i,1}s_{j,1}} \delta_{s_{i,2},s_{j,2}} \,, \tag{4.1}$$

where $s_{i,1} = 1, 2, \ldots, q$ and $s_{i,2} = 1, 2, \ldots, r$ are, respectively, the q-state and r-state color variables at site i. Hence, the index 1 will refer to the q-state sector of the coupled model, and index 2 to the r-state sector. Since our analysis will be performed directly in the continuum limit and will only rely on symmetry, our results for the critical points will cover all combinations of ferromagnetic and antiferromagnetic values of the couplings J_1, J_2 and J.

The implementation of the scattering description follows the steps already seen in section 1.5 for the basic Potts model. In the first place, there are particle excitations associated to each sector. We denote them $A_{\alpha_k \beta_k}$, where $k = 1, 2$ labels the two sectors, $\alpha_1, \beta_1 = 1, \ldots, q$ and $\alpha_2, \beta_2 = 1, \ldots, r$ ($\alpha \neq \beta$). Now the trajectory of a particle $A_{\alpha_k \beta_k}$ separates a region of space-time characterized by the colors α_1 in the q-state sector and α_2 in the r-state sector from a region in which sector k changes its color to β_k, with the color of the other sector remaining unchanged. It follows that the two-particle scattering amplitudes inequivalent under color permutations are those[4] depicted in figure 4.1. The first four amplitudes involve only particles belonging to the same sector, so that we keep for them the notation of section 1.5, up to the addition of the sector index k. On the other hand, the remaining three amplitudes involve particles from both sectors and are responsible for the coupling of the two Potts models.

[4]We also imply that the theory is invariant under time reversal and spatial reflection.

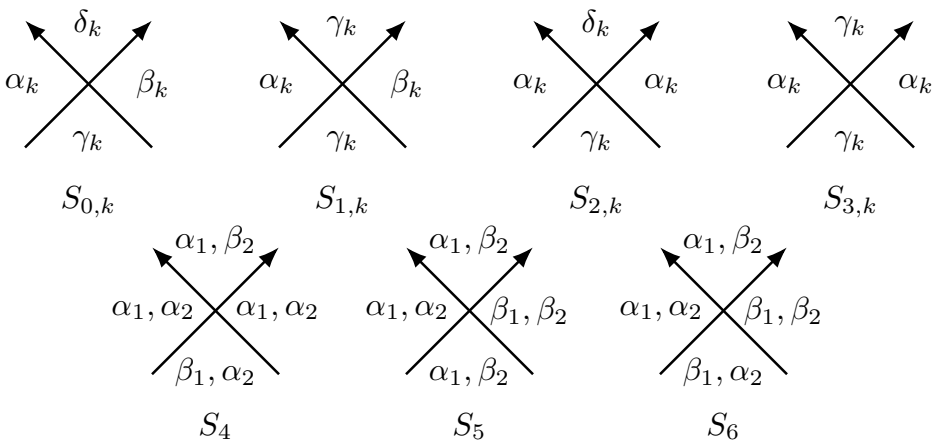

Figure 4.1: Scattering amplitudes for the coupled q-state and r-state Potts models. The label α_k refers to color α in the q-state model for $k = 1$, and in the r-state model for $k = 2$.

The crossing symmetry equations (3.1) now become

$$S_{0,k} = S_{0,k}^* \equiv \rho_{0,k}, \tag{4.2}$$
$$S_{1,k} = S_{2,k}^* \equiv \rho_{1,k} e^{i\phi_k}, \tag{4.3}$$
$$S_{3,k} = S_{3,k}^* \equiv \rho_{3,k}, \tag{4.4}$$
$$S_4 = S_5^* \equiv \rho_4 e^{i\theta}, \tag{4.5}$$
$$S_6 = S_6^* \equiv \rho_6, \tag{4.6}$$

with parametrizations in terms of $\rho_{1,k}$ and ρ_4 nonnegative, and $\rho_{0,k}$, $\rho_{3,k}$, ρ_6, ϕ_k and θ real. The unitarity equations (2.2) then take the form

$$0 = (q-4)\rho_{0,1}^2 + 2\rho_{1,1}\rho_{0,1}\cos\phi_1, \tag{4.7}$$
$$0 = (r-4)\rho_{0,2}^2 + 2\rho_{1,2}\rho_{0,2}\cos\phi_2, \tag{4.8}$$
$$1 = (q-3)\rho_{0,1}^2 + \rho_{1,1}^2, \tag{4.9}$$
$$1 = (r-3)\rho_{0,2}^2 + \rho_{1,2}^2, \tag{4.10}$$
$$0 = (q-3)\rho_{1,1}^2 + 2\rho_{1,1}\rho_{3,1}\cos\phi_1 + (r-1)\rho_4^2, \tag{4.11}$$
$$0 = (r-3)\rho_{1,2}^2 + 2\rho_{1,2}\rho_{3,2}\cos\phi_2 + (q-1)\rho_4^2, \tag{4.12}$$
$$1 = (q-2)\rho_{1,1}^2 + \rho_{3,1}^2 + (r-1)\rho_4^2, \tag{4.13}$$
$$1 = (r-2)\rho_{1,2}^2 + \rho_{3,2}^2 + (q-1)\rho_4^2, \tag{4.14}$$

$$0 = \rho_4 \left[\rho_{3,2} e^{i\theta} + \rho_{3,1} e^{-i\theta} + (q-2)\rho_{1,1} e^{-i(\theta+\phi_1)} + (r-2)\rho_{1,2} e^{i(\theta+\phi_2)}\right], \tag{4.15}$$

$$1 = \rho_4^2 + \rho_6^2, \tag{4.16}$$

$$0 = 2\rho_4\rho_6 \cos\theta. \tag{4.17}$$

Notice that $\rho_4 = 0$ directly yields $S_4 = S_5 = 0$; in addition (4.16) implies $S_6 = \pm 1$, namely absence of scattering between particles from different sectors. It follows that $\rho_4 = 0$ corresponds to the case in which the two Potts models decouple, and indeed the system (4.7)-(4.17) gives back[5], for each sector, the equations of section 1.5.

4.2.2 Solutions

The solutions of equations (4.7)-(4.17) yield the RG fixed points with $\mathbb{S}_q \times \mathbb{S}_r$ symmetry. It turns out that the space of solutions can be divided into three subspaces according to the values taken by ρ_4. The first subspace is that in which the q-state sector and the r-state sector are decoupled ($\rho_4 = 0$); in this case the solutions can be immediately traced back to those we saw in section 1.5 for a single Potts model and do not need further discussion. The second subspace is that in which ρ_4 varies; we will refer to the solutions in this subspace as solutions of type V. The third subspace is that of solutions with $\rho_4 = 1$, which we will call solutions of type S; clearly, in the S-type solutions the two sectors are always strongly coupled. We will also use the notations

$$x_k = \rho_{1,k} \cos\phi_k\,, \qquad y_k = \rho_{1,k} \sin\phi_k\,, \qquad k = 1, 2\,, \tag{4.18}$$

while the notation $(\pm)$ will indicate that both signs are allowed. As usual, given a solution of the crossing and unitarity equations, another solution is obtained reversing the sign of all amplitudes.

The Hamiltonian (4.1) and the equations (4.7)-(4.17) are invariant under the simultaneous exchanges

$$q \leftrightarrow r\,, \qquad \text{sector index } 1 \leftrightarrow \text{sector index } 2\,. \tag{4.19}$$

It follows that this exchange operation maps a solution of the fixed point equations into another solution. Some solutions will be mapped into themselves and will be called exchange-invariant solutions. In these invariant solutions the q-state sector and the r-state sector play a symmetric role: they are both ferromagnetic, or both antiferromagnetic on

[5]Notice that the parameter ρ of section 1.5 is now called ρ_1.

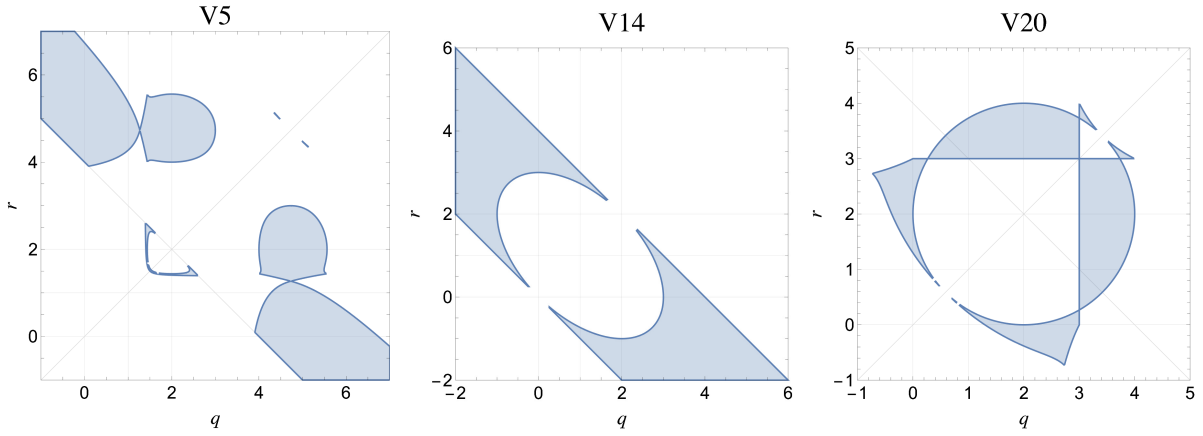

Figure 4.2: Domains of definition in the q-r plane for the solutions V5, V14 and V20.

the same lattice. This is the case normally considered when referring to coupled Potts models, and in this section we will list the exchange-invariant solutions. More generally – for example for the application to correlated percolation of the next section – it is relevant to know also the noninvariant solutions, which we then list in appendix 4.A. If a noninvariant solution possesses a decoupling limit $\rho_4 \to 0$, the amplitudes obtained in the limit for the q-state sector and for the r-state sector correspond to different solutions[6] of table 1.3.

Solutions with varying ρ_4

We give here the solutions of type V invariant under the exchange operation (4.19). They are denoted by V followed by a number distinguishing the different solutions. These numbers come from a different selection process and are not presented in progressive order.

A first group of solutions – V5, V14 and V20 – are defined in the ranges of q and r shown in figure 4.2. They read

[6]This was not possible in the case of [39], where n identical Potts replicas were considered for the purpose of studying quenched disorder ($n \to 0$).

• V5

$$\begin{aligned}
&\rho_{0,1}=\rho_{3,1}=\pm(r^2-6r+6)f(q,r),\quad \rho_{0,2}=\rho_{3,2}=\pm(q^2-6q+6)f(q,r)\\
&x_1=-\frac{q-4}{2}\rho_{0,1},\quad y_1=(\pm)\frac{r-2}{2}g(q,r),\quad x_2=-\frac{r-4}{2}\rho_{0,2},\quad y_2=-\frac{q-2}{r-2}y_1\\
&\rho_4=\sqrt{\frac{\frac{(q^2-6q+6)^2}{q^2-5q+5}(q-3)-\frac{(r^2-6r+6)^2}{r^2-5r+5}(r-3)}{\frac{(r^2-6r+6)^2}{r^2-5r+5}(q-1)-\frac{(q^2-6q+6)^2}{q^2-5q+5}(r-1)}},\quad \theta=(\pm)\frac{\pi}{2},\quad \rho_6=(\pm)\sqrt{1-\rho_4^2},\\
&f(q,r)=\sqrt{\frac{4-q-r}{(qr-q-r)[(q^2-5q+5)(r^2-5r+5)-qr+q+r-1]}},\\
&g(q,r)=\sqrt{\frac{(qr-2q-2r+6)[(q^2-6q+6)(r-2)+(q-2)(r^2-6r+6)]}{(qr-q-r)[(q^2-5q+5)(r^2-5r+5)-qr+q+r-1]}},
\end{aligned}\tag{4.20}$$

• V14

$$\begin{aligned}
&\rho_{0,1}=\rho_{0,2}=0,\quad \rho_{3,1}=2x_1,\quad \rho_{3,2}=2x_2,\quad x_1=\pm\frac{r}{2}\sqrt{\frac{4-q-r}{q+r-qr}},\\
&y_1=(\pm)\frac{r-2}{2}\sqrt{\frac{q+r}{q+r-qr}},\quad y_2=-\frac{q-2}{r-2}y_1,\quad x_2=\frac{q}{r}x_1,\\
&\rho_4=\sqrt{\frac{q^2+r^2-3(q+r)+qr}{q+r-qr}}\ ,\ \rho_6=(\pm)\sqrt{1-\rho_4^2},\quad \theta=(\pm)\frac{\pi}{2},
\end{aligned}\tag{4.21}$$

• V20

$$\begin{aligned}
&\rho_{0,1}=\pm\frac{r^2-4r+2}{\sqrt{1-(q-3)(q-1)(r-3)(r-1)}},\quad \rho_{0,2}=\frac{q^2-4q+2}{r^2-4r+2}\rho_{0,1},\\
&x_1=-\frac{q-4}{2}\rho_{0,1},\quad x_2=-\frac{r-4}{2}\rho_{0,2},\quad \rho_{3,1}=-(q-3)\rho_{0,1},\quad \rho_{3,2}=-(r-3)\rho_{0,2},\\
&y_1=(\pm)\frac{r-2}{2}\sqrt{\frac{4-(q-2)^2(r-2)^2}{1-(q-3)(q-1)(r-3)(r-1)}},\quad y_2=-\frac{q-2}{r-2}y_1,\\
&\rho_4=\sqrt{\frac{\left(q^2-4q+2\right)^2-\left(r^2-4r+2\right)^2}{\frac{q-1}{r-3}(r^2-4r+2)^2-\frac{r-1}{q-3}(q^2-4q+2)^2}},\quad \theta=(\pm)\frac{\pi}{2},\quad \rho_6=(\pm)\sqrt{1-\rho_4^2}.
\end{aligned}\tag{4.22}$$

Then we have the solutions V1, V15, V21 and V33 with $q=r$. They all possess a free parameter and correspond to lines of fixed points at fixed $q=r$ (see figure 4.5). For V15, V21 and V33 the free parameter is ρ_4 itself (figure 4.3). The four solutions are

• V1 defined in the interval $q=r\in(2,3)$

$$\begin{aligned}
&\rho_{0,1}=\rho_{3,1}=\rho_{0,2}=\rho_{3,2}=0,\quad \rho_{1,1}=\rho_{1,2}=1,\quad \phi_1=-\phi_2\in[0,2\pi),\\
&\rho_4=\sqrt{\frac{3-q}{q-1}},\qquad \theta=(\pm)\frac{\pi}{2},\qquad \rho_6=(\pm)\sqrt{2\,\frac{q-2}{q-1}},
\end{aligned}\tag{4.23}$$

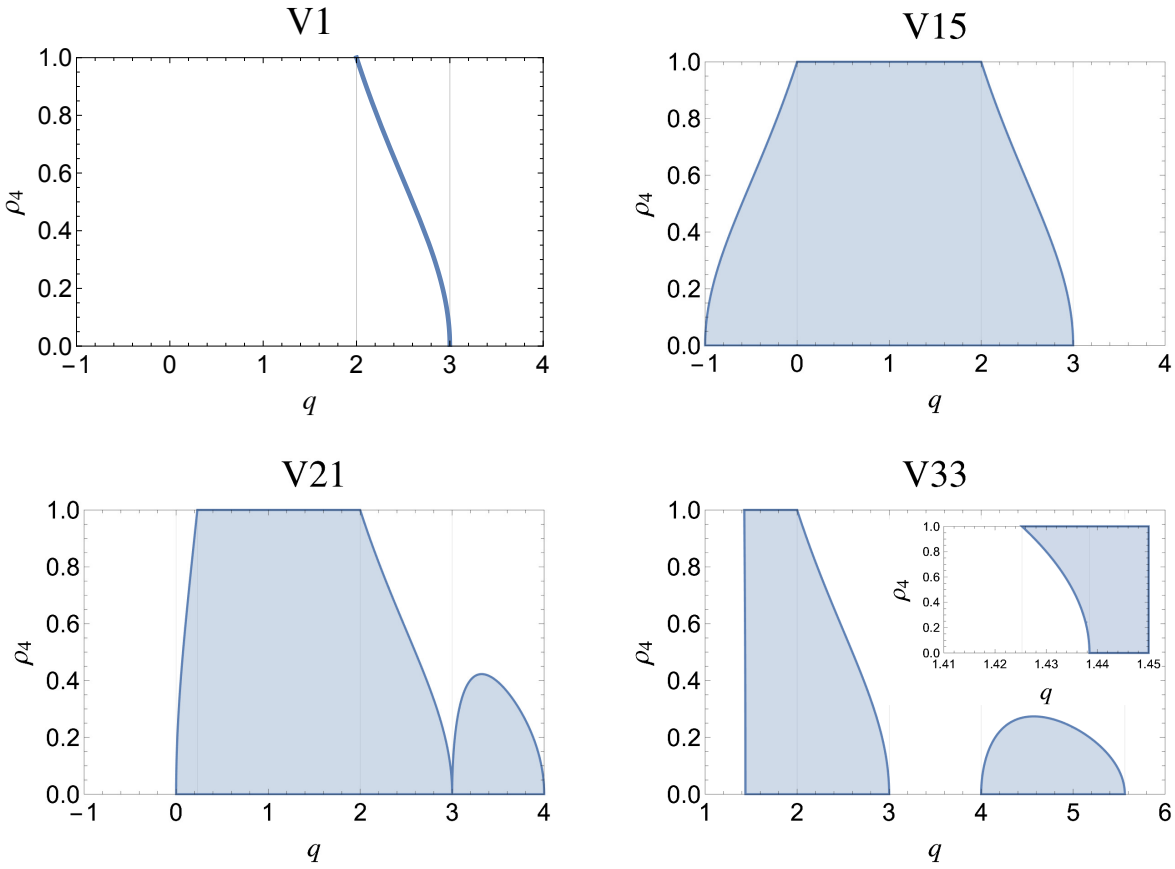

Figure 4.3: Ranges of variation of ρ_4 for the $q = r$ solutions V1, V15, V21 and V33.

- V15 defined in the interval $q = r \in (-1, 3)$

$$\rho_{0,1} = \rho_{0,2} = 0, \quad \rho_{3,1} = \rho_{3,2} = 2x_1, \quad \theta = (\pm)\frac{\pi}{2}, \quad \rho_6 = (\pm)\sqrt{1-\rho_4^2}$$
$$x_1 = x_2 = \pm\frac{1}{2}\sqrt{3-q+(q-1)\rho_4^2}, \quad y_1 = -y_2 = (\pm)\sqrt{1+q+(q-1)\rho_4^2}$$
$$0 < \rho_4 < \begin{cases} \sqrt{\frac{1+q}{1-q}}, & -1 < q < 0, \\ 1, & 0 \le q \le 2, \\ \sqrt{\frac{3-q}{q-1}}, & 2 < q < 3, \end{cases} \tag{4.24}$$

• V21 defined in the interval $q = r \in (0, 4)$

$$\begin{aligned}
&\rho_{0,1} = \rho_{0,2} = \pm\sqrt{1 + \frac{q-1}{q-3}\rho_4^2}, \quad x_1 = x_2 = -\frac{q-4}{2}\rho_{0,1}, \quad \theta = (\pm)\frac{\pi}{2}, \\
&y_1 = -y_2 = (\pm)\frac{1}{2}\sqrt{q(4-q) - \frac{(q-1)(q-2)^2}{q-3}\rho_4^2}, \quad \rho_{3,1} = \rho_{3,2} = -(q-3)\rho_{0,1}, \\
&\rho_6 = (\pm)\sqrt{1-\rho_4^2}, \quad 0 < \rho_4 < \begin{cases} \sqrt{\frac{q(q-3)(4-q)}{(q-1)(q-2)^2}}, & 0 < q \le q^* \text{ and } 3 < q < 4, \\ 1, & q^* < q \le 2, \\ \sqrt{\frac{3-q}{q-1}}, & 2 < q < 3\,, \end{cases}
\end{aligned} \tag{4.25}$$

where $q^* \approx 0.231\ldots$ is the real root of the polynomial $q^3 - 6q^2 + 10q - 2$.

• V33 defined in the interval $q = r \in (q', 3) \cup \left(4, \frac{7+\sqrt{17}}{2}\right)$

$$\begin{aligned}
&\rho_{0,1} = \rho_{0,2} = \rho_{3,1} = \rho_{3,2} = \pm\sqrt{\frac{q-3+(q-1)\rho_4^2}{q^2-5q+5}}, \qquad x_1 = x_2 = -\frac{q-4}{2}\rho_{0,1}, \\
&y_1 = -y_2 = (\pm)\frac{1}{2}\sqrt{\frac{(4-q)(q^2-7q+8) - (q-2)^2(q-1)\rho_4^2}{q^2-5q+5}}, \qquad \theta = (\pm)\frac{\pi}{2}, \\
&\rho_6 = (\pm)\sqrt{1-\rho_4^2}, \qquad \rho_4 \in \begin{cases} \left(\sqrt{\frac{(4-q)(q^2-7q+8)}{(q-2)^2(q-1)}}, 1\right), & q' < q < \frac{7-\sqrt{17}}{2}, \\ (0,1)\,, & \frac{7-\sqrt{17}}{2} < q < 2, \\ \left(0, \sqrt{\frac{3-q}{q-1}}\right), & 2 < q < 3, \\ \left(0, \sqrt{\frac{(4-q)(q^2-7q+8)}{(q-2)^2(q-1)}}\right), & 4 < q < \frac{7+\sqrt{17}}{2}, \end{cases}
\end{aligned} \tag{4.26}$$

where $q' \approx 1.425\ldots$ is the real root of the polynomial $q^3 - 8q^2 + 22q - 18$.

Finally there are solutions defined only for isolated values of q and r. The first is

• V13 defined for $r = q = 2$

$$\begin{aligned}
&\rho_{0,1} = \rho_{0,2} = \rho_{3,1} = \rho_{3,2} = x_1 = x_2 = \pm\sqrt{1-\rho_4^2}, \quad \theta = (\pm)\frac{\pi}{2} \\
&y_1 = (\pm)1, \quad y_2 = (\pm)1, \quad \rho_6 = (\pm)\sqrt{1-\rho_4^2}, \quad \rho_4 \in (0,1)\,,
\end{aligned} \tag{4.27}$$

while the others correspond to less interesting (irrational) values of q and r and will not be listed.

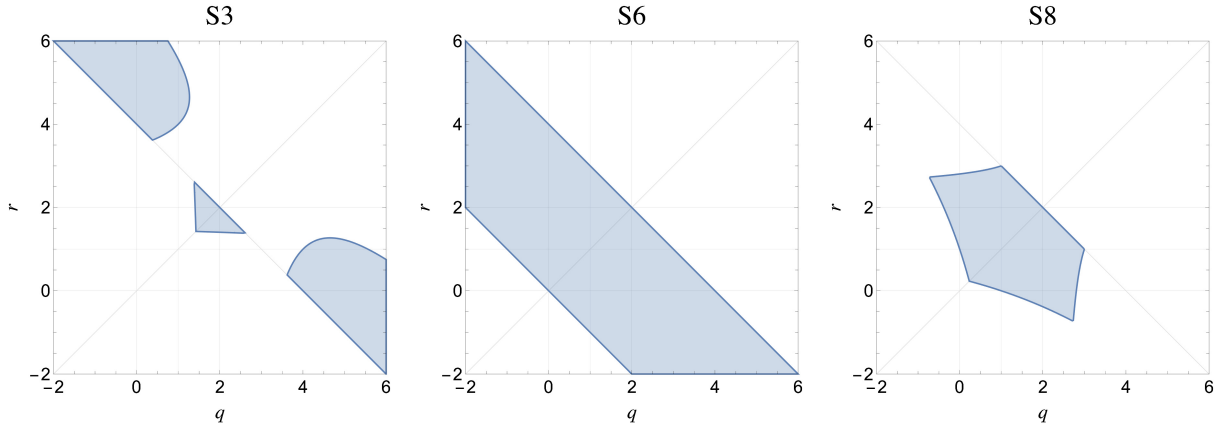

Figure 4.4: Domains of definition in the q-r plane for the solutions S3, S6, and S8

Solutions with $\rho_4 = 1$

When $\rho_4 = 1$ (and then $\rho_6 = 0$), it can be seen that (4.15) allows to express θ in the form

$$\tan(\theta + \pi j) = \frac{(q-2)\rho_{1,1}\cos\phi_1 + \rho_{3,1} + (r-2)\rho_{1,2}\cos\phi_2 + \rho_{3,2}}{(q-2)\rho_{1,1}\sin\phi_1 + (r-2)\rho_{1,2}\sin\phi_2}, \quad j = 0, 1\,, \tag{4.28}$$

with the condition

$$\begin{aligned}[(q-2)\rho_{1,1}\cos\phi_1 + \rho_{3,1}]^2 + (q-2)^2\rho_{1,1}^2\sin^2\phi_1 \\ = [(r-2)\rho_{1,2}\cos\phi_2 + \rho_{3,2}]^2 + (r-2)^2\rho_{1,2}^2\sin^2\phi_2\,.\end{aligned} \tag{4.29}$$

If $(q-2)\rho_{1,1}\cos\phi_1 + \rho_{3,1} = (q-2)\rho_{1,1}\sin\phi_1 = (r-2)\rho_{1,2}\cos\phi_2 + \rho_{3,2} = (r-2)\rho_{1,2}\sin\phi_2 = 0$, θ becomes a free parameter. We can solve for the remaining parameters, which satisfy the equations

$$\begin{aligned} 0 &= (q-4)\rho_{0,1}^2 + 2\rho_{1,1}\rho_{0,1}\cos\phi_1, & 0 &= (r-4)\rho_{0,2}^2 + 2\rho_{1,2}\rho_{0,2}\cos\phi_2, \\ 1 &= (q-3)\rho_{0,1}^2 + \rho_{1,1}^2, & 1 &= (r-3)\rho_{0,2}^2 + \rho_{1,2}^2, \\ 1-r &= (q-3)\rho_{1,1}^2 + 2\rho_{1,1}\rho_{3,1}\cos\phi_1, & 1-q &= (r-3)\rho_{1,2}^2 + 2\rho_{1,2}\rho_{3,2}\cos\phi_2, \\ 2-r &= (q-2)\rho_{1,1}^2 + \rho_{3,1}^2, & 2-q &= (r-2)\rho_{1,2}^2 + \rho_{3,2}^2\,. \end{aligned} \tag{4.30}$$

Notice that the last two equations imply that no solution in this class exists if both q and r are larger than 2.

We list here the exchange-invariant solutions, starting with

- S1 defined for $q + r = 4$

$$\rho_{0,1} = \rho_{0,2} = \rho_{3,1} = \rho_{3,2} = 0\ ,\ \phi_1, \phi_2 \in [0, 2\pi)\ ,\ \rho_{1,1} = \rho_{1,2} = 1\,. \tag{4.31}$$

The three solutions S3, S6 and S8 are instead defined for the values of q and r shown in figure 4.4. They read

• S3

$$\begin{aligned}
&\rho_{0,1} = \rho_{3,1} = (\pm)\sqrt{\frac{q+r-4}{q^2-5q+5}}, \qquad \rho_{0,2} = \rho_{3,2} = (\pm)\sqrt{\frac{q+r-4}{r^2-5r+5}}, \\
&x_1 = -\frac{q-4}{2}\rho_{0,1}, \quad y_1 = (\pm)\frac{1}{2}\sqrt{\frac{(4-q)\,(q^2-7q+8)-(q-2)^2(r-1)}{q^2-5q+5}}, \\
&x_2 = -\frac{r-4}{2}\rho_{0,2}, \quad y_2 = (\pm)\frac{1}{2}\sqrt{\frac{(4-r)\,(r^2-7r+8)-(r-2)^2(q-1)}{r^2-5r+5}},
\end{aligned} \tag{4.32}$$

• S6

$$\begin{aligned}
&\rho_{0,1} = \rho_{0,2} = 0, \quad \rho_{3,1} = 2x_1 \ , \ \rho_{3,2} = 2x_2 \\
&x_1 = (\pm)\frac{1}{2}\sqrt{4-q-r} \ , \ x_2 = (\pm)\frac{1}{2}\sqrt{4-q-r} \\
&y_1 = (\pm)\frac{1}{2}\sqrt{q+r} \ , \ y_2 = (\pm)\frac{1}{2}\sqrt{q+r},
\end{aligned} \tag{4.33}$$

• S8

$$\begin{aligned}
&\rho_{0,1} = (\pm)\sqrt{\frac{q+r-4}{q-3}} \quad \rho_{0,2} = (\pm)\sqrt{\frac{q+r-4}{r-3}} \\
&x_1 = -\frac{q-4}{2}\rho_{0,1}, \quad \rho_{3,1} = -(q-3)\rho_{0,1}, \quad x_2 = -\frac{r-4}{2}\rho_{0,2}, \quad \rho_{3,2} = -(r-3)\rho_{0,2} \\
&y_1 = (\pm)\frac{1}{2}\sqrt{\frac{4-r(q-2)^2-q(q-4)^2}{q-3}}, \quad y_2 = (\pm)\frac{1}{2}\sqrt{\frac{4-q(r-2)^2-r(r-4)^2}{r-3}}.
\end{aligned} \tag{4.34}$$

Finally, we have solutions defined for isolated values of q and r. The first one is

• S9 defined for $q = r = 2$

$$\rho_{0,1} = \rho_{0,2} = \rho_{3,1} = \rho_{3,2} = 0 \ , \ \phi_1, \phi_2, \theta \in [0, 2\pi) \ , \ \rho_{1,1} = \rho_{1,2} = 1 \, , \tag{4.35}$$

while the others are defined for less interesting values of q and r (irrational or zero) and will not be listed.

4.2.3 Some implications

We notice first of all that for $q = r = 2$ the Hamiltonian (4.1) becomes that of the Ashkin-Teller model (two coupled Ising models) [20]. The Ashkin-Teller model allows for lines of fixed points – along which the central charge is $c = 1$ and the critical exponents

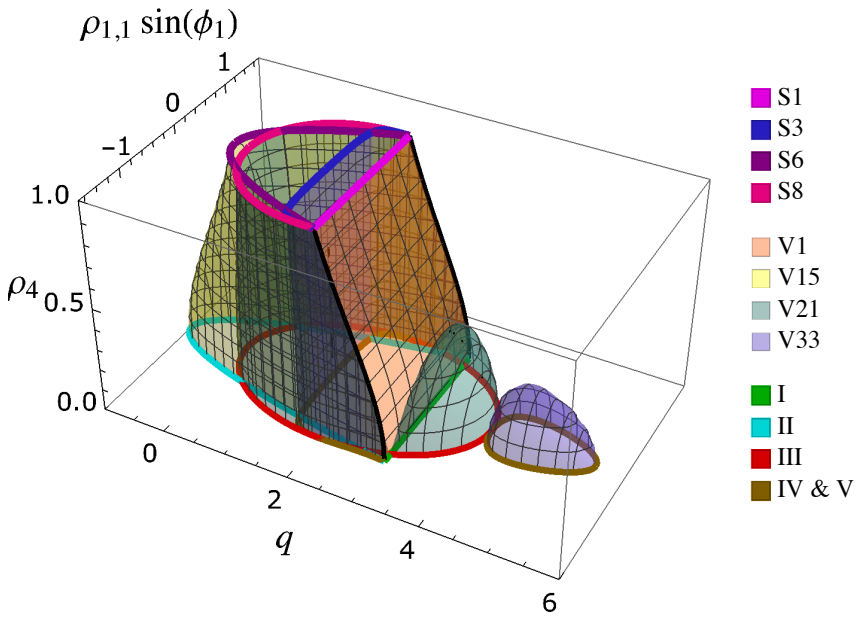

Figure 4.5: The solutions V1, V15, V21, and V33 in the parameter subspace ($\rho_{1,1}\sin\phi_1$, ρ_4) along with the decoupled solutions I, II, III, IV and V, and the strongly coupled solution S1, S3, S6, S8 for $q = r$. All the surfaces corresponding to the V-type solutions meet along the black lines for $2 < q < 3$.

vary continuously – identified perturbatively in [88, 129] and exactly in [130]. Also in our present formulation we see that at $q = r = 2$ the solutions V15, V21, V33, V13, S1 and S9 all possess a free parameter providing the coordinate along a critical line.

Excluding the Ashkin-Teller case, we also see that the only critical points corresponding to coupled models with q and r integers larger than 1 are provided by solution V5 for $(q, r) = (2, 5)$ and solution V33 for $q = r = 5$. Both V5 and V33 appear to be related to solution V of table 1.3 for a single Potts model. One implication is that for criticality in coupled ferromagnets we are left with Ashkin-Teller only. As a particular case, these results confirm the conclusion of theoretical and numerical studies [131, 132, 133, 134] which found no fixed points in two coupled Potts ferromagnets with $q = r = 3, 4, \ldots$.

The nontrivial phenomenon of a critical line with continuously varying exponents for fixed symmetry provided by the Ashkin-Teller model is made possible by the fact that at criticality this model renormalizes on the Gaussian model (free scalar boson), which in two dimensions allows for a continuous spectrum of scaling dimensions [6]. The same free

boson accounts for the line of fixed points of a single 3-state Potts model (solution I of table 1.3) [40], and is expected to generate all lines of fixed points at fixed symmetry in two dimensions. In particular, it should be contained in the field theories corresponding to the $q = r$ solutions V1, V15, V21 and V33, which span surfaces of fixed points as q varies (figure 4.5), and then lines of fixed points for q fixed. Quite interestingly a solvable square lattice realization of the $q = r$ model originally obtained in [135] and further studied in [136, 137] has been found in [138] to possess a continuous spectrum of critical exponents associated to a free boson. This lattice solution terminates at $q = 4$ and has $q = 3$ as a decoupling point; it should then be related to our solution V21. It can be seen also from figure 4.5 that in the decoupling limit $\rho_4 \to 0$ the solution V21 gives solution III for the two q-state models, and we saw in section 1.5 that solution III can describe both the ferromagnet and the square lattice antiferromagnet (recall table 1.4). In [138] the lattice solution results from the coupling of two antiferromagnets; on the other hand the central charge proposed in [137, 138] gives at the decoupling point $q = 3$ the value $8/5$, which is that of two ferromagnets. This point will deserve further investigation.

4.3 Correlated percolation

We already saw in section 1.5 how the FK representation (1.71) relates the Potts model to FK clusters. In order to make contact with spin clusters, correlated percolation in the q-state Potts ferromagnet was studied in [118] considering the coupling to an r-state Potts model realized by the Hamiltonian (4.1) with $J_2 = 0$. The site variables of the r-component are auxiliary and are eventually eliminated by the limit $r \to 1$. They allow a generalization of the FK expansion in which the clusters are made of connected bonds placed with probability (1.72) between nearest neighbors with the same value of the q-state Potts site variable. This comes from the fact that in (4.1) J is the coupling of the auxiliary variables to the q-state Potts variables. The approximated RG analysis of [118] gave two fixed points for the coupled ($J \neq 0$) model for $r \to 1$. Both of them have J_1 equal to the critical value J_c of the q-state Potts ferromagnet, consistently with the expectation for a fixed point of the $r \to 1$ model. One of the fixed points, for $J = J_c$, was argued to be repulsive and to correspond to the FK clusters. The other fixed point, for $J = J^* > J_c$, was argued to be attractive and to rule the critical behavior of spin clusters, which by definition correspond to $J = \infty$ ($p = 1$). The lines spanned by the two fixed points as a

function of q were conjectured in [118] to coalesce and terminate at $q = 4$, although this could not actually be seen within the approximated RG method.

We are now in the position of discussing Potts correlated percolation in light of our exact fixed point solutions. Observe first of all that for $r = 1$ the equations (4.7), (4.9), (4.11) and (4.13) exactly reproduce the system (1.67)-(1.70) which determines the fixed points of a decoupled q-state Potts model. This implies that, even in the coupled model ($\rho_4 \neq 0$), for $r \to 1$ the amplitudes of the q-state sector – namely the amplitudes $S_{i,1}$, $i = 0, 1, 2, 3$, involving only excitations in the q-state sector – coincide with one of the solutions of table 1.3 for the decoupled q-state Potts model. This can indeed be checked plugging $r = 1$ in the solutions of section 4.2.2. On the other hand, it must be taken into account that, even for $r \to 1$, the remaining amplitudes – involving excitations in the auxiliary r-state sector – cannot be forgotten, since also the auxiliary degrees of freedom will normally contribute to the results[7]. It follows that, taking into account the full set of amplitudes that determine a fixed point solution, the range of q in which the solution is defined for $r \to 1$ is in general smaller than that given in table 1.3 for the amplitudes of the q-state sector. This is due to the fact that in general the r-state (auxiliary) degrees of freedom are not critical in the full range in which the q-state degrees of freedom are critical. In particular, inspection of the solutions of section 4.2.2 and appendix 4.A shows that in the $r \to 1$ coupled model there is no critical line continuously defined in the whole range $q \in [2, 4]$. This excludes, in particular, that spin clusters can be fully described through some analytic continuation performed in this range, consistently with the numerical findings of [125, 126]. The possibility remains, however, that analytic continuation holds for some specific quantity that can be evaluated directly at $r = 1$, where the number of auxiliary degrees of freedom is strictly zero[8] and one can recover the branches of solution III of table 1.3 in their full range of definition $q \in [0, 4]$.

In light of our present results, it seems interesting to recall that different convergenge patterns of spin clusters towards a fixed point were observed below and above $q \approx 2.5$ in the numerical simulations performed in [125], where the range $q \in [1, 4]$ was scanned in steps of 0.25. This can be compared with our finding that in the $r \to 1$ coupled model

[7]This is immediately understood thinking to the basic example of random percolation as the limit $r \to 1$ of the r-state Potts model. In this case all the degrees of freedom are auxiliary, but nevertheless determine all the percolative properties. Extensive illustrations in the scattering formalism for the off-critical case are given in [139, 140, 141, 142, 143].

[8]We further illustrate this point in appendix 4.B.

there is a discontinuity in the critical properties at $q = 3$, since solution S8 provides a critical line in the range $q \in [0, 3]$, and solution $\tilde{\text{S5}}$ provides a critical line in the range $q \in (3, 4]$; here the tilde indicates the solution obtained from (4.43) under the exchanges (4.19). As $r \to 1$, both S8 and $\tilde{\text{S5}}$ tend to solution III of table 1.3 in the q-state sector and in their respective domains of definition.

4.A Appendix. Exchange-noninvariant solutions

We list in this appendix the solutions of the fixed point equations (4.7)-(4.17) which are noninvariant under the exchange operation (4.19). This operation maps each of the solutions below into another solution, which we do not list.

We first have the following solutions with varying ρ_4 and domains of definition shown in figure 4.6:

• V2

$$\begin{aligned}
&\rho_{0,1} = \rho_{3,1} = 0, \quad \rho_{0,2} = \rho_{3,2} = \pm\sqrt{\frac{(r-q)(r+q-4)}{(r-1)(r^2-5r+5)}}, \\
&x_1 = -\frac{(r^2-6r+6)}{2(q-2)}\rho_{0,2}, \quad x_2 = -\frac{r-4}{2}\rho_{0,2}, \quad \theta = (\pm)\frac{\pi}{2}, \\
&y_1 = -\frac{r-2}{q-2}y_2, \quad \rho_6 = (\pm)\sqrt{\frac{q+r-4}{r-1}}\ , \ \rho_4 = \sqrt{\frac{3-q}{r-1}}, \\
&y_2 = (\pm)\frac{1}{2}\sqrt{\frac{(q-3)(q-1)}{r-1} + \frac{(q-4)q-r+5}{r^2-5r+5} - r + 6},
\end{aligned} \tag{4.36}$$

• V6

$$\begin{aligned}
&\rho_{0,1} = \rho_{0,2} = \rho_{3,1} = 0, \qquad \rho_{3,2} = 2x_2, \qquad \theta = (\pm)\frac{\pi}{2}, \\
&x_1 = \frac{r}{q-2}x_2, \qquad x_2 = \pm\frac{1}{2}\sqrt{\frac{(q-r)(q+r-4)}{r-1}}, \qquad \rho_4 = \sqrt{\frac{3-q}{r-1}}, \\
&y_1 = -\frac{r-2}{q-2}y_2, \qquad y_2 = (\pm)\frac{1}{2}\sqrt{\frac{r^2-(q-2)^2}{r-1}}, \qquad \rho_6 = (\pm)\sqrt{\frac{r+q-4}{r-1}},
\end{aligned} \tag{4.37}$$

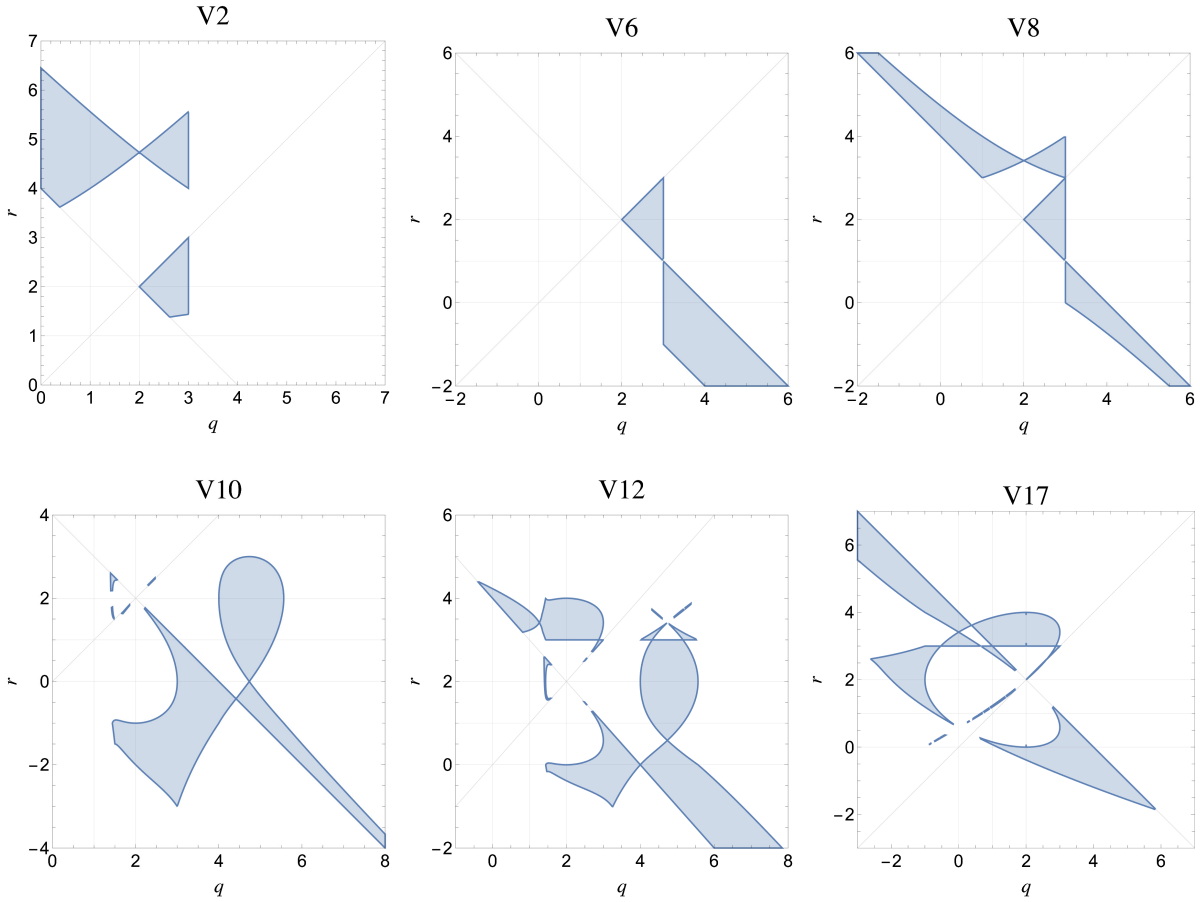

Figure 4.6: Domains of definition of the solutions V2, V6, V8, V10, V12 and V17.

- V8

$$\rho_{0,1} = \rho_{3,1} = 0, \quad \rho_{0,2} = \pm\sqrt{\frac{(r-q)(q+r-4)}{(r-1)(r-3)}}, \quad \rho_{3,2} = -(r-3)\rho_{0,2}, \quad \theta = (\pm)\frac{\pi}{2},$$
$$x_1 = -\frac{r^2-4r+2}{2(q-2)}\rho_{0,2}, \quad x_2 = -\frac{r-4}{2}\rho_{0,2}, \quad \rho_4 = \sqrt{\frac{3-q}{r-1}}, \quad \rho_6 = (\pm)\sqrt{\frac{q+r-4}{r-1}},$$
$$y_1 = -\frac{r-2}{q-2}y_2, \quad y_2 = (\pm)\frac{1}{2}\sqrt{\frac{(q-3)(q-1)}{(r-3)(r-1)}(r-2)^2 - r(r-4)}, \tag{4.38}$$

• V10

$$\rho_{0,1}=\rho_{3,1}=\pm r\sqrt{\frac{(q-r)(q+r-4)}{(q-1)(q^2-5q+5)r^2+(q^2-6q+6)^2(r-1)}},\quad \rho_{0,2}=0,$$
$$x_1=-\frac{q-4}{2}\rho_{0,1},\quad x_2=-\frac{q^2-6q+6}{2r}\rho_{0,1},\quad \rho_{3,2}=2x_2,\quad \theta=(\pm)\frac{\pi}{2},$$
$$y_1=(\pm)\frac{r-2}{2}\sqrt{\frac{(q-2)^2r^2-(q^2-6q+6)^2}{(q-1)(q^2-5q+5)r^2+(r-1)(q^2-6q+6)^2}},\quad y_2=-\frac{q-2}{r-2}y_1,$$
$$\rho_4=\sqrt{\frac{r^2(3-r)(q^2-5q+5)+(3-q)(q^2-6q+6)^2}{r^2(q-1)(q^2-5q+5)+(r-1)(q^2-6q+6)^2}},\quad \rho_6=(\pm)\sqrt{1-\rho_4^2},$$

(4.39)

• V12

$$\rho_{0,1}=\rho_{3,1}=\pm(r^2-4r+2)\alpha(q,r),\quad \rho_{0,2}=\pm(q^2-6q+6)\alpha(q,r),\quad \theta=(\pm)\frac{\pi}{2},$$
$$x_1=-\frac{q-4}{2}\rho_{0,1},\quad x_2=-\frac{(r-4)}{2}\rho_{0,2},\quad \rho_{3,2}=-(r-3)\rho_{0,2},\quad \rho_6=\pm\sqrt{1-\rho_4^2},$$
$$y_1=(\pm)\frac{r-2}{2}\beta(q,r),\quad y_2=-\frac{q-2}{r-2}y_1,\quad \rho_4=\sqrt{\frac{(r^2-4r+2)^2-\frac{(q-3)(q^2-6q+6)^2}{q^2-5q+5}}{\frac{(q^2-6q+6)^2(r-1)}{q^2-5q+5}-\frac{(q-1)(r^2-4r+2)^2}{r-3}}},$$
$$\alpha(q,r)=\sqrt{\frac{(r-q)(q+r-4)}{(q^2-6q+6)^2(r-3)(r-1)-(q-1)(q^2-5q+5)(r^2-4r+2)^2}},$$
$$\beta(q,r)=\sqrt{\frac{(q^2-6q+6)^2(r-2)^2-(q-2)^2(r^2-4r+2)^2}{(q^2-6q+6)^2(r-3)(r-1)-(q-1)(q^2-5q+5)(r^2-4r+2)^2}},$$

(4.40)

• V17

$$\rho_{0,1}=0,\quad \rho_{0,2}=q\sqrt{\frac{(q-r)(4-q-r)}{q^2(r-3)(r-1)+(q-1)(r^2-4r+2)^2}},\quad \theta=(\pm)\frac{\pi}{2},$$
$$x_1=-\frac{r^2-4r+2}{2q}\rho_{0,2},\quad x_2=-\frac{r-4}{2}\rho_{0,2},\quad \rho_{3,1}=2x_1,\quad \rho_{3,2}=-(r-3)\rho_{0,2},$$
$$y_1=(\pm)\frac{r-2}{2}\sqrt{\frac{q^2(r-2)^2-(r^2-4r+2)^2}{q^2(r-3)(r-1)+(q-1)(r^2-4r+2)^2}},\quad y_2=-\frac{q-2}{r-2}y_1,$$
$$\rho_4=\sqrt{\frac{(r-3)\left[(3-q)q^2-(r^2-4r+2)^2\right]}{q^2(r-3)(r-1)+(q-1)(r^2-4r+2)^2}},\quad \rho_6=(\pm)\sqrt{1-\rho_4^2}.$$

(4.41)

Then we have the following solutions with $\rho_4=1$ and domains of definition shown in figure 4.7:

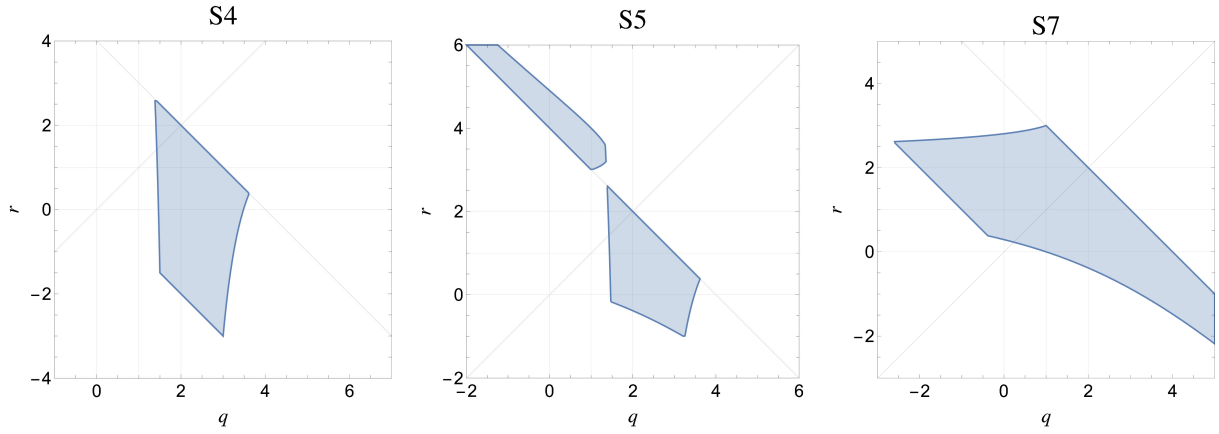

Figure 4.7: Domains of definition of the solutions S4, S5 and S7.

- S4

$$\begin{aligned}
&\rho_{0,1} = \rho_{3,1} = (\pm)\sqrt{\frac{q+r-4}{q^2-5q+5}}, \quad x_1 = -\frac{q-4}{2}\rho_{0,1}, \\
&y_1 = (\pm)\frac{1}{2}\sqrt{\frac{(4-q)\,(q^2-7q+8)-(q-2)^2(r-1)}{q^2-5q+5}}, \\
&\rho_{0,2} = 0, \quad \rho_{3,2} = 2x_2 = (\pm)\sqrt{4-q-r}, \quad y_2 = (\pm)\frac{1}{2}\sqrt{q+r},
\end{aligned} \tag{4.42}$$

- S5

$$\begin{aligned}
&\rho_{0,1} = \rho_{3,1} = (\pm)\sqrt{\frac{q+r-4}{q^2-5q+5}}, \quad \rho_{0,2} = (\pm)\sqrt{\frac{q+r-4}{r-3}}\ , \ \rho_{3,2} = -(r-3)\rho_{0,2}, \\
&x_1 = -\frac{q-4}{2}\rho_{0,1}, \quad y_1 = (\pm)\frac{1}{2}\sqrt{\frac{(4-q)\,(q^2-7q+8)-(q-2)^2(r-1)}{q^2-5q+5}}, \\
&x_2 = -\frac{r-4}{2}\rho_{0,2}, \quad y_2 = (\pm)\frac{1}{2}\sqrt{\frac{4-q(r-2)^2-r(r-4)^2}{r-3}},
\end{aligned} \tag{4.43}$$

- S7

$$\begin{aligned}
&\rho_{0,1} = 0, \quad \rho_{3,1} = 2x_1 \quad \rho_{0,2} = (\pm)\sqrt{\frac{q+r-4}{r-3}}, \quad \rho_{3,2} = -(r-3)\rho_{0,2}, \\
&x_1 = (\pm)\frac{1}{2}\sqrt{4-q-r}, \quad y_1 = (\pm)\frac{1}{2}\sqrt{q+r}, \\
&x_2 = -\frac{r-4}{2}\rho_{0,2}, \quad y_2 = (\pm)\frac{1}{2}\sqrt{\frac{4-q(r-2)^2-r(r-4)^2}{r-3}}.
\end{aligned} \tag{4.44}$$

Finally there are solutions defined only for isolated values of q and r, of which we only list those defined for nonzero integer values of q and r:

• V7 defined for $q = 3$, $r = 1$

$$\begin{aligned} &\rho_{0,1} = \rho_{0,2} = \rho_{3,1} = 0, \quad x_1 = x_2 = \frac{1}{2}\rho_{3,2} = \pm\frac{1}{\sqrt{2}}\sqrt{1-\rho_4^2}, \quad \theta = (\pm)\frac{\pi}{2}, \\ &y_1 = y_2 = (\pm)\frac{1}{\sqrt{2}}\sqrt{1+\rho_4^2}, \quad \rho_6 = (\pm)\sqrt{1-\rho_4^2}, \quad \rho_4 \in (0,1), \end{aligned} \tag{4.45}$$

• V9 defined for $q = 3$, $r = 1$

$$\begin{aligned} &\rho_{0,1} = \rho_{3,1} = 0, \quad \rho_{0,2} = 2x_1 = \frac{2}{3}x_2 = \frac{1}{2}\rho_{3,2} = \pm\sqrt{1-\rho_4^2}, \quad \theta = (\pm)\frac{\pi}{2}, \\ &y_2 = y_1 = (\pm)\frac{1}{2}\sqrt{3+\rho_4^2}, \quad \rho_6 = (\pm)\sqrt{1-\rho_4^2}, \quad \rho_4 \in (0,1), \end{aligned} \tag{4.46}$$

• V11 defined for $q = r = 2$

$$\begin{aligned} &\rho_{0,1} = \rho_{3,1} = \rho_{3,2} = x_1 = 2x_2 = \pm\sqrt{1-\rho_4^2}, \quad \rho_{0,2} = 0, \quad \theta = (\pm)\frac{\pi}{2}, \\ &y_1 = (\pm)1\ ,\ y_2 = (\pm)\frac{1}{2}\sqrt{3+\rho_4^2}\ ,\ \rho_6 = (\pm)\sqrt{1-\rho_4^2}\ ,\ \rho_4 \in (0,1), \end{aligned} \tag{4.47}$$

• V22 defined for $q = 3, r = 1$

$$\begin{aligned} &\rho_{0,1} = \rho_{0,2} = 2x_1 = \frac{2}{3}x_2 = \frac{1}{2}\rho_{3,2} = \pm\sqrt{1-\rho_4^2}, \quad \rho_{3,1} = 0, \quad \theta = (\pm)\frac{\pi}{2}, \\ &y_1 = y_2 = (\pm)\frac{1}{2}\sqrt{3+\rho_4^2}, \quad \rho_6 = (\pm)\sqrt{1-\rho_4^2}, \quad \rho_4 \in (0,1). \end{aligned} \tag{4.48}$$

4.B Appendix. Scattering eigenstates

Within the scattering description of the coupled q-state and r-state Potts models we consider the states

$$\psi_k = B_k \sum_{\substack{\gamma_1=1 \\ \gamma_1\neq\alpha_1}}^{q} A_{\alpha_1\gamma_1}A_{\gamma_1\alpha_1} + C_k \sum_{\substack{\gamma_2=1 \\ \gamma_2\neq\alpha_2}}^{r} A_{\alpha_2\gamma_2}A_{\gamma_2\alpha_2}\,, \qquad k = 1, 2\,, \tag{4.49}$$

which scatter into themselves through the phases Φ_k given by

$$\begin{aligned} \Phi_1 = \frac{1}{2}\Bigg[&(q-2)S_{2,1} + (r-2)S_{2,2} + S_{3,1} + S_{3,2} \\ &+ \sqrt{\Big((q-2)S_{2,1} - (r-2)S_{2,2} + S_{3,1} - S_{3,2}\Big)^2 + 4(q-1)(r-1)S_4^2}\Bigg], \end{aligned} \tag{4.50}$$

$$\begin{aligned} \Phi_2 = \frac{1}{2}\Bigg[&(q-2)S_{2,1} + (r-2)S_{2,2} + S_{3,1} + S_{3,2} \\ &- \sqrt{\Big((q-2)S_{2,1} - (r-2)S_{2,2} + S_{3,1} - S_{3,2}\Big)^2 + 4(q-1)(r-1)S_4^2}\Bigg]. \end{aligned} \tag{4.51}$$

The coefficients in (4.49) are given by

$$\begin{aligned} B_k &= S_{3,2} + (r-2)S_{2,2} - (r-1)S_4 - \Phi_k \,, \\ C_k &= S_{3,1} + (q-2)S_{2,1} - (q-1)S_4 - \Phi_k \,. \end{aligned} \tag{4.52}$$

In the decoupled case $S_4 = 0$ the phases Φ_1 and Φ_2 reduce to $(q-2)S_{2,1} + S_{3,1}$ and $(r-2)S_{2,2} + S_{3,2}$, respectively, as they should (recall (1.73)). As a generalization of (1.49), in the coupled case the relations

$$\Phi_k = e^{-2\pi i \, \Delta_{\eta_k}} \tag{4.53}$$

give the conformal dimensions Δ_{η_1} and Δ_{η_2} of the fields which create the particles in the q-state sector and in the r-state sector, respectively.

Notice that in the limit $r \to 1$ relevant for correlated percolation the phase Φ_1 for the q-state sector becomes

$$\Phi_1|_{r=1} = (q-2)S_{2,1} + S_{3,1} \,, \tag{4.54}$$

which is the value (1.73) for the decoupled q-state model. As a consequence (4.53) yields for $\Delta_{\eta_1}|_{r=1}$ the value of the decoupled model, in spite of the fact that the coefficients

$$B_1|_{r=1} = S_{3,2} - S_{2,2} - (q-2)S_{2,1} - S_{3,1} \,, \tag{4.55}$$

$$C_1|_{r=1} = -(q-1)S_4 \tag{4.56}$$

are both nonzero in the coupled case $S_4 \neq 0$. Hence, Δ_{η_1} provides an example of a quantity that can be evaluated directly at $r = 1$, where the degrees of freedom in the r-state sector play no role, since their number is strictly zero. Other quantities, on the other hand, will be determined by ratios in which both the numerator and the denominator vanish at $r = 1$. The limit $r \to 1$ exists, but is determined by evaluation at $r = 1 + \epsilon$, where the auxiliary r-state degrees of freedom are present and contribute. The three-point connectivity of random percolation provides an exact illustration of this mechanism [35].

Bibliography

[1] L.D. Landau and E.M. Lifshitz, Statistical Physics, part 1, 3rd edn, Elsevier, 1980.

[2] R.B. Potts, Proc. Cambr. Phil. Soc. 48 (1952) 106.

[3] F.Y. Wu, Rev. Mod. Phys. 54 (1982) 235.

[4] J. Cardy, Scaling and renormalization in statistical physics, Cambridge, 1996.

[5] K.G. Wilson and J. Kogut, Physics Reports 12 (1974) 75.

[6] P. Di Francesco, P. Mathieu and D. Senechal, Conformal field theory, Springer-Verlag, New York, 1997.

[7] A.A. Belavin, A.M. Polyakov and A.B. Zamolodchikov, Nucl. Phys. B 241 (1984) 333.

[8] D. Friedan, Z. Qiu and S. Shenker, Phys. Rev. Lett. 52 (1984) 1575.

[9] A.B. Zamolodchikov, JETP Lett. 43 (1986) 730.

[10] L. Onsager, Phys. Rev. 65 (1944) 117.

[11] C.N. Yang, Phys. Rev. 85 (1952) 808.

[12] B. Kaufman, Phys. Rev. 76 (1949) 1244.

[13] A.B. Zamolodchikov, Sov. J. Nucl. Phys. 44 (1986) 529.

[14] D.A. Huse, Phys. Rev. B 30 (1984) 3908.

[15] V.S. Dotsenko, Nucl. Phys. B 235 (1984) 54.

[16] J.L. Cardy, Nucl. Phys. B 270 (1986) 186.

[17] A. Cappelli, C. Itzykson and J.B. Zuber, Nucl. Phys. B 280 (1987) 445.

[18] S. Coleman, Phys. Rev. D 11 (1975) 2088.

[19] S. Mandelstam, Phys. Rev. D 11 (1975) 3026.

[20] J. Ashkin and E. Teller, Phys. Rev. 64 (1943) 178.

[21] L.P. Kadanoff and A.C. Brown, Ann. Phys. 121 (1979) 318.

[22] N.D. Mermin and H. Wagner, Phys. Rev. Lett. 17 (1966) 1133.

[23] P.C. Hohenberg, Phys. Rev. 158 (1967) 383.

[24] S. Coleman, Comm. Math. Phys. 31 (1973) 259.

[25] V.L. Berezinskii, Sov. Phys. JETP, 32 (1971) 493.

[26] J.M. Kosterlitz and D.J. Thouless, J. Phys. C 6 (1973) 1181.

[27] L.H. Ryder, Quantum Field Theory, Cambridge University Press, Second Edition, 1996.

[28] R.J. Eden, P.V. Landshoff, D.I. Olive and J.C. Polkinghorne, The analytic S-matrix, Cambridge, 1966.

[29] G. Delfino, Ann. Phys. 333 (2013) 1.

[30] G. Delfino and N. Lamsen, J. Stat. Mech. (2019) 024001.

[31] P.G. De Gennes, Phys. Lett. A 38 (1972) 339.

[32] B. Nienhuis, in Phase transitions and critical phenomena, edited by C. Domb and J.L. Lebowitz, vol. 11, p. 1, Academic Press, London, 1987.

[33] Vl.S. Dotsenko and V.A. Fateev, Nucl. Phys. B 240 (1984) 312.

[34] A.B. Zamolodchikov, Mod. Phys. Lett. A 6 (1991) 1807.

[35] G. Delfino and J. Viti, J. Phys. A 44 (2011) 032001.

[36] G. Delfino and J. Viti, Nucl. Phys. B 852 (2011) 149.

[37] L. Chim and A.B. Zamolodchikov, Int. J. Mod. Phys. A 7 (1992) 5317.

[38] V.V. Bazhanov and Y.G. Stroganov, Nucl. Phys. B 205 (1982) 505.

[39] G. Delfino, Phys. Rev. Lett. 118 (2017) 250601.

[40] G. Delfino and E. Tartaglia, Phys. Rev. E 96 (2017) 042137.

[41] C.M. Fortuin and P.W. Kasteleyn, J. Phys. Soc. Jpn. Suppl. 26 (1969) 11; Physica 57 (1972) 536.

[42] D. Stauffer and A. Aharony, Introduction to Percolation Theory, 2nd edn, Taylor & Francis, London, 1992.

[43] R.J. Baxter, Exactly Solved Models of Statistical Mechanics, Academic Press, London, 1982.

[44] G. Delfino, Phys. Lett. B 450 (1999) 196.

[45] G. Delfino and P. Grinza, Nucl. Phys. B 682 (2004) 521.

[46] G. Delfino and J. Cardy, Phys. Lett. B 483 (2000) 303.

[47] B. Nienhuis, A.N. Berker, E.K. Riedel and M. Schick, Phys. Rev. Lett. 43 (1979) 737.

[48] E.H. Lieb and F.Y. Wu, in Phase Transitions and Critical Phenomena, edited by C. Domb and M.S. Green (Academic, New York, 1972), Vol. 1, p. 331.

[49] J.K. Burton, Jr. and C.L. Henley, J. Phys. A 30 (1997) 8385.

[50] J. Cardy, J.L. Jacobsen and A.D. Sokal, J. Stat. Phys. 105 (2001) 25.

[51] J.-P. Lv, Y. Deng, J.L. Jacobsen and J. Salas, J. Phys. A: Math. Theor. 51 (2018) 365001.

[52] R.J. Baxter, Proc. Roy. Soc. London A 383 (1982) 43.

[53] H. Saleur, Nucl. Phys. B360 (1991) 219.

[54] J.L. Jacobsen and H. Saleur, Nucl. Phys. B743 (2006) 207.

[55] Y. Ikhlef, Mod. Phys. Lett. B 25 (2011) 291.

[56] A.B. Zamolodchikov and V.A. Fateev, Sov. Phys. JETP 62 (1985) 215.

[57] A. Aizenman and J. Wehr, Phys. Rev. Lett. 62 (1989) 2503.

[58] K. Hui and A.N. Berker, Phys. Rev. Lett. 62 (1989) 2507.

[59] Y. Deng, Y. Huang, J.L. Jacobsen, J. Salas, and A.D. Sokal, Phys. Rev. Lett. 107 (2011) 150601.

[60] J. Salas, Phys. Rev. E 102 (2020) 032124.

[61] G. Delfino and P. Grinza, Nucl. Phys. B 791 (2008) 265.

[62] L. Lepori, G.Z. Toth and G. Delfino, J. Stat. Mech. (2009) P11007.

[63] G. Delfino and N. Lamsen, to be published.

[64] P.G. de Gennes and J. Prost, The Physics of Liquid Crystals, Oxford University Press, Oxford, 1993.

[65] N.D. Mermin and H. Wagner, Phys. Rev. Lett. 17 (1966) 1133.

[66] V.L. Berezinskii, Sov. Phys. JETP, 32 (1971) 493.

[67] K. Harth and R. Stannarius, Front. Phys. 8 (2020) 112.

[68] Z. Zhang, O.G. Mouritsen and M. Zuckermann, Phys. Rev. Lett. 69 (1992) 2803.

[69] D.L. Stein, Phys. Rev. B 18 (1978) 2397.

[70] N.D. Mermin, Rev. Mod. Phys. 51, 591 (1979).

[71] H. Kunz and G. Zumbach, Phys. Rev. B 46 (1992) 662.

[72] A.I. Farinas-Sanchez, R. Paredes and B. Berche, Phys. Lett. A 308 (2003) 461.

[73] S. Dutta and S.K. Roy, Phys. Rev. E 70 (2004) 066125.

[74] S. Shabnam, S.D. Gupta and S.K. Roy, Phys. Lett. A 380 (2016) 667.

[75] C. Chiccoli, P. Pasini and C. Zannoni, Physca A 148 (1988) 298.

[76] R. Paredes R., A.I. Farinas-Sanchez and R. Botet, Phys. Rev. E. 78 (2008) 051706.

[77] A.I. Farinas-Sanchez, R. Botet, B. Berche and R. Paredes, Condens. Matter Phys. 13 (2010) 13601.

[78] Y. Tomita, Phys. Rev. E 90 (2014) 032109.

[79] B. Kamala Latha and V.S.S. Sastry, Phys. Rev. Lett. 121 (2018) 217801.

[80] D.K. Sinclair, Nucl. Phys. B 205 (1982) 173.

[81] S. Caracciolo, R.G. Edwards, A. Pelissetto and A.D. Sokal, Nucl. Phys. B (Proc. Suppl.) 30 (1993) 815.

[82] F. Niedermayer, P. Weisz and D.-S. Shin, Phys. Rev. D 53 (1996) 5918

[83] M. Hasenbusch, Phys. Rev. D 53 (1996) 3445.

[84] S.M. Catterall, M. Hasenbusch, R.R. Horgan, R. Renken, Phys. Rev. D 58 (1998) 074510.

[85] S. Caracciolo, R.G. Edwards, A. Pelissetto and A.D. Sokal, Phys. Rev. Lett. 71 (1993) 3906.

[86] C. Bonati, A. Franchi, A. Pelissetto and E. Vicari, Phys. Rev. D 102 (2020) 034513 [arXiv:2006.13061].

[87] G. Delfino, Annals of Physics 360 (2015) 477.

[88] J.V. José, L.P. Kadanoff, S. Kirkpatrick and D.R. Nelson, Phys. Rev. B 16 (1977) 1217.

[89] G. Delfino and N. Lamsen, J. Phys. A: Math. Theor. 52 (2019) 35LT02.

[90] L. A. Fernandez, V. Martin-Mayor, D. Sciretti, A. Tarancon and J. L. Velasco, Phys. Lett. B 628 (2005) 281.

[91] A.C.D. van Enter and S.B. Shlosman, Phys. Rev. Lett. 89, 285702 (2002).

[92] E. Domany, M. Schick and R.H. Swendsen, Phys. Rev. Lett. 52, 1535 (1984).

[93] H.W.J. Blote, W.N. Guo and H.J. Hilhorst, Phys. Rev. Lett. 88, 047203 (2002).

[94] R.L.C. Vink, Phys. Rev. Lett. 98, 217801 (2007).

[95] N. Magnoli, F. Ravanini, Z. Phys. C 34 (1987) 43.

[96] H. Kunz and G. Zumbach, J. Phys. A 22 (1989) L1043.

[97] A.D. Sokal and A.O. Starinets, Nucl. Phys. B 601 (2001) 425.

[98] O. Tchernyshyov and S.L. Sondhi, Nucl. Phys. B 639 (2002) 429.

[99] S. Caracciolo, B.M. Mognetti and A. Pelissetto, Nucl. Phys. B 707 (2005) 458.

[100] H. Eichenherr, Nucl. Phys. B 146 (1978) 215.

[101] A. D'Adda, M. Luscher and P. Di Vecchia, Nucl. Phys. B 146 (1978) 63.

[102] E. Witten, Nucl. Phys. B 149 (1979) 285.

[103] A. Nahum, P. Serna, A.M. Somoza and M. Ortuño, Phys. Rev. B 87 (2013) 184204.

[104] F. Delfino, A. Pelissetto and E. Vicari, Phys. Rev. B 91 (2015) 052109.

[105] G. Delfino, Eur. Phys. J. B 94 (2021) 65.

[106] G. Delfino and N. Lamsen, J. Stat. Mech. (2019) 024001.

[107] A.B. Zamolodchikov and Al.B. Zamolodchikov, Annals of Physics 120 (1979) 253.

[108] B. Berg and P. Weisz, Commun. Math. Phys. 67 (1979) 241.

[109] Y.Y. Goldschmidt and E. Witten, Phys. Lett. B 91(1980) 392.

[110] M.E. Fisher, Physics 3 (1967) 255.

[111] H. Muller-Krumbhaar, Phys. Lett. A 48 (1974) 459.

[112] A. Coniglio and W. Klein, J. Phys. A 13 (1980) 2775.

[113] A. Coniglio, C. Nappi, F. Peruggi and L. Russo, J. Phys. A 10 (1977) 205.

[114] M.F. Sykes and D.S. Gaunt, J. Phys. A 9 (1976) 2131.

[115] B. Nienhuis, J. Phys. A 15 (1982) 199.

[116] B. Nienhuis, in Phase transitions and critical phenomena, edited by C. Domb and J.L. Lebowitz, vol. 11, p. 1, Academic Press, London, 1987.

[117] A. Stella and C. Vanderzande, Phys. Rev. Lett. 62 (1989) 1067.

[118] A. Coniglio, F. Peruggi, J. Phys. A 15 (1982) 1873.

[119] R.J. Baxter, J. Phys. C 6 (1973) L445.

[120] C. Vanderzande, J. Phys. A 25 (1992) L75.

[121] J.L. Cardy, M. Nauenberg and D.J. Scalapino, Phys. Rev. B 22 (1980) 2560.

[122] Y. Deng, H.W.J. Blöte and B. Nienhuis, Phys. Rev. E 69 (2004) 026123.

[123] R.M. Ziff, J.J.H. Simmons and P. Kleban, J. Phys. A: Math. Theor. 44 (2011) 065002.

[124] M. Picco, R. Santachiara, J. Viti and G. Delfino, Nucl. Phys. B, 875 (2013) 719.

[125] G. Delfino, M. Picco, R. Santachiara and J. Viti, J. Stat. Mech. (2013) P11011.

[126] I.A. Kovacs, E.M. Elci, M. Weigel and Ferenc Igloi, Phys. Rev. B 89 (2014) 064421.

[127] J. Cardy and I. Peschel, Nucl. Phys. B 300 (1988) 377.

[128] M. Picco and R. Santachiara, On the CFT describing the spin clusters in 2d Potts model, arXiv:2111.03846.

[129] L.P. Kadanoff, Annals of Physics 120 (1979) 39.

[130] G. Delfino and N. Lamsen, J. Phys. A: Math. Theor. 52 (2019) 35LT02.

[131] I. Vaysburd, Nucl. Phys. B 446, 387 (1995).

[132] P. Pujol, Europhys. Lett. 35 (1996) 283.

[133] V. Dotsenko, J.L. Jacobsen, M.-A. Lewis and Marco Picco, Nucl. Phys. B 546 (1999) 505.

[134] Y. Gandica and S. Chiacchiera, Phys. Rev. E 93 (2016) 032132.

[135] H. Au-Yang and J.H.H. Perk, Intern. J. Mod. Phys. A7 Suppl. 1B (1992) 1025.

[136] M.J. Martins and B. Nienhuis, J. Phys. A: Math. Gen. 31 (1998) L723.

[137] P. Fendley and J.L. Jacobsen, J. Phys. A: Math. Theor. 41 (2008) 215001.

[138] E. Vernier, J.L. Jacobsen and H. Saleur, J. Stat. Mech, P10003 (2014).

[139] G. Delfino and J. Cardy, Nucl. Phys. B 519 (1998) 551.

[140] G. Delfino, Nucl. Phys. B 818 (2009) 196.

[141] G. Delfino, J. Viti and J. Cardy, J. Phys. A: Math. Theor. 43 (2010) 152001.

[142] G. Delfino and J. Viti, Nucl. Phys. B 840 (2010) 513.

[143] G. Delfino and J. Viti, J. Phys. A: Math. Theor. 45 (2012) 032005.